Distribution Agreement

In presenting this thesis or dissertation as a partial fulfillment of the requirements for an advanced degree from Emory University, I hereby grant to Emory University and its agents the non-exclusive license to archive, make accessible and display my thesis or dissertation in whole or in part in all forms of media, now or hereafter known, including display on the world wide web. I understand that I may select some access restrictions as part of the online submission of this thesis or dissertation. I retain all ownership rights to the copyright of the thesis or dissertation. I also retain the right to use in future works (such as articles or book) all or part of this thesis or dissertation.

Signature

_____ _____

Eric David Heuer Date

Neonatal lesions of the hippocampus in the rhesus macaque:
Testing the validity of the early hippocampal lesion model of schizophrenia in a non-human primate.

By

Eric David Heuer
Doctor of Philosophy

Graduate Division of Biological and Biomedical Sciences
Neuroscience

_____
Jocelyne Bachevalier, Ph.D.
Advisor

_____
Elizabeth Buffalo, Ph.D.
Committee Member

_____
Leonard Howell, Ph.D.
Committee Member

_____
Richard Saunders, D.Phil.
Committee Member

_____
Stuart Zola, Ph.D.
Committee Member

Accepted:

_____
Lisa A. Tedesco, Ph.D.
Dean of the James T. Laney School of Graduate Studies

_____
Date

Neonatal lesions of the hippocampus in the rhesus macaque:
Testing the validity of the early hippocampal lesion model of schizophrenia in a non-human primate.

By

Eric David Heuer
B.S., Allegheny College, 2003

Advisor: Jocelyne Bachevalier, Ph.D.

An abstract of
a dissertation submitted to the Faculty of the Graduate School of Emory University
in partial fulfillment of the requirements for the degree of Doctor of Philosophy
in Graduate Division of Biological and Biomedical Science
Neuroscience
2010

Abstract

Neonatal lesions of the hippocampus in the rhesus macaque:
Testing the validity of the early hippocampal lesion model of schizophrenia in a non-human primate.
By Eric David Heuer

Schizophrenia is a neurodevelopmental disorder of unknown etiology that has a varied developmental progression. Research in schizophrenia has found the primary sites of disease pathology to be the dorsolateral prefrontal cortex (dlPFC) and hippocampus, which are associated with impairments in working memory and sensory-motor gating. From the knowledge gained from schizophrenia research, investigators have developed a rodent model in which neonatal damage to the ventral hippocampus recapitulates a host of neuropathological, behavioral and cognitive symptoms of the disease state, including impairment in working memory and sensory-motor gating. Although this rodent model has provided an important tool to better understand the origins of the disease, interpretation of the cognitive and sensory filtering processes is problematic because the primary site of pathology in schizophrenia, i.e. the dlPFC, does not truly exist in the rodent. Thus, to properly address the cognitive problems in schizophrenia and their neural origin, the use of an animal model with a well-developed prefrontal cortex is required. Toward this end, the aim of the current studies was to select a battery of neuropsychological, neuroimaging and sensory-motor assays to measure the effects of neonatal neurotoxic lesions of the hippocampus in adult monkeys, which have prefrontal regions homologous to those found in humans. Using monkeys that had received neonatal hippocampal lesions in the first 2 weeks of life (Neo-H) and sham-operated controls, four experiments were designed. The first two experiments used cognitive tasks specifically designed to assess monitoring working memory processes mediated by the dorsolateral prefrontal cortex (i.e. object self-order task and serial order task) and maintenance working memory processes mediated by the ventrolateral prefrontal cortex (session-unique delayed non-matching to sample). As compared to controls, monkeys with Neo-H lesions were impaired on the two former tasks but not on the later, indicating a selective dlPFC dependent working memory deficit that mirrors that described in schizophrenia. The results suggest a putative role for the hippocampus in the development of the prefrontal cortex. To investigate this further, the third experiment directly examined the integrity of prefrontal cortex regions (dlPFC and vlPFC) in monkeys with Neo-H and their sham-operated controls using magnetic resonance spectroscopy (MRS). N-acetyl-aspartate (NAA) is an amino acid, produced exclusively in neurons and consistently associated with cellular integrity and activity, which can be measured by MRS. The results showed no alterations in the NAA levels within the dlPFC indicating no evidence of ultra-structural or morphological changes associated with the Neo-H lesion. By contrast, increased NAA levels were found in the vlPFC, suggesting that this PFC region may have compensated for a dysfunctional dlPFC by increasing its' activity levels and subsequently NAA levels. However, given that the vlPFC cannot fully substitute for all dlPFC functions, monitoring working memory processes mediated by the dlPFC were disrupted. Lastly, we sought to examine sensory-motor gating following the Neo-H lesion using the pre-pulse inhibition paradigm (PPI). PPI is known to be sensitive to the disruption of the ventral striatal circuitry, the same theoretical circuitry whereby early hippocampal lesions are thought to impact working memory. The results showed no alterations in the baseline startle response but impairment in inhibition at long pre-pulse intervals. As a whole, these results suggest that the neonatal lesion model of schizophrenia is tenable in the primate but that the nature of observed changes may be different than in rodents. Future studies in the primate should be directed at examining the neural basis for the observed behavioral changes associated with a Neo-H lesion in a monkey and how it applies to humans.

Neonatal lesions of the hippocampus in the rhesus macaque:
Testing the validity of the early hippocampal lesion model of schizophrenia in a non-human primate.

By

Eric David Heuer
B.S., Allegheny College, 2003

Advisor: Jocelyne Bachevalier, Ph.D.

A dissertation submitted to the Faculty of the Graduate School of Emory University
in partial fulfillment of the requirements for the degree of Doctor of Philosophy
in Graduate Division of Biological and Biomedical Science
Neuroscience
2010

Contents

List of Figures

List of Tables

Acknowledgements

I would first like to thank my mentor Dr. Jocelyne Bachevalier, who has supported my scientific development throughout the past six years. In working with her I have learned what it takes to be a successful scientist and how she has gotten where she is today. One of the best lessons that I learned from her was that good science is not done behind closed doors, but through a free exchange of ideas and collaboration.

I would also like to thank my class, Emory Neuroscience 2004, who I've come to know well over these past six years. Since arriving in Atlanta we've been there for the each other during: ups, downs, highs and lows. I'm not sure I could've made it though without the support of my class. I sincerely hope that future generations of Emory neuroscientists are fortunate enough to have such a great relationship with their peers. I would also like to thank the program in general, including the students and administrators.

It also naturally follows that I thank my thesis committee: Dr. Elizabeth Buffalo, Dr. Leonard Howell, Dr. Richard Saunders and Dr. Stuart Zola. In the last several years I have really come to learn how important a good thesis committee can be facilitating a PhD students progress and development. During my time at Emory I have had extensive guidance from

each of the members of my committee and I know that because of them I am a better scientist. A PhD is not just the work of one person but is formulated under the guidance of good mentorship.

I was also fortunate enough to receive intellectual contributions from within my laboratory. As a primate laboratory we are required to share animals, equipment and physical space, which can test the patience of even the most tempered individual. Fortunately, despite having being such a large lab we were able to make it work so that everybody could accomplish what was necessary.

Outside collaborators have also been extremely helpful in my adventures into applying new techniques to monkey neuropsychology. I would like to thank Dr. Xiaodong Zhang for his expertise in the magnetic resonance spectroscopy study. Dr. Michael Davis was instrumental in getting the startle apparatus up and running, allowing me to examine startle and pre-pulse inhibition.

I think it is also important to acknowledge all the technical support that I have received in one way or another throughout my time here. Each of these people, in varying ways, assisted with the completion of these projects: Martin O'Malley, Becca Grizzard, Amy Mahan, Brittany Copp, Bronwyn Welsh and Anthony Gazy.

It certainly goes without saying that I would also like to thank my family, specifically my parents. My mother and stepfather have always placed a priority on education and started me on this path many years ago. I cannot thank them enough for I certainly would not be where I am today without their support.

Lastly, I'd like to thank my partner, Catherine C. Capello. Catie, you have helped me through the toughest adventure of my scientific career. Thank you for your support.

Chapter 1

Introduction and Background

Overview

Schizophrenia is a severely debilitating psychiatric disorder, with a variety of symptoms that affects millions of people worldwide. As a result, mental health professionals and basic science researchers alike have sought to bring novel treatments in an attempt to improve the quality of life for affected individuals. Recent research of the disorder has highlighted impaired cognitive functions, and more particularly memory deficits. The focus on these cognitive components, or "endophenotypes", has recently been highlighted by the Measurement and Treatment Research to Improve Cognition in Schizophrenia (MATRICS) Panel, which identified deficits in several cognitive domains in schizophrenia, including episodic and working memory (WM) that are generally refractive to treatment with antipsychotics and which has recommended that these endophenotypes be used and modeled in animal studies [1-3]. Although current rodent models are well suited to investigate the genetic, neurochemical and molecular

components of the disease, they offer limited advantages for the study of higher cognitive processes, such as working memory processes mediated by the lateral prefrontal cortex. The main reason being that rodents have a poorly developed prefrontal cortex. Thus, nonhuman primates, which have prefrontal regions homologous to those of humans [4,5], may be better suited to model the working memory deficits found in schizophrenia.

This introduction reviews the available literature on the background of the disease and its' anatomical substrates. In relation to the studies designed for the present thesis , the current rodent model utilizing neonatal hippocampal lesions is described and its main disadvantages are highlighted. Finally, accounts are provided for why the development of a primate model is necessary to address the question of whether or not early hippocampal lesions may trigger maldevelopment of the lateral prefrontal cortex, resulting in working memory deficits that could model those found in schizophrenia.

Schizophrenia Background

Schizophrenia is a psychiatric diagnosis of a neuro-developmental disorder that likely encompasses several disorders, which are generally grouped due to an overlap in observable symptoms. As per the Diagnostic and Statistical Manual IV, schizophrenia symptoms are grouped into three categories: Positive, Negative and Cognitive [6]. Positive symptoms, by definition mental processes existing in the disease state that do not exist in a normal individual, including: hallucinations (visual, auditory or tactile), delusions of grandeur, motor stereotypies and disorganized speech patterns. In contrast, Negative symptoms are defined as processes that are absent or reduced in the disease state, as compared to normal individuals and include: low emotionality, low energy, flattened affect, social isolation and impaired sensory-motor gating. The last and most recently

identified of the three major categories of schizophrenia symptoms are Cognitive symptoms, which include: working memory impairments, poor attention and reduced cognitive processing speed.

Recent epidemiological studies of schizophrenia have confirmed that the prevalence of schizophrenia has not changed over time, unlike other comparable developmental disorders such as Autism, which seems to be showing an increase in incidence [7]. Consistent with older studies, the prevalence of schizophrenia has remained constant with approximately 1 in 100 individuals being affected in any given population [8]. In addition, there seems to be a strong sex difference in the affected patient population with a greater male to female ratio of approximately 1.4:1 [8]. The sex differences are often attributed to a difference in vulnerability during the prenatal period, insofar as estrogen seems to provide some level of neuro-protection in the females. Researchers point to prenatal susceptibility as a potential explanation for the observed sexual dimorphism. This assertion is supported by evidence showing that prenatal factors, such as poor maternal nutrition [9], maternal infection during the second to third trimester [10,11] and paternal age [12], greatly increase the likelihood of disease onset. It certainly should be mentioned that the populations cited in these studies were extremely homogeneous, limited in scope and cannot account for all potential risk factors, however they provide the strongest controlled and well documented evidence for an association between prenatal vulnerability and schizophrenia.

In viewing the clinical picture of schizophrenia, it is clear that this disease is extremely pervasive as it impacts all aspects of the patients' life, often making it impossible for many to function on any reasonable level within society. A recent study

of the economic effects of schizophrenia estimated that the annual direct cost of healthcare, in the United States alone, for diagnosed patients to be $22.7billion [13]. The additional costs of providing housing (inpatient or outpatient), lost income from not working and legal problems, to name a few, have been estimated at over $67 billion annually. Lastly, a frequently overlooked cost of schizophrenia is the effect it has on the primary caregiver. Caregivers of patients suffer a reduced quality of life, are often more susceptible to illness, show a reduced work output and suffer a significant financial burden [14]. In sum, these data suggest that all efforts should be made to provide the most effective treatment for schizophrenia, as it is clearly in the interest of both the patient and society as a whole.

In order to examine the effectiveness of recent advances in schizophrenia treatments a large-scale clinical trial was recently conducted. The trial, so-named Clinical Antipsychotic Trials for Intervention Effectiveness (CATIE), was focused on examining the effectiveness first and second generation antipsychotics [15]. The goal of the study was to determine if anecdotal evidence that the second-generation antipsychotics were truly more effective and more tolerable than classic medications. The results of the study found that only 26% of the patient populous adhered to their assigned medication, regardless of the type of medication (first or second generation). Overall, both medication types were equally effective at relieving the psychotic symptoms of the disease state but neither tended to convey a significant advantage in terms of providing a truly stable baseline that allowed patients to function normally. Unfortunately, this study suggests that, despite advances in pharmacotherapy for the treatment of schizophrenia, little advances have been made in providing effective treatment for affected individuals.

Further, it suggests a re-evaluation of the available literature on the disorder and a paradigm shift in terms of how novel therapies may be identified, classified and evaluated.

Schizophrenia Research

Many brain structures have been found to be altered in schizophrenia, but the dorsolateral prefrontal cortex (dlPFC; see Fig. 1.1 Top) and the hippocampus within the medial temporal region (Fig. 1.1 Bottom) have received the most attention. The primary neuropathology in schizophrenia has long been linked to a dysfunction of the dlPFC, the area of the brain that is responsible for executive function and working memory [5]. In considering the clinical profile of schizophrenia it should come at no surprise that this area seems to be grossly underdeveloped in the disease. Previous studies have found alterations in the overall architecture of the dlPFC, dopaminergic and GABAergic innervation. The second site of gross pathology associated within the disease state is the medial temporal lobe, more specifically the hippocampus (see Fig. 1B), an area of the brain that mediates episodic memory processes and stress-related responses. An overview of neuropathology studies of both regions in schizophrenia is presented in the following sections.

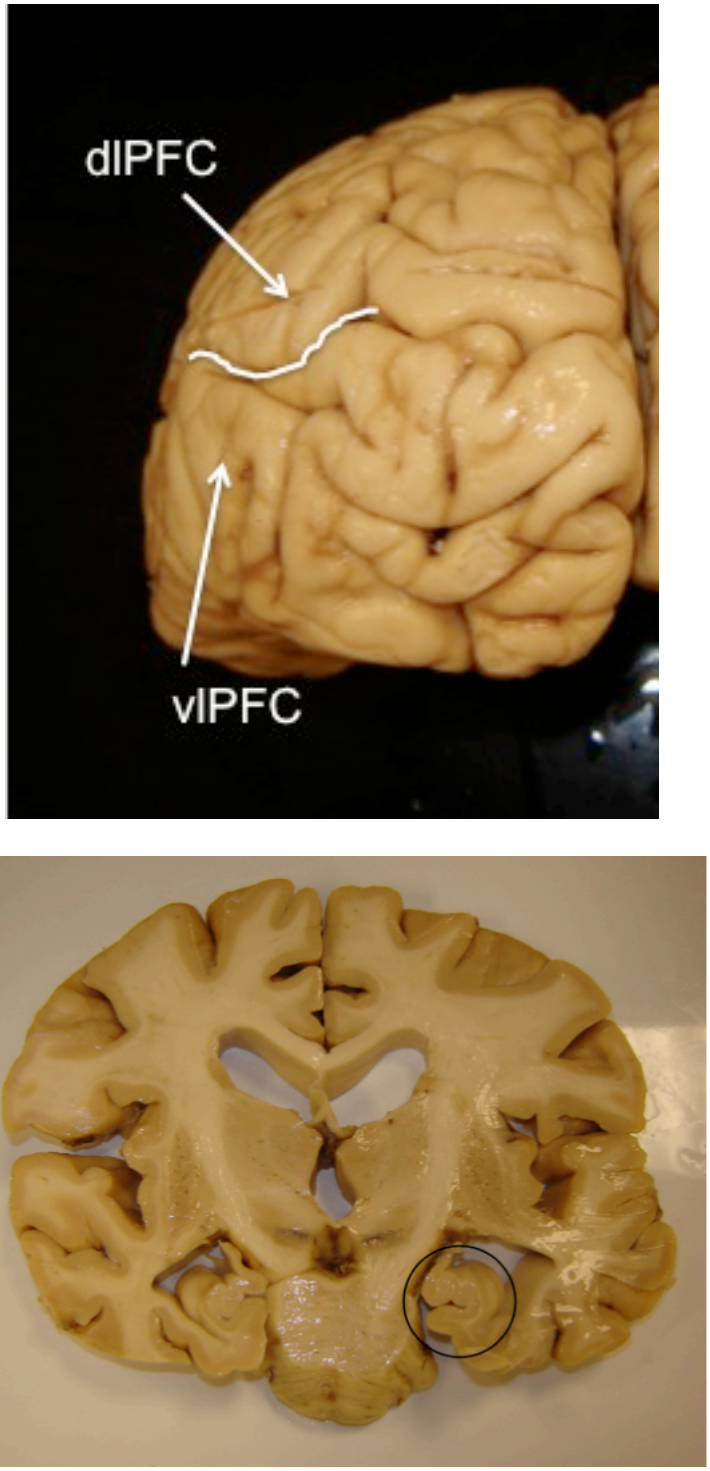

Figure 1.1: Human brain. External frontal of right hemisphere of the human brain (top) and coronal (bottom). The top image shows the dlPFC and vlPFC, separated by the inferior frontal sulcus (white line) as defined by Petrides [5]. The bottom image highlights the human hippocampus (circle). Images provided by Dr. Yoland Smith, Yerkes National Primate Research Center.

Neuropathological processes in the dlPFC

Post-mortem studies: Post mortem studies of schizophrenic patients have shown increases in the density of cells in the dlPFC, but not increases in overall cell numbers [16]. This increased packing density was actually the result of an abnormally thin cortical mantle, a condition that could potentially reduce overall neurotransmission and limit plasticity. Subsequent research has demonstrated that spine density within cortical layer III is reduced within the dlPFC of schizophrenia patients [17,18], a finding consistent with the idea that neurotransmission to the dlPFC is altered in the disorder. Interestingly, the studies showed that the reduction of spine density is predominantly observed in deep layer III, the predominant layer that receives thalamic inputs critical for conveying information from other association areas [19]. A recent study found a global reduction of dlPFC synaptophysin, a docking protein located at the pre-synaptic terminal known to be important in vesicular release [20]. A general reduction in the levels of synaptophysin with in a cortical area is consistent with a reduction in overall activity of that area, which could also be related to the decreased spine density and thinned cortical mantle.

Neuroimaging studies: A large body of neuroimaging data in schizophrenia patients, employing methods such as: structural Magnetic Resonance Spectroscopy (MRS) and Diffusion Tensor Imaging (DTI), structural Magnetic Resonance Imaging (MRI), functional Magnetic Resonance Imaging (fMRI) and Positron Emission Tomography (PET) have been used to examine the frontal cortex in the disease state. The results of these studies will be briefly described in the following. Magnetic Resonance Spectroscopy (MRS) studies have found reduced levels of n-acetyl-aspartate (a known marker of neuronal integrity) within the dlPFC in schizophrenia [21-23]. Recent advances in

neuroimaging such as Diffusion Tensor Imaging (DTI) have allowed investigators to examine the functional integrity of white matter tracts *in vivo.* Numerous DTI studies have found alterations and reduced integrity of frontal lobe white matter in schizophrenia [24-31], supporting the findings of MRS studies in schizophrenia. In parallel, functional imaging (PET and fMRI) have shown that schizophrenia patients fail to activate their dlPFC sufficiently during working memory tasks, further supporting the dlPFC as a site of primary dysfunction in schizophrenia [32-34]. Despite seeing changes in prefrontal integrity there is no real evidence to support volume reductions of the prefrontal cortex, for a review see [35]. The results of the imaging data provide direct confirmation post-mortem studies of the dlPFC. In sum, these results indicate that the gross architecture of the dlPFC in schizophrenia has been dramatically altered.

Neuropathological processes in the medial temporal lobe

Post-mortem studies: The medial temporal lobe, specifically the hippocampus and related structures, also show consistent pathology in schizophrenia. Additionally, schizophrenia patients show abnormal cell orientation within the granule cell layer of the dentate gyrus [36]. Interestingly it was found that the degree of disorganization within the dentate gyrus correlated with symptom severity, such that greater dentate cell disorganization equates with greater symptom severity. Subsequent studies of the hippocampus found a second level of disorganization within the hippocampus of schizophrenia patients, but in this case within the pyramidal cell layer at both the CA1-2 and CA2-3 junctions [37]. Like for the dlPFC, investigators have also found reduced synaptophysin within the subiculum and dentate gyrus of the hippocampus and the parahippocampal gyrus [38].

Neuroimaging studies: In parallel to studies of the frontal cortex in schizophrenia, researchers have applied the same technology to investigating the nature of hippocampal dysfunction in schizophrenia. Structural MRI studies have consistently found the overall volume of the hippocampus to be reduced in the disease state [35,39-44] and reduced levels of n-acetyl-aspartate within the hippocampus and the medial temporal lobe, as a whole [21,45,46]. DTI studies, as in the case of the dlPFC, have found alterations in white matter tracts leaving the hippocampus [25,27,29-31]. Lastly, while the hippocampus has been shown to co-activate with the dlPFC during working memory, it fails to do so in schizophrenia [47]. In sum, the results suggest that the hippocampus, much like the dlPFC, is profoundly affected in schizophrenia.

To summarize, the cumulative evidence seems to implicate both the dlPFC and hippocampus as primary sites of pathology in the schizophrenia.

Behavioral and Cognitive deficits in schizophrenia

A large body of literature has been directed at characterizing behavioral and cognitive impairments related to the schizophrenia. The investigation of behavioral metrics of schizophrenia is particularly important as they can provide a measure of pharmacotherapeutic efficacy that is independent of self-report. For the purpose of the studies presented in this thesis, we will focus on sensory-motor gating and working memory deficits.

Sensory-motor gating: Sensory-motor gating can simply be defined as the ability to filter and process information in a short temporal window in order to modulate responses to external stimuli. Empirically, sensory-motor gating is typically measured by the pre-

pulse inhibition paradigm (PPI), which utilizes the natural tendency to startle to acoustic stimuli. Initially, the individuals startle response is measured and then it is calculated in the presence or absence of a preceding stimulus of a lesser magnitude in close temporal proximity. Inherently, mammals reduce their startle response to an acoustic noise in the presence of a pre-pulse, proportionate to the intensity and temporal proximity of the pre-pulse. Deficits in pre-pulse inhibition are thought to reflect aberrant neural circuitry involving the connections between the brainstem and the cortex, although the exact mechanisms are still debated [48].

The initial report of sensory-motor gating deficits in schizophrenia spurred great interest as a potential mechanism to measure the efficacy of therapeutics in schizophrenia [49]. Subsequent studies have shown PPI deficits to be one of the most consistent behavioral impairments associated with the disease state [50-56]. It should be mentioned, however, that there has been some discrepancy as to whether PPI deficits correlate with the expression of the general symptoms associated with schizophrenia [53,57,58]. Thus, a recent review concluded that PPI is not an adequate diagnostic of schizophrenia and suggested that an alternative behavioral measure is needed to evaluate future advances in treatment [59].

Working memory: A more recent line of neuropsychological studies has focused on working memory deficits associated with schizophrenia. The initial paper by Park and Holzman [60] documented a clear working memory impairment in delayed response tasks restricted to functions dependent upon the dlPFC. Subsequent studies have demonstrated that this deficit is extremely robust and reproducible in vastly different patient populations and can be evidenced by a variety of established dlPFC-dependent

working memory tasks, including n-back, spatial working memory span and self-ordered tasks [32,61,62]. A recent meta-analysis of over 150 studies in schizophrenia found working memory deficits to be a core feature of the disease and are modality and delay independent, but can be exaggerated by increasing the memory load [63]. Recently, neuro-imaging studies were used to characterize the neural origin of the working memory impairment and reported that it is associated with a failure to sufficiently activate the dlPFC [33,64-66], thus strengthening the connection between dlPFC pathology and working memory deficits. Interestingly, newer imaging methods also enabled investigators to study the functional significance of hippocampal pathology in schizophrenia. These fMRI studies showed that in normal individuals performing working memory tasks, activity of the hippocampus synchronizes with that of the dlPFC, but this synchronization failed in schizophrenic patients. The failure of the hippocampus and dlPFC to synchronize directly correlated with subjects' performance on working memory tasks [47,67], establishing a functional link between the hippocampus, the dlPFC and working memory impairments. Thus, working memory may provide a potential metric that could be used to study disease state progression, response to therapy and potentially used in animal models to screen novel medications.

In sum, the volume of research on schizophrenia has been extensive. Early research into the disease was focused on detailing the primary and secondary neuropathology, whereas recent research has focused on more discrete behavioral and cognitive impairments and neuro-imaging. The culmination of this large body of research suggests that early dysfunction of the frontal and medial lobe temporal systems may lead to a predisposition to the disease state, as reflected by the nature of cognitive

impairments seen in schizophrenia. Additionally, recent behavioral work in schizophrenia has illustrated the flaws in using the PPI paradigm to examine treatment efficacy in animal models [59]. Thus, despite sensory-motor gating deficits being one of the most consistent findings in schizophrenia, it may not provide the best behavioral metric to test therapeutic agents. By contrast, studies of working memory can be used as a diagnostic tool for human patients and as a metric in animal models to evaluate potential novel treatments.

Schizophrenia Animal Models-Rodent

As with any psychiatric disorder, researchers often turn to animal models with the goal to better understand the disorder and also provide a tool to screen potential novel therapeutic agents. Empirical data on schizophrenia patients, namely the developmental nature of the disease and the pathology within the dlPFC and hippocampus, were integrated to create an animal model that comprises not only the theoretical end product of the disease state but also potential etiology [68]. The theoretical framework of the model proposed that some events (genetic, environmental or more likely a combination of the two) occurring prenatally, alter the hippocampus, which in turn triggers a maldevelopent of the prefrontal cortex. Lodge and Grace [69] proposed a mechanistic model (Figure 1.2) to explain how early damage to the hippocampus might impact frontal cortical function. Essentially, the theoretical model suggests that early damage to the hippocampus will preclude the disinhibition of the ventral tegmental area dopamine release to the dlPFC, via the nucleus accumbens and ventral pallidum. In this way, the dopamine transmission

to the prefrontal cortex is greatly reduced and results in maldevelopment of the prefrontal cortex.

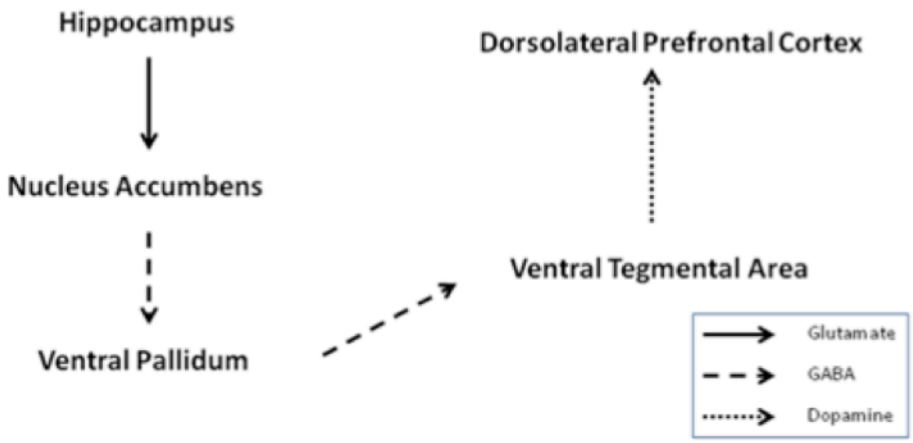

Figure 1.2: Proposed dlPFC-hippocampus connectivity model. The schematic demonstrates how early damage to the hippocampus could lead to decreased dopamine transmission to the prefrontal cortex, resulting in a state similar to schizophrenia as in the disease model. Adapted from Lodge and Grace [69].

The following studies were conducted in the rat, which is an easily accessible animal model with known behavioral and neurobiological correlates to humans. In this case, the construct of the model involved creating a neonatal lesion of the ventral hippocampus (Neo-H) and subsequently studying the animal using a variety of behavioral, physiological and chemical assays to determine if they could recapitulate the developmental and neurobiological aspects of the disorder. As recently reviewed by Tseng and colleagues [70], the neonatal ventral hippocampal lesion model is associated with a number of behavioral, molecular and physiological changes reminiscent of a variety of aspects of schizophrenia that emerge at a particular time in development, i.e., around young adulthood/adolescence (Figure 1.3).

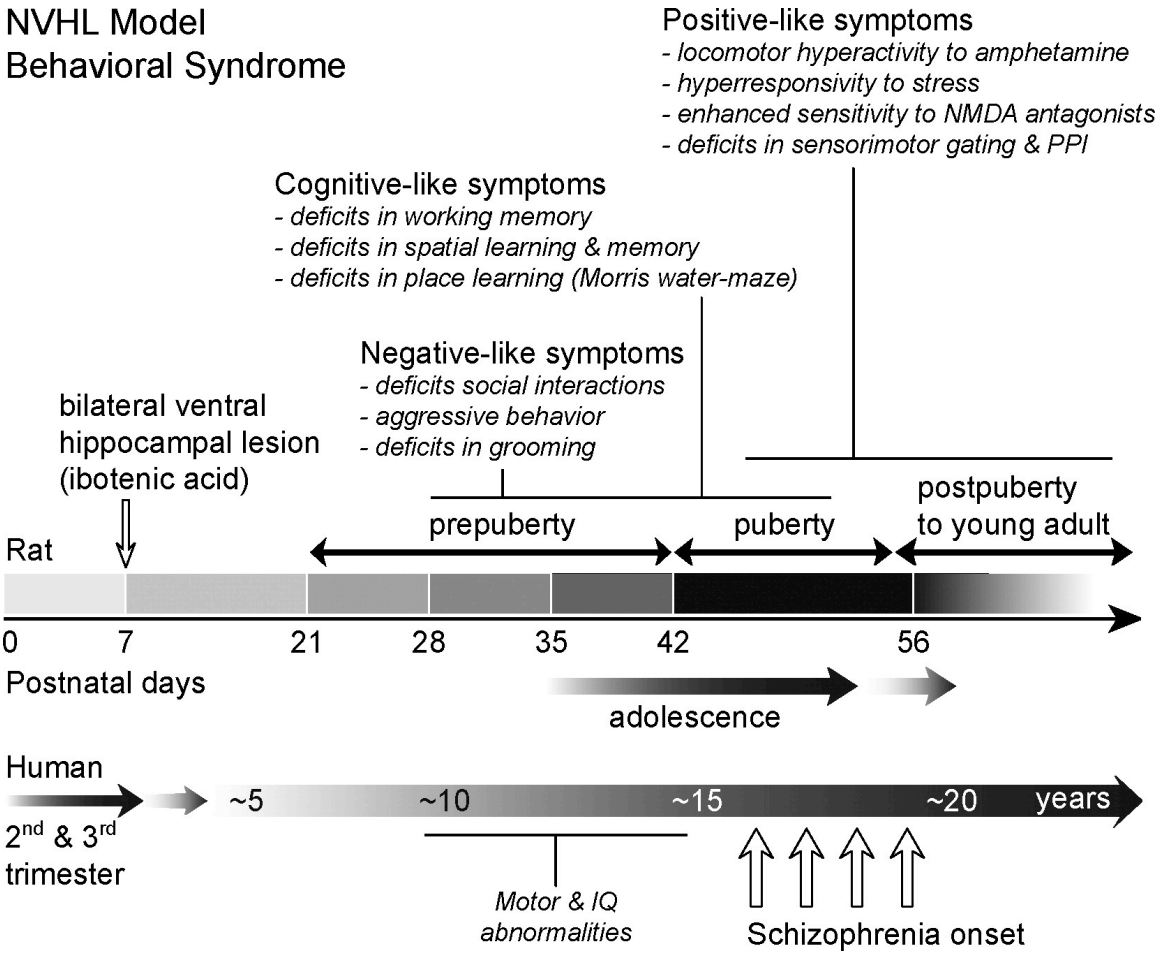

Figure 1.3: Overview of rodent schizophrenia model. Early lesions of the hippocampus not only recapitulate a number of the symptoms of schizophrenia, but also seems to mirror the time-course of these same effects in disease state. The above figure illustrates the temporal progression of the rodent model in relation to schizophrenia. Reprinted from Tseng and colleagues [70], with permission.

Typically, the first step in the validation of any animal model is to examine the behavioral profile of the animal for correlates to the disease state. As impairments in sensory-motor gating have been consistently found in schizophrenia, it was used as a metric to evaluate its presence in the disease model. In both human and animal subjects sensory-motor gating is assessed by pre-pulse inhibition. Briefly, pre-pulse inhibition (PPI), is the natural tendency of mammals to reduce the magnitude of startle to a stimulus when the stimulus is preceded, in close temporal proximity, by a stimulus of lesser magnitude (see description in Schizophrenia section for greater detail). Numerous studies of this model have consistently shown that early lesions of the ventral hippocampus impair sensory-motor gating, as evidenced by deficits in PPI [71-76]. The second major behavioral correlate examined in animal models is the presence of spontaneous hyper-locomotion, a measure often equated to the motor stereotypies exhibited by schizophrenia patients. Once again, numerous studies have demonstrated that Neo-H lesions produce a behavioral repertoire comparable to the disease states as hyper-locomotion has been ubiquitously found in this model [76-78]. Lastly, working memory deficits in the Neo-H rats have been documented on several measures of working memory, such as the win-shift paradigm [79], continuous and discrete alternation [80] and the radial arm maze [81].

A number of investigators have also characterized the neuro-chemical and electrophysiological changes associated with early damage to the hippocampus. In line with the dopamine hypothesis of schizophrenia [69], gross alterations in various levels of the dopamine system have been found in this model including: decreased dopamine transporter mRNA in both the substantia nigra and ventral tegmental area [82], abnormal

dopamine responsivity in the nucleus accumbens [83] and dopamine insensitivity within the medial prefrontal cortex [84]. In contrast, examinations of GABAergic alterations in this model have been far less consistent. One recent study showed that glutamate decarboxylase 67 (GAD-67), the rate limiting enzyme of GABA synthesis, is globally reduced in the Neo-H schizophrenia model [85] and a second indicated alterations in one subunit of the GABA-A that may impair its functionality [86]. In contrast, two other studies found no alterations in the overall expression of GAD67 globally [82] or specifically in the medial prefrontal cortex [84]. Despite the disparity of findings in the neuro-chemical data, recent electrophysiological studies have consistently demonstrated functional deficits within the medial prefrontal cortex. Following neonatal hippocampal lesions, mPFC pyramidal neurons display patterns of over-excitability when the ventral tegmental area is stimulated [83,87]. The electrophysiology data seem to support the idea that early lesions of the hippocampus are sufficient to alter the dopaminergic tone of the prefrontal cortex, resulting in a sensitization to dopamine and altered neuronal function. Lastly, a magnetic resonance spectroscopy study of Neo-H rats showed decreased levels of NAA within the mPFC[88], further suggesting that the early hippocampal lesions have compromised the integrity of the mPFC and providing further parallels between the disease state and the model.

In sum, the early hippocampal lesion rat model has been proposed as an heuristic neurodevelopmental model of schizophrenia and has shown a great deal of promise. It is clear that the model is able to recapitulate many of the symptoms of the disorder including behavioral, neuro-chemical, electrophysiological and even ultra-structural. Additional support for this model has come from a follow-up study demonstrating that a

complete ventral hippocampal lesion is not necessary to create the array of symptoms, but that a temporary inactivation of the structure in early life is sufficient to create the same phenotype [89]. As schizophrenia patients do not have gross lesions of the hippocampus, but rather show marginal reductions in overall volume, this model would be much more akin to the disease state. However, as with any animal model there are certainly limitations and concerns that will be described in the following section.

Limitations of the rodent model

It certainly goes without saying that any model has physical and practical limits that are directly related to the construct from which they have been made. In this case there are two predominant issues that should be considered when assessing the future utility of the rodent schizophrenia model as follows: (1) Neuro-anatomical disparities between rodents and humans, specifically within the prefrontal cortex and (2) The behavioral assays which can be employed in the current model.

As discussed previously, the primary pathology in schizophrenia is within the prefrontal cortex, specifically areas 46 and 9, comprising the middle frontal gyrus and the area dorsal to the middle frontal gyrus (see Fig 1.1 Top). In trying to identify a comparable area in the rodent brain, many investigators have often pointed to the medial prefrontal cortex. However, this assertion has been highly disputed in the literature [90,91]. The main argument is that this area of the prefrontal cortex is the most developed area of the brain in the primate and does not exist or at least is poorly developed in the rodent [5,92]. Furthermore, the lateral frontal cortex of the primate can be subdivided into different

regions that differ anatomically and functionally. Such lateral prefrontal subregions do not exist in rodents [93].

The second major issue is the utility of the animal model, in this case the ability of the model to differentiate subtle differences in clinical effects of novel and traditional pharmacotherapies for the treatment of schizophrenia. A recent clinical study of schizophrenia patients suggested that one of the greatest potential screens for the effectiveness of antipsychotic medications is the ability of the compounds to recover working memory function [94]. In this light an animal model that could assay the ability of a pharmacotherapy to recover working memory function would be particularly useful. Unfortunately, one of the few studies using the rodent model to examine the effects of an antipsychotic on working memory found that the antipsychotic clozapine actually impaired the performance of the animal [81]. Additionally, it is not possible to assay working memory in rodents in the same way as a human, as working memory tasks in rodents essentially all measure maintenance working memory. This point is captured by examining the adaptation of serial order tasks to rodent studies [95], as rodents are unable to distinguish neighboring pairs of objects, but seem rather to utilize a different strategy all together.

In conclusion, the literature suggests that, although the rodent model has contributed greatly to our knowledge of schizophrenia, there is a need to improve the model, particularly by increasing research on the working memory deficits and their neurobiological origin given that working memory seems to be a reliable predictor of antipsychotic efficacy and provides a useful metric to assess new therapeutic agents.

Rhesus Monkey as Model of Human Cognition

Rhesus monkeys (Macaca mulatta) have long been utilized as an animal model of human cognition in general and working memory more specifically. Early investigators such as Jacobsen, Pribram and Mishkin successfully employed the rhesus monkey and discovered that it is a highly adaptable and intelligent creature suited to studies of higher order cognition [96,97]. Later studies focused on the degree of homology of the prefrontal cortex as anatomists such as Goldman-Rakic and Petrides attempted to link cognitive processes to specific anatomical loci [98-103]. Additionally, the protracted development of the rhesus monkey affords investigators the ability to study the maturation of these cognitive processes in a model that had a great deal of similarity to the human [104]. Each of these issues will be discussed in the remainder of this introduction in an effort to fully elucidate the utility of the rhesus monkey as model organism for studying cognitive deficits in schizophrenia.

Working Memory

Working memory has been defined, quite simply, as working with memory but theorists such as Baddeley [105]. Obviously, this simplistic definition does not speak to the broad scope of working memory and the sub-types of working memory processes that can be parsed out, both behaviorally and anatomically. A more complete definition has been offered: "The term working memory refers to a brain system that provides temporary storage and manipulation of the information necessary for such cognitive tasks as language comprehension, learning and reasoning…" [105]. This definition encompasses not only the components of working memory but also the other main function of the

dlPFC, the so-called central executor. As the purpose of this document is to outline a potential metric to assay dlPFC function in the non-human primate, the remainder of this section will focus on categorizing the subcomponents of working memory, both cognitively and anatomically. The discussion will begin by outlining classical and contemporary working memory tasks in rhesus monkeys and conclude with a thorough discussion of the anatomy of the dlPFC and potential relationship with the hippocampus.

In the non-human primate literature working memory tasks can be divided into two distinct groups: Classical and Contemporary. The classical working memory tasks generally fall under the title of delayed response tasks and have been based on the idea that the dlPFC exclusively processes spatial information. In contrast, contemporary working memory utilizes the monitoring of temporal order and is based on the assumption that the dlPFC functions to monitor stimuli to guide future actions, irrespective of modality.

Working memory has a long history within the animal literature, as there have certainly been many iterations of working memory tasks that have shown dependence on the lateral prefrontal cortex. Perhaps the earliest establishment of a structure-function relationship, with respect to the lateral prefrontal cortex, was a study conducted by Jacobsen [106]. This early study established a functional link between the frontal lobes (via complete frontal lobectomy) and working memory (delayed response) in two non-human primate species. The establishment of a link between the frontal lobes and working memory was later replicated in the rhesus monkey [107]. Following this early work, several studies have established that the impairment on the delayed response task was more specifically attributable to damaging the lateral frontal cortex [97,108-110]. However, it was

not until the studies of Mishkin [111] that the locus of higher order working memory processes was determined to be the dorsolateral prefrontal cortex. In this study, small lesions of the principal sulcus (part of the homolog of the human dlPFC [5,92]) were made in the rhesus monkey and resulted in a severe impairment on the spatial delayed alternation task. The structure function relationship established in this study was later confirmed [112] and initiated a line of research into the neural substrates of working memory that has continued to this day.

To further characterize the nature of neuronal activity during the delayed response tasks investigators have used electrophysiology, cellular imaging and pharmacologic manipulations of the dlPFC in the monkey. Early electrophysiology studies in monkeys were aimed at recording the neuronal activity of cells within the principal sulcus [113,114], which showed that pyramidal neurons in the principal sulcus display bursting activity during the delay period of the delayed response task. This delay related activity has been since referred to as the neural substrate of working memory. In general, it is thought that the bursting of these neurons reflects the individuals' active maintenance of items within working memory. The relationship between dlPFC activity and working memory was further established by Friedman and Goldman-Rakic, who used the 2-deoxyglucose (2-DG) technique to examine relative metabolic activity of cells within and outside of the dlPFC during performance on working memory tasks [115]. Essentially, 2-DG is a radioactive analog of glucose that is taken up by cells in proportion to their relative activity. The glucose analog then becomes trapped in the cytosol and can be detected in post-mortem tissue using autoradiography. It was determined that monkeys performing delayed response tasks show a preferential increase in 2-DG labeling within the dlPFC

but not during control memory tasks. This result provided independent confirmation of the previous physiology data and further supported dlPFC burst firing as the neural substrate of working memory.

It is clear that a lot of what is known about the working memory system and its' dependence upon the dlPFC has been gained by employing the delayed response tasks. However, it is equally important to note certain considerations when employing these tasks that make them less appealing for use in the current research. The first major concern is the number of alternative solutions to any particular trial of either the spatial delayed alternation (SDA) or the delayed response (DR) tasks. While the animal can certainly "hold on-line" the object that contains the food reward in memory buffer, the subject can also use a positional or motoric strategy to solve this problem. As an example monkeys have been observed to either shift their body position to the side of the testing apparatus that contains the rewarded object. Alternatively the animal may place a hand on the side of the cage that will contain the reward on the subsequent trial. These non-cognitive strategies provide opportunities for the subject to solve the task without requiring any form of working memory. It is certainly possible that, due to the way in which science was conducted historically, i.e. one animal group for one study, animals were less skilled at finding alternative solutions to the problem. However, in current research environment, any given animal may run dozens of behavioral tasks, the likelihood of animals identifying alternative strategies is greatly increased. As such, the delayed-response tasks, may be of less utility in current working memory research. Inherently, as the nature of science changes the need for better metrics arise. Thus, the

need to develop working memory tasks that provide fewer alternative solutions that are modality independent and get at the nature of the function of the dlPFC became critical.

In contrast to the first generation of working memory tasks, SDR and SDA, the second generation of working memory tasks did not utilize spatial memory as a basic component of the task. These tasks, which will be referred to as monitoring tasks, were focused on the idea that the dlPFC is responsible for tracking the order events in a temporally limited window to guide further action. The earliest description of a monitoring task showing its' relation to frontal cortical function was performed in chimpanzees in by Jacobsen nearly 75 years ago [106]. Although the lesions were large, encompassing the entire frontal cortex, this study was successful in demonstrating that the ability to perform an externally ordered sequential task was inherently dependent upon the frontal cortex. However, this line of research was seemingly abandoned until 1965 where monkeys with complete lateral prefrontal lesions were tested on another monitoring task [116]. In this case subjects with lateral PFC lesions were tested on a similar paradigm but required to track their own responses to correctly complete the task, the idea being that it doesn't matter if the task is internally (self) or externally (experimenter) ordered, it is the process of monitoring that is critical. The results of the study demonstrated that, regardless of the nature of the order, the lateral frontal cortex was necessary for monitoring of sequences of stimuli held in working memory. Interestingly, as before this line of work was seemingly abandoned within the monkey literature for almost another 30 years.

The more recent development of monitoring tasks in monkeys came with a series of lesion studies conducted by Petrides [101-103]. In these experiments, performance on an

internally (self) and an externally (experimenter) ordered tasks of animals with lesions of the dlPFC were compared to that of animals with lesions of the periarcuate region (encompassing tissue surrounding and including the arcuate sulcus). In the self-ordered task the subject was allowed to select from three rewarded objects and was required to monitor their selection in order to select an object they had not previously selected, on subsequent trials. The experimenter ordered task was designed as a serial order task in which the subject was presented with a series of objects and then presented with a recency discrimination between two objects of the series. To complete the task correctly, the subject had to select the object earlier in the series, regardless of which two objects in the series were presented. In both tasks, the data demonstrated that subjects with lesions of the dlPFC were profoundly impaired, whereas those with periarcuate lesions performed normally. Additionally, despite their working memory impairment, animals with dlPFC lesions performed normally on tests of visual recognition memory, thus confirming that the impairment on the monitoring tasks was not due to disturbances of visual, motor or reward systems [101]. In contrast to the limited earlier studies, these experiments utilized focal lesions of the dlPFC and conclusively demonstrated that it is essential for the monitoring of stimuli in working memory. In contrast, another study claims to have conflicting data concerning the attribution of a structure-function relationship between the dlPFC and the monitoring tasks [4]. However, the study did not use full lesions of the dlPFC that encompasses both Area 9 and the superior bank of the principal sulcus (Area 46) so no such can conclusion can be drawn from this study (Figure 1.4). Further, a recent electrophysiology study of the self-ordered task indicated delay-related activity in neurons of the superior dlPFC region (Area 9) and the superior

bank of the principal sulcus (Area 46), comparable to that seen in previous studies using delayed response tasks [117]. In sum, these studies support the idea that the dlPFC (including area 9 and 46) is a critical mediator of monitoring working memory processes and demonstrate that monitoring tasks are useful tools to assess the functional integrity of the dlPFC.

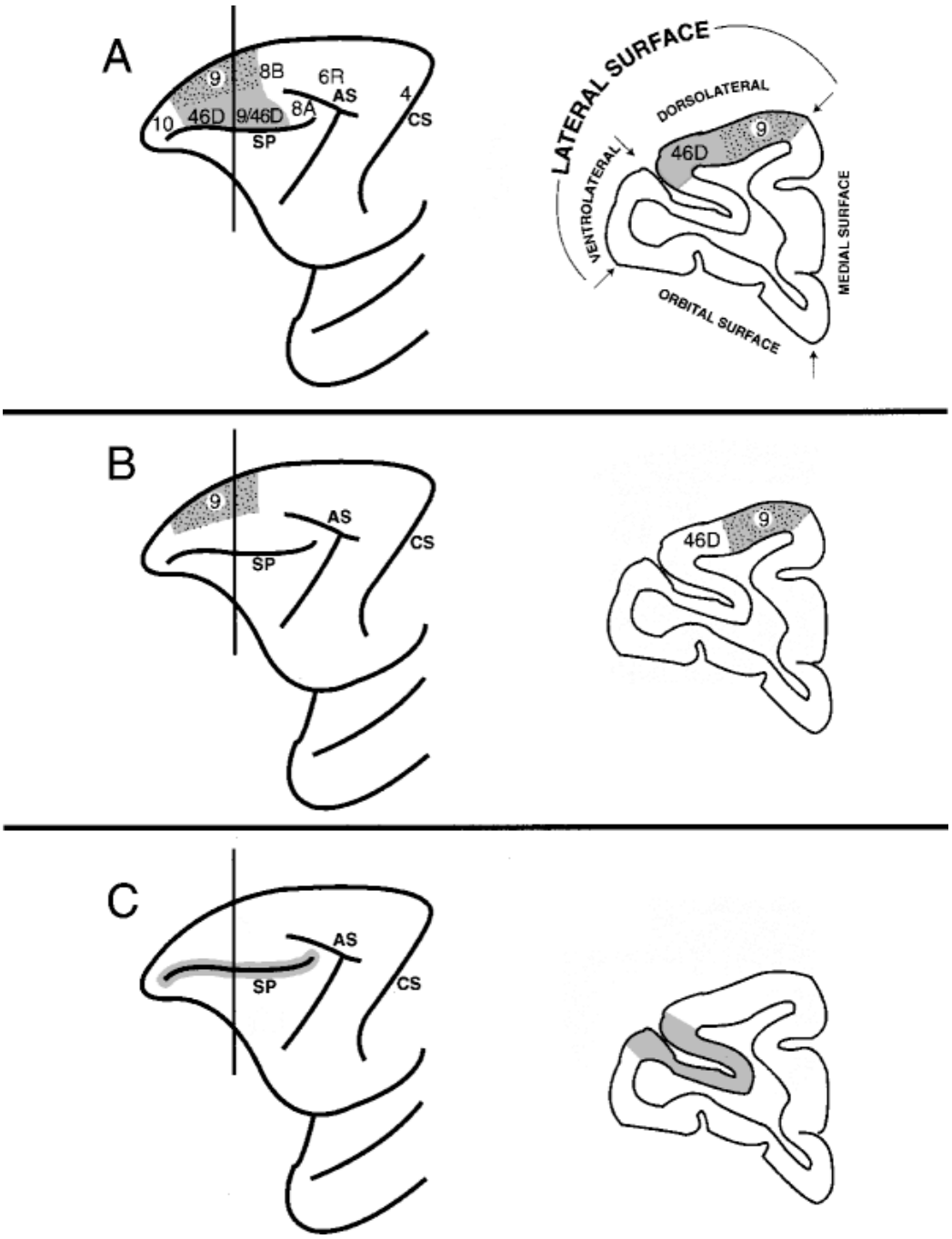

Figure 1.4: Comparison of dlPFC lesions. A. Typical mid-dlPFC lesion made by Petrides, which encompasses both the dorsal segment (Area 9) and the principal sulcus (Areas 46 and 9/46). **B.** A superior dlPFC lesion containing damage to only area 9. This was the lesion used to make the comparison to Petrides findings [102,103] by Levy [4] and as shown is not comparable to the mid-dlPFC lesion. **C.** Typical principal sulcus lesion, which includes only area 46. Reprinted from Petrides [92] with permission.

Anatomy and Connectivity of dlPFC and hippocampus

Now that the processes and types of working memory have been characterized it seems only logical to discuss the neural substrates that support this function. In this case the primary locus of working memory, confirmed through years of both human and nonhuman primate neuropsychology, is the dorsolateral prefrontal cortex [5]. In addition to the dlPFC the gross anatomy and functional connectivity of the hippocampus will also be reviewed. The goal of this discussion is to put into perspective the potential mechanisms whereby the hippocampus can act as a functional regulator of the dlPFC function, and by inference, working memory.

The dorsolateral prefrontal cortex:

The dorsolateral prefrontal cortex, more specifically the mid-dorsolateral prefrontal cortex, is a functional unit of the brain located, as its' name would suggest, in the dorsal and lateral portion of the prefrontal cortex of the primate brain. The original view of dlPFC function operated on the hypothesis of domain specific function, in this case spatial working memory [100]. In essence, the domain specific model seems to have arisen from examining its anatomical connectivity, specifically the projections to the parahippocampal gyrus [118] and series of studies in non-human primates highlighting deficits in spatial working memory following lesions of the principal sulcus [100]. In contrast, the process-specific of the dlPFC has been based upon comparative cytoarchitechtonic, electrophysiological and lesion studies in both human and non-human primates [5,119]. Additional support for the process model comes from the human neuroimaging literature showing activation of the dlPFC during verbal and object working memory tasks [120]. After consideration of all available evidence the functional

model versus the domain specific model seems to be more strongly supported by all available data and as such this document will utilize the process-specific definition of the prefrontal cortex [121]. However, this is not to say that there is not merit to the role in which the dlPFC plays in spatial working memory, but rather that it is not exclusively limited to spatial processing.

In the non-human primate the dlPFC consists of the middle third of the principal sulcus (Broadmann's areas 46, 9/46 dorsal and 9/46 ventral) and the area directly dorsal, up to the midline (Broadmann's area 9). The following section will discuss the functional connectivity of the dlPFC both afferent and efferent, emphasizing the areas of overlap and differences between areas 9 (dorsal) and 46, 9/46 (principal sulcus).

The afferent connectivity of the dlPFC is extremely diffuse, although it seems that the major projections are predominantly received from other prefrontal areas. The dorsal component receives projections from frontal polar cortex (BA 10), the orbital frontal cortex (BA 11), the principal sulcus (BA 46), the ventrolateral prefrontal cortex (BA 47/12) and the ventromedial prefrontal cortex (BA 14) [121]. Outside of the prefrontal cortex, additional projections to the dorsal segment of the dlPFC are received from both the anterior and posterior cingulate cortex and the superior temporal gyrus [121]. The principal sulcus shares a similar projection pattern as compared to the dorsal segment (BA 9), including a reciprocal projection from BA 9, except that it does not receive an afferent from the ventromedial prefrontal cortex. Lastly, the dlPFC receives significant afferent projections from the lateral segment of the mediodorsal thalamic nucleus [122,123].

Efferent projections of the dlPFC are also even more diverse than the afferent projections as the dlPFC seems to project to a wider range of structures than those from

which it receives projections. However, as a higher order modulator, it makes more sense that the dlPFC is able to exert top-down function regulation, i.e. directly modulating the functions of other cortical areas rather than being modulated by them. The dorsal component of the dlPFC projects to: the thalamus (mediodorsal nucleus), frontopolar cortex, ventromedial PFC, the anterior and posterior cingulate cortex, retrosplenial cortex and the pre-subiculum [124]. In addition, it also projects widely to the posterior parietal cortex and the parahippocampal gyrus [125]. Efferent projections originating from the principal sulcus share a lot of targets with the dorsal segment including: anterior and posterior cingulate, pre-subiculum, reciprocal projection with the dorsal segment, mediodorsal thalamus and a projection to the parahippocampal gyrus [124,126]. However, projections from the principal sulcus also terminate diffusely in the basal ganglia and send a distinct projection to the fundus of the rhinal sulcus [118].

In sum, the anatomical studies of the dlPFC highlights its widespread connectivity that presumably enables it to exert functional influences on cognition as a whole. The functional model of Petrides is supported by the empirical data detailing the significant overlap in connectivity of the two sub-regions of the dlPFC [121]. Further, the differences in connectivity with the dorsal segment receiving more subcortical afferent projections and the principal sulcus sending more subcortical efferent projections suggests that there may exist a relative segregation of information flow. It is possible that the dorsal segment acts more as a receiver and the principal sulcus acting more as a transmitter to coordinate the functions of subcortical structures. This segregation may not hold when it comes to other frontal structures as both areas are widely reciprocally connected to the rest of the frontal cortex. Lastly, the two projections originating from the dlPFC and

terminating in the parahippocampal gyrus and the rhinal sulcus provide a mechanism whereby the dlPFC can modulate the function of the hippocampus. However, it seems that there is no afferent projection from the medial temporal lobe to the dlPFC that could allow for a loop of information passage through the two regions. As such, a thorough examination of hippocampal projections may provide an answer to this question.

As discussed earlier in this document, there seems to be a preponderance of evidence suggesting that the hippocampus plays a critical role in working memory function. The evidence of hippocampal involvement in working memory is vast, including but not limited to human neuro-imaging literature, studies of schizophrenia patients and studies of lesions in rodent animal species. Thus, it is imperative to discuss the anatomy of the hippocampus in line with that of the dlPFC and examine points of connectivity that might allow for the hippocampus to be a dynamic modulator of the dlPFC and by inference, working memory.

The hippocampus:

The afferent projections to the hippocampus originate from practically all areas of the brain. This diversity of hippocampal connectivity is illustrated in Figure 1.5. It should be noted that, although the majority of inputs into the hippocampus is filtered through the entorhinal cortex, there are in fact several direct projections to the CA1 field of the hippocampus [127]. Also illustrated in the figure is the segregation of inputs to the entorhinal cortex from the perirhinal (35/36) and parahippocampal (TH/TF) cortices. For the sake of clarity afferents will be discussed in the following order: Direct to CA1,

Indirect to subiculum via the perirhinal (35/36) and indirect to the subiculum via parahippocampal (TH/TF) cortices.

The direct projections to the CA1 field of the hippocampus originate from the perirhinal and parahippocampal cortices, the basolateral amygdala and the superior temporal gyrus [128-130]. In addition, the hippocampus receives monoamine and cholinergic inputs from the ventral tegmental area, raphae nuclei, the locus coereleus and the basal nucleus of meynert, respectively [129]. Lastly, CA1 also receives direct projections from the orbital frontal cortex (Area 13), retrosplenial cortex, septal nucleus and the thalamus (anterior and midline nuclei).

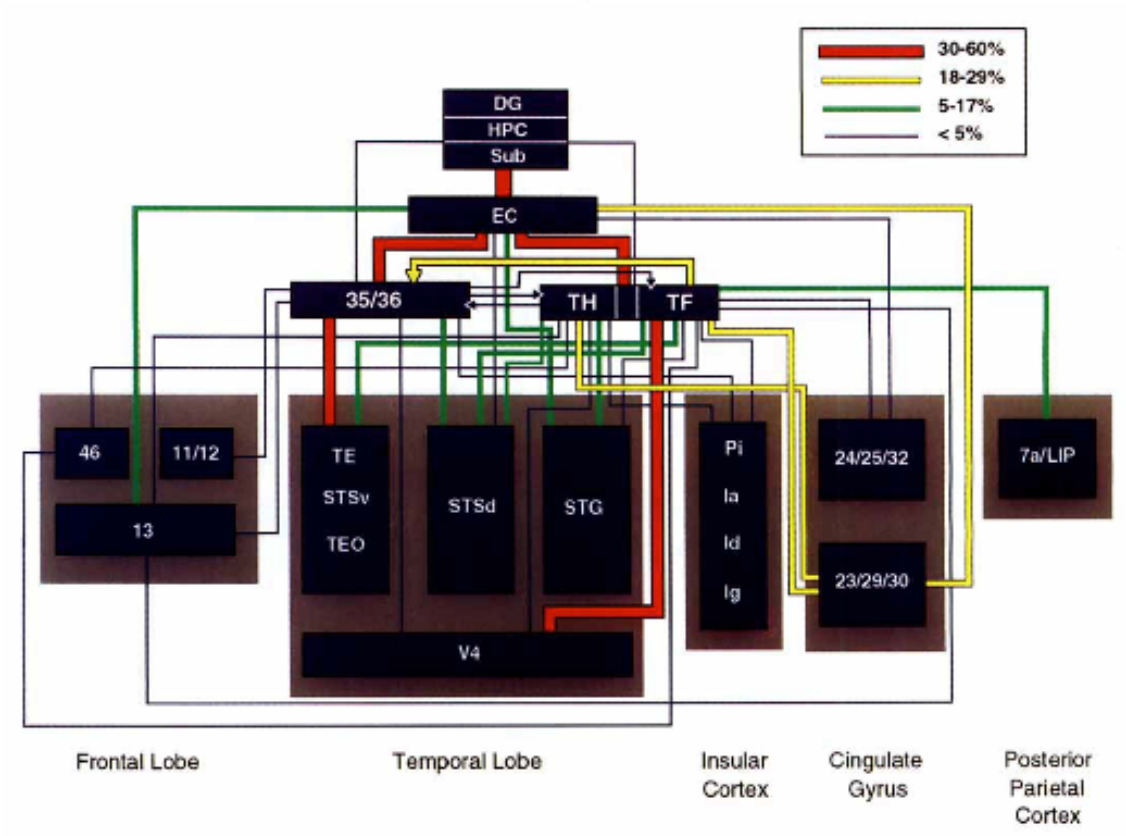

Figure 1.5: Schematic of indirect afferents to the hippocampus. The illustration diagrams the segregation of inputs into the hippocampus from the perirhinal cortex (35/36) and the parahippocampal gyrus (TH/TF) via the entorhinal cortex (EC). The diagram shows the diversity of inputs that travel to the hippocampus in a segregated manner through the temporal cortices and eventually terminate in the subiculum. It should be noted that this diagram does not detail afferent projections that terminate directly into the hippocampus, with the exception of those coming from 35/36 and TH/TF. The legend details the strength of input as a function of the number of cells found labeled with the anterograde and retrograde tracers. This figure has been reprinted from Suzuki and Amaral [127], with permission.

As stated previously, indirect afferents also enter the hippocampus through the subiculum. In general, these afferents originate in the perirhinal or parahippocampal cortices and are routed through the entorhinal cortex prior to terminating in the subiculum [127]. Afferents from the perirhinal cortex originate from the temporal lobe (Area TE), the frontal cortex (Areas 11, 12, 13 and slight projections from 45 and the caudal principal sulcus) and the retrosplenial cortex [127]. In a similar manner, afferents originating the parahippocampal gyrus originate in the temporal lobe (Area TE and the superior temporal gyrus), frontal cortex (Areas 13 and 46), retrosplenial cortex, insular cortex and the visual cortex (Area V4) [127].

The efferent outputs of the hippocampus seem to show a similarly diverse connectivity, in terms of structures with whom it is connected. The presubiculum and CA1 fields both project to the entorhinal, perirhinal and parahippocampal cortices [131,132]. The hippocampus also projects to the prefrontal cortex (Areas 11, 13 and 14) and thalamus (anterior and dorsal) [132,133]. However, the only reciprocal connectivity with the monoaminergic system seems to be a projection to the ventral tegmental area (eminating from presubiculum and CA1) [134].

The examination of hippocampal anatomy has illustrated that it is a structure with broad connectivity to the association cortices and other medial temporal structures. As one would expect, its' afferent input from higher order association areas (frontal and parietal) is much broader than it's efferent input to these same structures. The data to date demonstrate no direct anatomical reciprocal connectivity between the hippocampus and the dlPFC, although there seems to be two distinct projections whereby the dlPFC can modulate hippocampal function. However, the connectivity of the hippocampus with

the midbrain dopamine system (ventral tegmental area) suggests that the hippocampus may be well positioned to regulate dopamine concentrations in the dlPFC. As it has long been known that dopamine is a critical modulator of working memory[135-138], the hippocampus could dynamically regulate these cognitive processes, as well as receive feedback information from the dlPFC. However, the role of development in the interaction between the dlPFC and the hippocampus must also be considered.

Development

The earlier portion of this document was focused on detailing a mechanism whereby the hippocampus can functionally regulate the dlPFC, however given the developmental nature of this study it is equally important detail the temporal development (post-natal) of these structures, with respect to one another. Thus, the following section will discuss the post-natal development of the dlPFC and that of the hippocampus using available behavioral and neuro-anatomical data.

The dlPFC has one of the most protracted developmental periods of any brain structure and as a result can be impacted by different factors. Research in normal human subjects has demonstrated a dual-plateau model of working memory development [139-141]. The model postulates that at the youngest age subjects cannot complete the task with any level of competency, during adolescence they achieve a moderate level of performance and at some point during post-adolescence they achieve adult performance levels. Theoretically, this three part behavioral transition corresponds to global neural immaturity, functional maturity of lower order frontal areas and finally the functional maturity of the dlPFC, respectively. This process is supported by the work of Goldman-

Rakic in a series of developmental studies aimed at assaying working memory function following early and late selective lesions of the frontal lobe [104,142,143]. Cumulatively, these studies confirmed earlier work indicating that lesions of the dlPFC, in the adult monkey, were sufficient to impair working memory performance but that early lesions of the dlPFC were insufficient to impair performance in a young animal. In contrast, late lesions of the orbital frontal cortex had no impact on working memory but early lesions of the orbital frontal cortex produced a working memory impairment comparable to adult dlPFC lesions. The conclusion of these studies was that early in life the orbital frontal cortex subserves the functions of the dlPFC, at a moderate performance level. Once the dlPFC becomes functionally mature the orbital frontal cortex no longer has any involvement in working memory, as the dlPFC now supports working memory. This study was replicated by using a temporary inactivation method, cryogenic depression, which confirmed the early dependence of working memory on the orbital frontal cortex, during late childhood to early adolescence, that switches to the dlPFC during the transition to adulthood [144]. Thus, the behavioral data in both the human and non-human primate seem to support the idea that the dlPFC is a late developing structure that gains full functional activity by adulthood.

Interestingly, recent neuro-anatomical evidence about the development of the dlPFC seems to parallel the older behavioral findings, further supporting working memory as a functional mechanism to assay the development of the dlPFC. As seen in Figure 1.6, chandelier neuron density increases from birth, reaching an early plateau around 3 months of age, a maxima at 1.5 years and a drop to adult levels by the 3.5-4 years of age [145]. These relative changes in interneuron density are closely paralleled by

alterations in the density of spines of pyramidal neurons and dopamine varicosities within the dlPFC. Interestingly, CCK neurons do not follow the same pattern and seem to play a less critical role in the development of the dlPFC, at least as described here [145]. Overall, measures of cellular development in the dlPFC greatly overlap the observed functional development and perhaps provide a mechanistic explanation for a long supported idea within the neuropsychology literature.

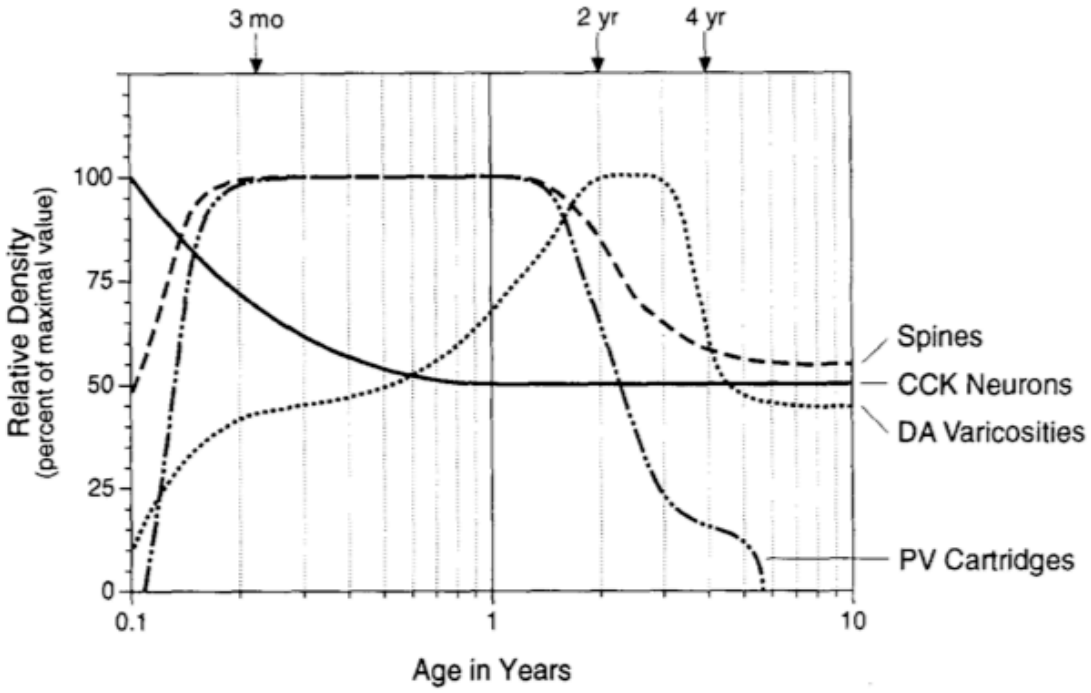

Figure 1.6: Postnatal development of dlPFC. The above graph showing age related changes in spine density, interneuron number (CCK and PV cartridges) and dopamine varicosities[145]. Reprinted from Anderson et al (1995) with permission.

As the hippocampus is an evolutionary older structure than the dlPFC it would likely follow that it matures at an earlier developmental age. Behaviorally, the development of the hippocampus has been studied extensively in primates by using the visual paired comparison paradigm (VPC). VPC, a behavioral measure of incidental recognition memory, takes advantage of the inherent primate preference for novelty. The VPC paradigm is relatively simple in that an object is presented and the subject is allowed to look upon the object for a fixed habituation time. After a delay, the animal is re-presented with the original object and a novel object. To assess novelty preference, the cumulative time the animal spends looking at the novel and habituated objects are calculated. A recent study characterized the development of novelty preference in VPC and found that the novelty preference is present as early as 1.5 months of age but that it strengthens to adult performance levels by six months of age [146]. Interestingly, measurable delay dependent performance decrements are not detectable at six months of age, but are present by 18 months of age. It was argued that the delay dependent effects could represent functional development of the hippocampus. This proposal was confirmed in this same study by demonstrating that selective neonatal lesions of the hippocampus do not impair recognition memory, as assessed by VPC, until 18 months of age. By contrast, a follow-up study showed that neonatal perirhinal lesions are sufficient to impair VPC performance as early as 1.5 months of age, suggesting a dependence of VPC performance on the perirhinal cortex prior to the development of the hippocampus[147]. This finding mirrors studies showing that working memory is dependent upon the orbital frontal cortex prior to the development of the dlPFC [104,142,143]. Additionally, these studies suggest that the hippocampus becomes functionally mature

prior to the dlPFC, although an examination of anatomical evidence would add credence to this argument.

Anatomical studies of hippocampal development seem to point to the same developmental time points as the behavioral literature. A recent neuro-imaging study of hippocampal volume in rhesus macaques shows that hippocampal volume increases over the first two years of life but seems to reach a plateau by 11 months of age [148]. Similarly a study of developing hippocampal neurons found that synaptogenesis increases from birth to five months of age and then is pruned back until approximately 11 months of age [149]. Additionally, it seems that the hippocampal GABAergic system is present in primates at birth [150] but is modified postnatally [151], presumably the result of life experience. In sum, the anatomical evidence, both grossly and at the cellular level, seems to indicate that the hippocampus reaches a level of functional maturity by one year of life, supporting behavioral studies of the hippocampus.

The preponderance of evidence seems to indicate that the dlPFC is a late developing structure that only reaches functional maturity in late adolescence. In contrast, multiple lines of evidence indicate that the hippocampus is an earlier developing structure that becomes functional by 1 to 1.5 years of life. Prior to functional maturation, the function of both the dlPFC and hippocampus seem to be supported by the orbital frontal and perirhinal cortices, respectively. In sum, the evidence supports the idea that early damage to the hippocampus could impact the development of the dlPFC given their respective developmental trajectories.

Conclusion

Overall, the current state of the literature suggests that schizophrenia patients show clear pathology within the dlPFC and hippocampus. As a result of this pathology patients suffer from a variety of symptoms but also show profound impairments in working memory. In an effort to both provide a greater understanding of the disorder and a potential tool with which to test novel pharmacotherapies, several investigators have created an animal model of schizophrenia in the rodent. The model was based on the idea that pathology of an early developing structure, in this case the hippocampus, may trigger maldevelopment in a late developing structure, in this case the dlPFC. The construct of the model involved lesioning the hippocampus early in life and examining the animal for a variety of behavioral and physiological changes that correlate with the disease state. In theory, early damage to the hippocampus should result in a maldeveloped prefrontal cortex, presumably by altering the function of the mesolimbic dopamine system. The empirical evidence supports the neonatal ventral hippocampal lesion model of schizophrenia as a valid model encompassing many facets of the disease state. However, any animal model has limitations and in this case the main limitation lies in the selection of the animal species. Insofar as the rats do not possess a true dlPFC, the most affected brain region in schizophrenia, the model is inherently limited in its' ability to test functions dependent upon this region, namely working memory. This idea is supported by the fact working memory tasks cannot assess the same functions in rodents as you can in primates. The limitation of working memory assessment is particularly troubling in this model, as working memory has been shown to be a reliable predictor of symptom severity in schizophrenia. As a result, it is important to determine if the early hippocampal lesion model of schizophrenia is tenable in a primate species, which have a

far greater degree of neurobiological and neuropsychological similarities with humans. Thus, the following study will examine adult rhesus monkeys, which received neonatal lesions of the hippocampus in infancy, and sham operated controls as a potential non-human primate model of the working memory deficits in schizophrenia.

Hypothesis and Aims:

Neonatal hippocampal lesions in rhesus monkeys is sufficient to disrupt the function of the dorsolateral prefrontal cortex, presumably via the mesolimbic dopamine system. In order to test this hypothesis the following experiments were performed:

Aim 1: To characterize the working memory processes affected by neonatal hippocampal lesions in the rhesus macaque

Aim 1a. *To dissociate the effects of neonatal lesions of the hippocampus on maintenance processes and monitoring processes.* In this first experiment monkeys with neonatal hippocampal lesions were tested on two working memory tests: Session Unique-Delayed Non-Match to Sample (SU-DNMS) measuring maintenance of information mediated by the ventrolateral prefrontal cortex and Object Self-Ordered Task (Obj-SO) measuring monitoring of information mediated by the dorsolateral prefrontal cortex. If the rodent model is tenable in the primate Neo-H monkeys, I hypothesized that animals with Neo-H lesions should be impaired on the dlPFC dependent task (Obj-SO), while performing as well as controls in a recency paradigm known to be dependent upon the vlPFC (SU-DNMS).

Aim 1b. *To examine serial order working memory function following neonatal lesions of the hippocampus.* In this experiment Neo-H monkeys and their sham-operated

controls were tested on the serial order memory task (SOMT) to confirm the results found in Aim 1a. In this case only one task is needed because the SOMT allows for the dissociation of both dlPFC-dependent and vlPFC-dependent functions, independently. As in Aim 1a, I hypothesize that Neo-H monkeys will be impaired on dlPFC-dependent components of the SOMT, but show a sparing of function on the vlPFC-dependent components.

Aim 2. *Examination of dlPFC integrity in adult monkeys with neonatal lesions of the hippocampus using Magnetic Resonance Spectroscopy.*

In this experiment the functional integrity of the dlPFC and vlPFC was examined using Magnetic Resonance Spectroscopy to measure n-acetyl-aspartate (NAA), a known marker of neuronal integrity. In addition, the primary somatosensory cortex was also examined as an additional control region of interest. I hypothesize that Neo-H monkeys will show a reduction in NAA within the dlPFC, but that the vlPFC and somatosensory cortex will show NAA levels comparable to the control group.

Aim 3. *To assess sensory-motor gating in Neo-H and sham operated control animals using the Pre-Pulse Inhibition Paradigm (PPI).*

In this experiment Neo-H animals and control subjects were tested on the PPI paradigm to determine if Neo-H monkeys show deficits in sensory-motor gating. As sensory-motor gating is a core symptom of schizophrenia it will be important to determine if the non-human primate model also demonstrates deficits in this process. I hypothesize that Neo-

H monkeys will show reduced PPI, which is indicative of an impairment in sensory-motor gating.

Chapter 2.

Monitoring, but not maintenance, working memory processes are impaired following selective neonatal lesions of the hippocampus in the rhesus macaque.

Introduction

In the last decade, studies in rodents have provided mounting evidence to suggest that neonatal damage to the ventral hippocampus alters the normal development and function of the prefrontal cortex for a review see, [70]. Focal neonatal neurotoxic lesions (Neo-H) of the hippocampus yield prefrontal cortex dysfunction as revealed by behavioral, electrophysiological, neurochemical and ultra-structural studies. This prefrontal cortex dysfunction is also associated with impaired working memory as assessed by a number of

working memory tasks, such as the radial arm maze, delayed and discrete alternation, win-shift paradigm, set-shifting and spatial working memory [79-81,152-154]. In addition, animals with Neo-H lesions exhibit altered ventral prefrontal cortical firing patterns following dopaminergic and glutamatergic stimulation [87,155], decreased dopamine transporter in the ventral tegmental area and decreased GAD-67, the rate limiting enzyme of gamma-aminobutyric acid (GABA) synthesis [82,85] as well as ultra-structural changes in the prefrontal cortex, such as reduced number of interneurons and decreased spine density of pyramidal neurons [85,152]. Thus, the rodent literature clearly established a causal link between neonatal damage to the ventral hippocampus and prefrontal cortical development, suggesting that dopamine control of prefrontal mechanisms are compromised in the absence of functional hippocampal inputs during development.

While these studies have been extremely valuable in establishing a putative role for the hippocampus in the development of the prefrontal cortex, some of their limitations reside in the ability to use the rodent results to make inferences on the effects of neonatal hippocampal dysfunction on prefrontal cortex development in humans. In particular, although rats have a defined medial prefrontal cortex, they do not have the functionally distinct subdivisions of the primate lateral prefrontal cortex. Recent reviews have concluded that rats do in fact have rudimentary elements of the lateral prefrontal cortex (medial in the rodent) but that this area cannot be clearly delineated from another area believed to be the homolog of the anterior cingulate cortex in primates [90,91]. The issue of structural homology of the prefrontal cortex becomes more problematic when employing behavioral measures to dissociate structure-function relationships of different lateral prefrontal subregions. In this domain, studies in nonhuman primates offer important

advantages since in both monkeys and humans working memory processes are segregated within defined sectors of the lateral prefrontal cortex. Within the dorsal and ventral sectors of the lateral prefrontal cortex, working memory processes are organized according to the type of processing required (process-specific) rather than according to the domain of the information being processed (material-specific) for a review see, [5,119,120]. Thus, simple maintenance of information in a working memory buffer is inherently dependent upon the ventrolateral prefrontal cortex [93,102,156]. In contrast, higher order working memory processes, such as monitoring of sequential actions and of temporal order of information and manipulation of this information, is dependent upon the dorsolateral prefrontal cortex [101,102,157,158]. Given this division of labor in the lateral prefrontal cortex in primates, it became critical to evaluate whether neonatal hippocampal damage in monkeys will, as in rodents, yield deficit in working memory processes mediated by the prefrontal cortex, and if yes, to determine which sector of the lateral prefrontal cortex may be more specifically impacted by the absence of functional hippocampal inputs during development. To this end, we tested adult rhesus monkeys that had received neonatal neurotoxic lesions of the hippocampus and their sham-operated controls on two tasks of working memory. The Session-Unique Delayed NonMatch-to-Sample measures maintenance of information in working memory and assesses functioning of the ventrolateral prefrontal cortex. The Object-Self Ordered task measures monitoring of information and assesses functioning of the dorsolateral prefrontal cortex. Preliminary data of this study were already reported in abstract form [159].

Methods

Subjects

Eleven adult rhesus macaques (*Macaca mulatta*), aged 5 - 6 years and weighing between 5 to 8 kg, were used in this study. They were acquired as newborns from the breeding colony of the University of Texas, M.D. Anderson Cancer Center Science Park (Bastrop, TX) and brought to the nursery at M.D. Anderson Cancer Center where they were surrogate nursery raised in age- and sex-matched cohorts of 4 animals each [160]. Infant monkeys were individually housed but permitted social contacts with other animals in adjoining cages until one month of age. In addition, a plush surrogate was provided to the animals of approximately 30cm in length. A principal human caregiver spent roughly 6 h/day, 5 days/week in the nursery with the infant monkeys. On weekends, the infants were handled 2-3 times per day and received a total of 2-4 hours of social interactions with familiar experimenters. From one to nine months of age infants received daily social interactions for 3-4 hours, 5 days/week with age/sex matched peers and by 1 year of age, each cohort was socially housed until approximately 3 years of age. They were then moved to the Yerkes National Primate Research Center at Emory University (Atlanta, GA) where they were housed individually in rooms with a 12 hour light/dark cycle (7AM:7PM). All monkeys were fed Purina Old World Primate chow supplemented with fresh fruit and during behavioral testing, food was minimally restricted to sufficiently motivate the animal. Their weight was closely monitored to maintain it at or above 85% of their full feed weight and water was provided *ad libitum.*

All monkeys had received brain surgeries when they were infants (10-15 days post-natally) consisted of either sham-operations (Group Neo-C, 2 males, 3 females) or neurotoxic lesions of the hippocampus (Group Neo-H-ibo, 4 males, 2 females).

All experimental procedures were approved by the Institutional Animal Care and Use Committee at the University of Texas at Houston and Emory University and were conformed to the NIH Guide for the care and use of Laboratory Animals (HHS publication 85-23, 1985).

Neuroimaging and Surgical Procedures

All neuroimaging and surgical procedures have been described extensively in an earlier report [160] and will be briefly summarized below

Neuroimaging procedures: On the day of surgery, the infant monkeys were placed in an induction box saturated with isoflurane gas (1.0-3.0%, v/v, to effect), intubated and maintained under isoflurane gas throughout the procedure. They were then placed in a non-ferromagnetic stereotaxic apparatus (Crist Instruments, Damascus, MD) and centered in the scanner. Two types of MR images were acquired with a GE Signa 1.5 Tesla Echo Speed scanner (GE Medical Systems, Milwaukee, WI) using a 5-inch surface coil. A series included a 3D T1-weighted fast spoiled gradient (FSPGR)-echo MR images (echo time (TE) = 11ms, repetition time (TR) = 450ms in contiguous 4mm sections, 12cm field of view (FOV), 256 x 256 matrix) and the other included Fluid-Attenuated Inversion Recovery (FLAIR) images (TE = 140ms, TR = 10,000ms, inverstion time (TI) = 2200ms, contiguous 3mm sections, 14cm FOV, 256 x 256 matrix). These two series of MR images were repeated 6-8 days after the surgical procedures. The pre-surgical T1W images were used to select stereotaxic coordinates for the neurotoxin injection sites for

group Neo-H-ibo [161] and the post-surgical FLAIR images indicated areas of high water density and were matched with both the pre-surgical T1W and FLAIR images to verify the location and extent of lesions to the targeted area as well as to evaluate any inadvertent damage to adjacent structures [162,163]. Further investigation of the lesion extent was performed at approximately 1 to 1.5 year after surgery, when all animals received another scanning procedure using T1-W MR images to estimate the percent reduction of hippocampal volume.

Surgical procedures: At completion of the pre-surgical MRI, the animal was maintained under gas anesthesia and immediately transported to the surgical suite. The scalp was disinfected with Nolvasan solution and an intravenous drip containing 5% dextrose and 0.5% sodium chloride was infused to maintain hydration. The animal was maintained on a heating pad to maintain core temperature, and all vital signs (core temperature, pulse, blood pressure and expired CO_2) were continuously monitored until the end of the procedure. Marcaine (25%, 1.5m., s.c.) was injected along the midline incision of the scalp from the occiput to a point in between the eyebrows. The skin was incised and the connective tissue was displaced laterally to expose the skull in which two craniotomies were made in the left and right hemispheres just above the hippocampus followed by small slits in the dura.

For the hippocampal lesions, two 10µl Hamilton syringes attached to a Kopf electrode manipulators (David Kopf Instruments, Tujunga, CA) were used to simultaneously deliver the neurotoxin in the left and right hippocampus. A total of 2.8-4.2µl ibotenic acid (Biosearch Technologies, Novato, CA, 10mg/ml in PBS, pH 7.4) was injected into 7-8 sites along the hippocampus and was intended to target the uncus and

hippocampus along its entire length. The needles were slowly lowered at each injection site and 0.4-0.6µl of ibotenic acid was manually injected at a rate of 0.2µl/min. After each injection, the needles were left in place for an additional 3-min period to allow diffusion of the drug at the tip of the needle and minimize its spread in the needle track during retraction of the needles. After each injection the needles were cleaned with cotton-tipped applicators to remove any residual neurotoxin or tissue along the needle.

The procedures for the sham lesions were identical to those used for the neurotoxic acid lesion of the hippocampus except that no needle was lowered into the brain.

Following the completion of the surgical procedure, the incision was closed in anatomical layers and the infant was placed in an incubator to maintain core temperature. The post-operative care included a seven-day regimen of dexamethasone sodium phosphate (0.3mg/kg i.m.) to reduce swelling, Cefazolin (25mg/kg i.m.) to minimize infection, and acetaminophen for pain management.

Lesion Assessment

Because all animals are undergoing behavioral testing, extent of lesions was estimated from the MR images [163]. Pre- and post-surgical FLAIR images were matched to corresponding pre-surgical T1-weighted images and coronal drawings of a normal one-week-old rhesus monkey template brain (J. Bachevalier, unpublished data). Hypersignals on FLAIR MR images were identified, plotted onto corresponding coronal drawings from the template brain, and drawings were imported into a Java-based image analysis program (ImageJ®; http://rsb.info.nih.gov/ij/) to measure the surface area (in pixels^2) of

damage for intended targets, as well as all areas sustaining unintended damage (entorhinal and perirhinal cortex and amygdala). For any given region of interest (ROI), the measured surface area of damage on each section through each hemisphere was summed and then multiplied by image thickness to calculate a total volume of damage [164]. The volume of damage was then divided by the normal volume of the ROI and multiplied by 100 to indicate a percent of the total volume damaged.

In addition, the total hippocampal volume reduction was calculated using the 1-year post-surgical T1-weighted MR images. For each animal, the coronal MR images were imported into the Java-based image analysis program (ImageJ®; http://rsb.info.nih.gov/ij/). Images containing the hippocampal formation were identified and surface area measurements were recorded for the left and right hemispheres separately. Descriptions of borders used to define the hippocampal formation on MR images have been previously described [148]. Briefly, the first image posterior to the optic chiasm was used as the most anterior border in which the hippocampal formation appeared ventral to the amygdala and the tail of the lateral ventricle was often visible on the lateral and superior aspects of the hippocampal formation. The most posterior measurement for the hippocampal formation was made on the image that clearly showed the crus of the fornix emerging from the hippocampal formation. The gyrus fasciolaris and the fornix were excluded from the measurements. On all images between these two extremes, the hippocampal formation was bounded ventrally and medially by the white matter separating it from the parahippocampal gyrus, and laterally and dorsally, by the temporal horn of the lateral ventricle. Thus, the volume of the hippocampal formation included the CA fields, dentate gyrus, subicular complex and fimbria, but excluded the

entorhinal, perirhinal, and parahippocampal cortices. For each hemisphere, separately, the hippocampal volume (in mm^3) was calculated by summing hippocampal surface areas on each image and multiplying by the distance between the images (i.e. 1 mm), using Cavalieri's principle [164] For each animal in Group Neo-H-ibo, the hippocampal volume in each hemisphere was then compared to the averaged hippocampal volume from 6 normal male (n=3) and female (n = 3) monkeys of the same age (approximately 1 year of age). Percent volume reduction was then calculated using the following formula: [100-total H volume remaining/average H volume in normal subject]*100). Two trained observers measured the volume of hippocampal formation in normal animals and animals of Group Neo-H-ibo (Cronbach's alpha; $p < 0.01$ for all inter- and intra-observer reliabilities).

Behavioral procedures

As the animals were part of a developmental study examining the effects of neonatal hippocampal lesions on learning and memory processes, emotion regulation, social behavior and decision-making skills, they had received extensive, but identical, behavioral testing from infancy through the start of this experiment. This behavioral testing included measures of recognition memory at 1.5, 6, 18 and 48 months [165], non-spatial relational memory at 3 and 15 months, spatial memory at 8 and 24 months, object discrimination reversals 48-60 months, , food preference and shift in choice selection after food devaluation at 60 months, dyadic social interactions (3, 6, and 36 months), emotional reactivity to human intruder at 2 and 4.5 months and social attachment to caregiver at 9 months [160].

Apparatus and stimuli

Monkeys were tested in a darkened room containing a white noise generator to mask extraneous noise. For both the Session Unique Delayed NonMatch-toSample (SU-DNMS) and the Object Self-Ordered Task (Obj-SO) animals were transferred from their home cage to a Wisconsin General Testing Apparatus (WGTA), and positioned in front of a testing tray containing three recessed food wells (2 cm in diameter, 1 cm deep and 13 cm apart from each other).

The SU-DNMS task utilized a set of 1000 junk objects that differed in color, size and shape, although only a single pair of objects was used for any given daily test session. The Obj-SO task employed a single set of three junk objects for all daily sessions. Correct choices were rewarded with a generally preferred food (i.e. m&m, marshmallow, peanut etc).

Session Unique Delayed Non-Match to Sample (SU-DNMS)

The procedures for SU-DNMS are similar to those of the Trial Unique-DNMS [166], except that only a single pair of objects was used on each trial of a daily session instead of using new pairs of stimuli for each trial as for the Trial Unique DNMS task. This manipulation changes the DNMS paradigm from a purely recognition memory task to a recency memory task [167]. For each daily session a pair of objects was presented for 30 trials separated by a 30-s interval, such that both objects served as the sample or the choice in a random order. On each trial, a single one overlayed the center well baited with a food reward. After the subject displaced the sample object to retrieve the food reward, a 5-s delay was imposed during which the view of the testing tray was obstructed by a screen. For the choice test, the sample object now unbaited was presented together with the other baited object with both objects positioned over the lateral wells of the test

tray. Thus, starting with the second trial both objects had been seen and successive performance on the task required the animal to remember the object seen during the sample phase, i.e. the object he had seen the most recently. The following day a new pair of objects was selected for training and so on for all subsequent testing days, until the monkey achieved a score of 27 (or better) correct choices out of 30 trials on one day followed by a score of 24 (or better) correct choices out of 30 trials on the following day or until reaching the learning criterion of 1000 trials. After reaching criterion using the 5-s delay, testing continued in the same way with a longer delay of 30 seconds. Animals were given 20 trials per day at this longer delay and again a different pair of objects was used on each testing day until performance averaged85% correct across two consecutive test sessions or to a limit of 500 trials.

Object Self-Ordered Task (Obj-SO)

The Obj-SO task was delivered according to procedures described by [101,102]. The Obj-SO task requires the animal to choose different objects, one by one, on successive trials of a daily session. Because the positions of the objects are shuffled spatially on each trial, to solve the task, the animal cannot simply rely on the locations of each object on the tray, but rather has to make choices based on their actions in previous trials of the daily session. Specifically, on each day, animals received three successive trials using the same set of three objects until learning criterion was met. In Trial 1, the subject was presented with the three objects covering each of the three baited wells on the testing board. After the animal displaced one of the three objects and retrieved the food reward, a 10-s delay was imposed during which the view of the testing tray was obstructed by a screen. During this delay, the locations of the objects were re-ordered on the three wells

and only the two objects that were not selected on the first trial were baited. After selecting one of the two baited objects in Trial 2, a 10-s delay was again imposed during which the three objects were again re-ordered on the three wells, but this time only the object that had not been selected on the two previous trials was now baited. After selecting the last baited object on Trial 3, the daily session ended, and the next day, the three objects were again used and presented over the same three trials, but their positions on the wells varied randomly each day. Thus, because all three objects are baited in Trial 1, the animal could commit an error only in the second and/or third trials. If at any time during Trials 2 and 3, the animal incorrectly selected the unbaited object, this was scored as a primary error and a correction procedure was given. That is, a 10-s delay was imposed during which the three objects were re-ordered on the tray and represented to the animal for choice. This correction procedure was repeated until the animal correctly selected a baited object. The number of time the correction procedure was repeated for a given trial was used as a measure of perseverative errors. Testing for the Obj-SO task continues until the animal made three or less errors on both phases 2 and 3 (85% correct) across 10 consecutive days of testing (i.e. 20 trials). Testing was discontinued after a maximum of 50 daily sessions (100 trials).

Statistical Analysis

Between group comparisons for the behavioral measures were made using independent samples t-tests. When data sets are not normally distributed or if zero occurrences of a particular behavior exist, group comparisons were evaluated using nonparametric Mann-Whitney U test. Lastly, potential relationships between lesion

extent and behavioral measures were made using a correlation matrix (Pearson's r), corrected for multiple comparisons.

Results

Assessment of Lesion Extent

Table 2.1 provides an estimate of extent of hippocampal damage as well as unintended damage to adjacent structures. Two animals (Neo-H-ibo2 and Neo-H-ibo3) received extensive damage to the hippocampus bilaterally, averaging 67.6 and 87.4% damage, respectively. Three others (cases Neo-H-ibo-1, -4 and -5) had asymmetrical lesions with extensive damage on one hemisphere (average: 72%), but moderate damage on the other hemisphere (average: 15%). Only, case Neo-H-ibo-6 had relatively small hippocampal damage on each side (7.9 and 0% for the left and right hemispheres, respectively). Unintended damage in each case was almost non-existent, except for very small damage to the posterior amygdala (from 0 to 7% bilaterally) and to areas TH/TF (from 0 to 12.1%). The percent volume reduction calculated from the one year post-lesion MRI scans (Table 2.2) confirmed the FLAIR MRI estimation of the hippocampal lesions, and resulted in a positive correlation between the two methods ($r = 0.805$, $p = 0.05$). Thus, four animals (Neo-H-ibo-2 to Neo-H-ibo-5) showed rather substantial hippocampal volume reduction, averaging 47.6 to 67%, whereas two others (Neo-H-ibo-1 and -6) had only slight reduction of hippocampal volume, averaging 19% and 15%, respectively. Figure 2.1 displays extent of hippocampal volume reduction in a representative case (Neo-H-ibo-2).

Table 2.1: Lesion Extent as estimated via the FLAIR MR images

Group	Intended Damage				Unintended Damage							
Subjects	**Hippocampus**				**Amygdala**				**TH/TF**			
Neo-H-ibo	L%	R%	X%	W%	L%	R%	X%	W%	L%	R%	X%	W%
Neo-H-ibo-1	63.8	2.9	33.2	1.8	14.0	0.0	7.0	0.0	3.1	0.5	1.8	0.0
Neo-H-ibo-2	54.4	80.9	67.6	44.0	0.0	0.0	0.0	0.0	21.4	2.7	12.1	0.6
Neo-H-ibo-3	78.5	96.3	87.4	75.6	1.7	0.0	0.8	0.0	6.1	5.5	5.8	0.3
Neo-H-ibo-4	20.3	67.3	43.8	13.6	0.0	4.7	2.4	0.0	15.3	0.0	7.6	0.0
Neo-H-ibo-5	20.7	84.0	52.6	17.5	0.0	4.9	2.5	0.0	6.1	4.0	5.1	0.2
Neo-H-ibo-6	7.9	0.0	3.9	0.0	0.0	0.0	0.0	0.0	0.0	0.0	0.0	0.0
Mean	**40.9**	**55.2**	**48.0**	**25.4**	**2.6**	**1.6**	**2.1**	**0.0**	**8.6**	**2.1**	**5.4**	**0.1**

Note: L% percent damage in the left hemisphere; R%: percent damage in the right hemisphere; X% average damage to both hemispheres; W%: weighted average damage to both hemispheres (W% = L% x R%)/100; weighted index as defined by Hodos and Bobko [168]). TH/TF: ventral cortical area of the temporal lobe as defined by Bonin and Bailey, 1947)

Table 2.2: Volumetric Reduction of the Hippocampus

Group	Volume Reduction		
Subjects	**Hippocampus**		
Neo-H-ibo	L%	R%	X%
Neo-H-ibo-1	27.6	10.6	19.1
Neo-H-ibo-2	61.1	72.8	67.0
Neo-H-ibo-3	54.7	47.8	51.3
Neo-H-ibo-4	33.6	61.6	47.6
Neo-H-ibo-5	49.1	64.0	56.6
Neo-H-ibo-6	21.3	8.3	14.8
Mean	**41.2**	**44.1**	**42.7**

L% = Percent reduction of hippocampal volume in left hemisphere, R% = Percent reduction of hippocampal volume in right hemisphere, X% = Average percent reduction in both hemispheres.

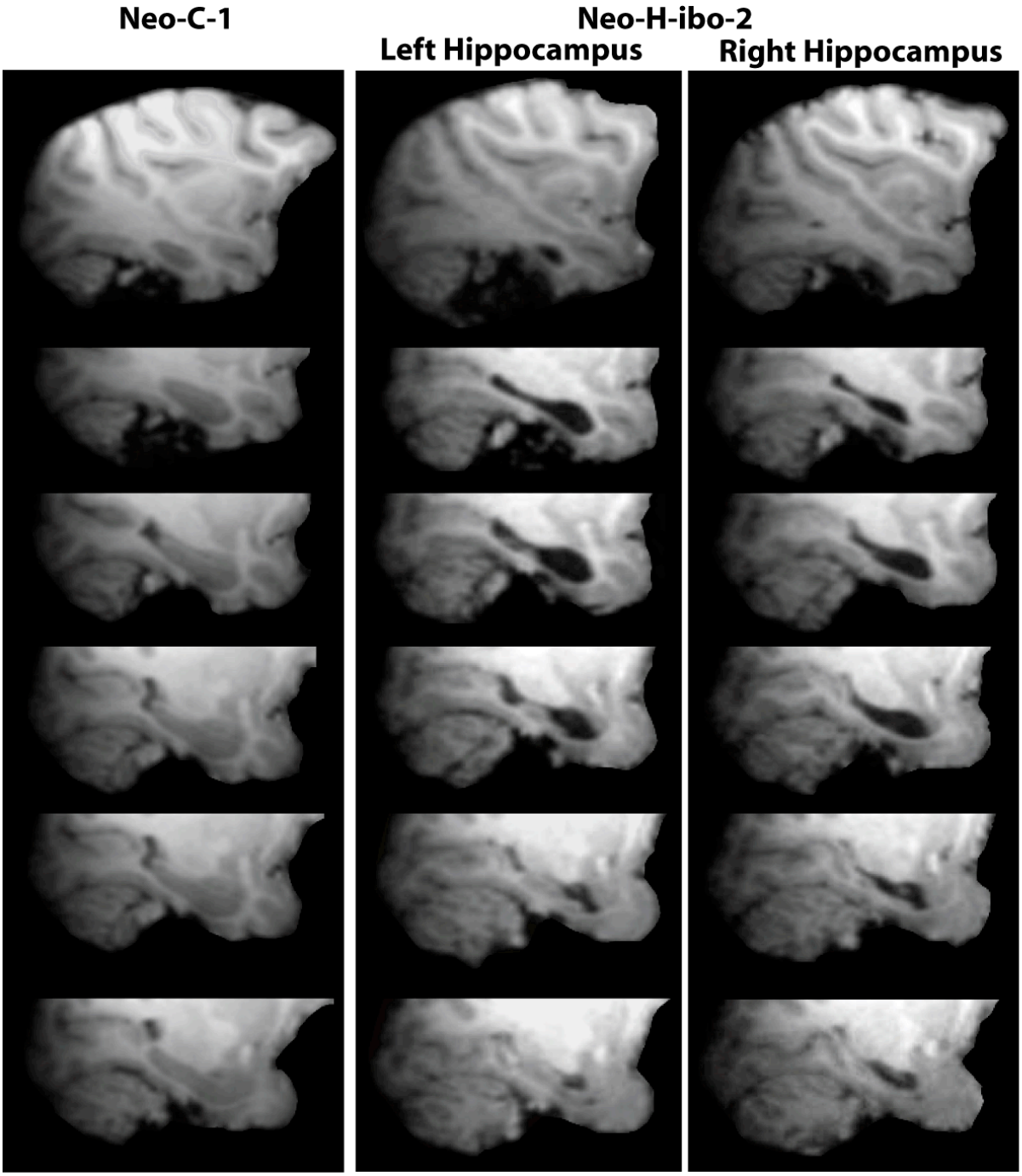

Figure 2.1: Example Hippocampal Lesion The left column shows a normal hippocampus from a sham lesioned control monkey (Neo-C-1) in the saggital plane. The middle and right columns show the left and right hippocampus, respectively an example lesion (Neo-H-ibo-2) also in the saggital plane.

Session Unique-Delayed NonMatch-to-Sample (SU-DNMS)

Individual scores at the 5 and 30s delays for both groups are shown in Table 3.

All animals successfully completed SU-DNMS at both delays well within the learning criterion limits of 1000 and 500 trials, respectively. Animals with neonatal hippocampal lesions took slightly longer to acquired the SU-DNMS at the 5-s delay, averaging 170 trials (50 errors) as compared to sham-operated controls (102 trials and 27 errors), although this group difference did not reach significance for both trials [$t(1,9) = 0.607$, $p = 0.559$] or errors [$t(1,9) = 0.635$, $p = 0.541$]. At the 30-s delay, animals with neonatal hippocampal lesions reached criterion slightly faster (53 trials and 16 errors) than sham-operated controls (80 trials and 26 errors), but again this group difference did not reach significance [$t(1,9) = 0.395$, $p = 0.702$ and $t(1,9) = 0.476$, $p = 0.646$, for trials and errors, respectively] Finally, none of the scores obtained by animals in Group Neo-H-ibo correlated significantly with extent of hippocampal lesions, demonstrating that although animals in Group Neo-H-ibo had extent of damage that varied greatly between animals, this variation was not reflected in performance on the SU-DNMS task.

Table 2.3: Session Unique Delayed Non-Match-to-Sample

Subjects	5 Second Delay		30 Second Delay	
	T	E	T	E
Neo-C				
Neo-C-1	0	0	0	0
Neo-C-3	150	35	320	114
Neo-C-4	240	68	80	16
Neo-C-5	120	30	0	0
Neo-C-6	30	6	80	18
Mean	**102.0**	**26.6**	**80.0**	**26.0**
Neo-H-ibo				
Neo-H-ibo-1	0	0	220	55
Neo-H-ibo-2	30	4	40	11
Neo-H-ibo-3	570	190	40	17
Neo-H-ibo-4	60	9	20	10
Neo-H-ibo-5	330	91	0	0
Neo-H-ibo-6	30	5	0	0
Mean	**170.0**	**49.8**	**53.3**	**15.5**

Scores are the number of trials (T) or of errors (E) committed prior to reaching criterion at each of the two delays for animals with neonatal hippocampal lesions (Neo-H-ibo) and sham-operated controls (Neo-C).

Object Self-Ordered Task (Obj-SO)

Individual scores for animals with neonatal lesions of the hippocampus and sham operated controls are shown in Table 4.

All subjects in the control group reached criterion well within the task limits (i.e. 50 daily sessions or 100 trials), completing the task in an average of 9 trials (i.e. 5 daily sessions). In contrast, all but one of the animals with neonatal hippocampal lesion (Neo-H-ibo-3) failed to reach criterion within the limit of testing, averaging 88 trials (i.e. 44 daily sessions). This group difference reached significance [$U(1,9) = 4.50$, $p = 0.05$]. This impairment in learning the Obj-SO task in monkeys with neonatal hippocampal

lesions was also reflected in the increased number of primary errors they made on Trial 2 and Trial 3 (34 errors) as compared to control animals (5 errors). The group effect was significant for the total number of errors [$t(1,9) = 3.331$, $p = 0.009$] as well as for number of errors committed on Trial 2 [$t(1,9) = 2.934$, $p = 0.017$] and Trial 3 [$t(1,9) = 3.711$, $p = 0.005$]. Finally, animals with neonatal hippocampal lesions also showed more preservative errors (35 errors) than sham-operated control (6 errors), but this group difference reached significance only for preservative errors made on Trial 3 [$t(1,9) = 3.556$, $p = 0.006$] but not on those made on Trial 2[$t(1,9) = 1.756$, $p = 0.113$]. It is interesting to note that case Neo-H-ibo-3, which learned the task immediately and performed as well as controls, had the most extended hippocampal damage (87%) as shown on FLAIR MR images. However, there were no significant correlations between the errors on SU-DNMS [$r = - 0.011$, $p = 0.984$] or Obj-SO [$r = -0.422$, $p = 0.491$] and lesion extent.

Table 2.4: Object Self Ordered Task

Subjects	Sessions	Errors by Trial				Total Errors	
		Trial 2 Error	Trial 2 PE	Trial 3 Error	Trial 3 PE	Errors	PE
Neo-C							
Neo-C-1	0	0	0	0	0	0	0
Neo-C-3	11	2	0	8	16	10	16
Neo-C-4	6	2	0	5	13	7	13
Neo-C-5	5	4	1	3	0	7	1
Neo-C-6	1	1	0	0	0	1	0
Mean	**4.6**	**1.8**	**0.2**	**3.2**	**5.8**	**5**	**6**
Neo-H-ibo							
Neo-Hibo-1	50*	8	1	27	28	35	29
Neo-Hibo-2	50*	13	11	33	52	46	63
Neo-Hibo-3	0	0	0	0	0	0	0
Neo-Hibo-4	50*	15	3	28	39	43	42
Neo-Hibo-5	50*	17	3	32	39	49	42
Neo-Hibo-6	50*	8	2	26	34	34	36
Mean	**44.1**	**10.2**	**3.3**	**24.3**	**32**	**34.5**	**35.3**

Scores are the number of sessions to reach criterion and the number of primary errors on Trials 2 and 3 and cumulative errors on both trials. PE= Perseverative Error made on Trials 2 and 3 and cumulative perseverative errors *Failed to reach criterion within the 50 session limit.

Discussion

The present experiment demonstrated that early lesions of the hippocampus impair working memory processes in monkeys. More importantly, the findings revealed that the working memory impairment was specific to monitoring processes while maintenance processes were not disrupted. These data demonstrated for the first time that malfunctioning of the hippocampus in early infancy may impact the normal maturation of the dorsolateral prefrontal cortex in the primate. After discussing the impact of neonatal hippocampal lesions on working memory processes, the putative

mechanisms by which these early lesions disrupt prefrontal maturation and the implication of the results in relation with schizophrenia will be reviewed.

Impact of Neonatal Hippocampal lesions on dlPFC working memory processes

In the SU-DNMS task, which measures the ability to maintain mental representations in a memory buffer mediated by the ventrolateral prefrontal cortex), animals with neonatal lesions of the hippocampus displayed normal performance even at the long delay of 30 seconds. This finding replicates that of an earlier study [169] showing that nonselective damage to the hippocampus spared recency judgments even at long delays and extends this earlier study by showing that the sparing holds true for both hippocampal lesions acquired in adulthood or in infancy. By contrast, in the Obj-SO task, all animals with neonatal hippocampal lesions but one failed to reach the learning criterion, indicating severe impairment in working memory task measuring the ability to monitor mental representations mediated by the dorsolateral prefrontal cortex. The normal performance of case Neo-H-ibo-3 (Table 3) is puzzling, given that this animal has one of the most extended hippocampal lesions (87%) of the group despite an impairment in recognition memory tasks known to be hippocampal-dependent as did the other animals of the group [165]. A possible explanation for the normal performance of this animal in the Obj-SO task may be the development of an alternative strategy of selecting the three objects in the same order across multiple days. However, inspection of this animal's performance on a daily basis did not reveal the use of such a strategy during the task. Another possibility is that only partial lesions of the hippocampus, as the ventral hippocampal lesions in rodents, may result in prefrontal dysfunction. Inspection of the lesion in this case did not reveal a greater sparing of the anterior hippocampus (homolog

of ventral sector in rodents). Although good performance of this case remains unexplained, it is clear that neonatal hippocampal lesions impact significantly working memory processes.

The results of this study indicate that the early damage to the hippocampus significantly disrupts the normal function of the dlPFC and supports the proposal that the hippocampus as a critical regulator of prefrontal development and working memory functions. It is important to note that at the current time, it is difficult to conclude whether the deficits in working memory processes are due to a direct effect of the early lesions on the dlPFC maturation, the hippocampus being a critical regulator of dlPFC function even in the adult monkey, or both. However, the pattern of results following neonatal hippocampal lesions mirrors the pattern results reported by Petrides[102] and indicating impaired performance on the Obj-SO task following selective mid-dorsolateral but not posterior dorsolateral lesions in adult monkeys. Secondly, rodent behavioral studies of hippocampal lesions on temporal order tasks have shown that hippocampal lesions produce global impairments in working memory [95,170], which is what would be expected if a primary locus of a process (i.e. working memory) was damaged, the combined data (SU-DNMS and Obj-SO) of the current investigation indicate a selective effect that affect only monitoring working memory processes mediated by the dorsolateral prefrontal cortex.

One issue worth discussing is the possibility that the rearing conditions could have impacted the development of the prefrontal cortex. As detailed in the Method section (see also [24]), animals in the current study were raised in a nursery with peers. As reported earlier [171], monkeys raised in nursery reared with peers showed reduced

prefrontal cortical white matter volumes, reduced volume of the corpus callosum associated with impaired performance on the Trial Unique Delayed Non-Match-to-Sample (TU-DNMS- a measure of recognition memory) as compared to animals raised in a semi-naturalistic field setting. . One important difference in the rearing of the monkeys in the present experiment is the substantial interactions with human caregivers and the intense cognitive testing they had received from infancy through adulthood. The infant monkeys' rearing conditions used in the present study were based on those developed by Sackett and collaborators (Survival, growth, health, and reproduction following nursery rearing compared with mother rearing in pigtailed monkeys (Macaca nemestrina) [172] These authors have shown in a large longitudinal study that infants monkeys reared without their biological mother but receiving intensive human handling as well as daily social interactions with peers, and frequently subjected to learning and cognitive testing, did not differ from mother-reared infants in terms of survival, growth, clinical treatments for disease or bite wounds, or pregnancy outcome and neonatal death. Thus, we indeed found that animals in Group Neo-C's performance on the TU-DNMS [173] was comparable to that of mother-reared monkeys in the Sanchez et al.'s study [35). In addition, the callosal volume of Group Neo-C was also comparable to that reports for mother-reared monkeys [35]. In addition, Group Neo-C performed in the Obj-SO task similarly, or even better, to the normal adults that were raised in more naturalistic conditions [19]. Thus, the rearing environment does not seem to have negatively impacted the cognitive development of animals in Group Neo-C and is unlike to be a significant factor to explain the group difference. Future studies are required to systematically investigate the impact

of the rearing environment on the cognitive effects of neonatal hippocampal lesions in monkeys.

These results support a large body of literature in the rodent suggesting a functional link between the developing prefrontal cortex and early damage to the hippocampus [68]. However, there is a distinction to be made between the rat and monkey concerning the types of working memory processes disrupted by the neonatal hippocampal lesions. Given that all working memory assays in the rodent measure maintenance working memory [79-81], a distinction between maintenance and monitoring processes was impossible to draw. By contrast, the current results demonstrated a sparing of maintenance working memory processes (vlPFC dependent) but severe impairment in monitoring working memory processes (dlPFC dependent). This distinction is important, as the lack of functional segregation within the lateral prefrontal cortex in rodents, inherently limits the ability to generalize their findings to the human.

Putative mechanisms:

How could a neonatal lesion of the hippocampus impact the development of a distal structure like the dlPFC, considering that there are no direct projections from the hippocampus to the dlPFC? A model proposed by Lodge and Grace [69] has indicated an indirect action of the hippocampus, via the ventral striatum, that disinhibits the ventral tegmental area eliciting dopamine release into the prefrontal cortex. It should be noted that this model was originally proposed and designed using the known connectivity of these systems in the rat, however sufficient data has shown that this system is

functionally conserved in the primate [134,174,175]. Further, years of non-human primate research have elucidated the profound role that the dopamine release plays in regulating dlPFC function, specifically working memory [135,137,176]. Additionally, although there is no direct connectivity between the hippocampus and dlPFC, alternative direct connections from the dlPFC, via the cingulum bundle and the retrosplenial cortex [118] exists. In this way the dlPFC is positioned to regulate hippocampal output, which in turn modulates dopaminergic tone in the dlPFC and subsequently working memory. Indeed, it is interesting to note that neonatal hippocampal lesions result in a decrease resting state metabolic activity in the retrosplenial cortex [177] and that animals in Group Neo-Hibo showed decreased volume of the posterior sectors of the corpus callosum [178].

Aside from the ventral striatum and midbrain dopamine system, other brain areas known to be involved in the regulation of working memory include the posterior parietal cortex [179,180] and the medial dorsal thalamic nucleus [19]. Given that the posterior parietal cortex projects to the parahippocampal gyrus [127], it is possible that early damage to the hippocampus could have impacted this connection, causing distal effects on the dlPFC. Alternatively, as both the dlPFC and the posterior parietal cortex project to the retrosplenial cortex [118,181], which subsequently projects to the hippocampus [127], it is also possible that disruption of this pathway may have played a role in the working memory impairment observed. Additionally, we cannot exclude the possibility that the early hippocampal lesion have altered thalamic circuitry important for working memory as both the dlPFC and the hippocampus project to and receive projections from the dorsal thalamic nuclei [129,182]. Thus, future studies are required to identify the specific neural underpinning of the working memory impairment found after neonatal hippocampal

lesions. To this end the use of neuroimaging and post-mortem histological methods on the monkeys of the present study will be crucial to determine the mechanism whereby early hippocampal lesions impact the functional development of the dlPFC.

Neonatal hippocampal lesions and schizophrenia

In conclusion, this study has demonstrated, for the first time, that early lesions of the hippocampus are sufficient to selectively impair working memory that is dependent upon the dlPFC in the primate. Although future studies should be aimed at confirming this novel finding and examining the neural basis of this impairment, the neonatal hippocampal lesion model has important implications to better understand the neurobiological basis of schizophrenia. Schizophrenia patients consistently show pathology within the developing hippocampus, as evidenced by reduced overall volume [40] and reduced n-acetyl-aspartate levels [21,46] (a marker of neuronal integrity). In addition, working memory deficits, dependent upon the dlPFC, have been described as a core symptom of the disease state [63]. Thus, the present study may provide a potential explanation for the working memory deficits commonly observed in the disease state and offer an important primate model to develop new therapeutic tools to improve the cognitive deficits associated with the disease.

Chapter 3

Dorsolateral prefrontal working memory processes are impaired after selective neonatal lesions of the hippocampus in adult rhesus macaques

Introduction

A recent study in this laboratory, found that monkeys with neonatal lesions of the hippocampus were found to have impaired monitoring working memory [183]. In contrast, these same animals performed comparably to controls on maintenance working memory. Anatomical distinctions have been made between the loci of these two working memory processes in the primate, which allows a neuropsychological driven approach attribute cognitive impairment to regional brain dysfunction. In both monkeys and humans, it has

been found that monitoring and maintenance working memory are dependent upon the dorsolateral and ventrolateral prefrontal cortex, respectively [93,101,102,157,158]. This finding represented the first time that a causal functional link was made between the hippocampus and the dorsolateral prefrontal cortex in the primate, despite mounting evidence from different fields that these two regions are functionally linked [47,184,185].

The novel finding of neonatal hippocampal lesions impacting dlPFC function, as measured by the Object-Self Ordered (Obj-SO) task needs to be substantiated. To independently measure monitoring working memory the serial order memory task (SOMT) was selected as this task has also been established to be dependent upon the dlPFC, in both monkeys and humans [102,103,186]. Essentially, both the Obj-SO and SOMT task measure the same processes, the monitoring of external stimuli, albeit in Obj-SO the subject (internal) controls the order and in SOMT the experimenter (external) controls the order. In essence, the monitoring requirement is what engages dlPFC function, irrespective of the source of stimuli order.

Serial order memory, put simply, is the process of monitoring and momentarily remembering the temporal sequence of a list of items. The implementation of a true serial order task in monkeys was driven by a desire to create a metric that would mirror the demands of the self-ordered task and by inference independently measure the function of the dorsolateral prefrontal cortex [103]. It should be noted however, that the serial order task as described by Petrides, has the added benefit of testing the functions of the dlPFC dependent and dlPFC independent working memory processes. As such, the serial order memory task exists as a useful metric to confirm previous results obtained using the self-

ordered task and offers a built in control, which enables the experimenter to infer functional specificity.

To date no studies have examined the effects of hippocampal lesions on serial order memory in the non-human primate. However, several investigators have examined the effects of hippocampal lesions on temporal order memory in the rat [170,187,188]. These previous studies found that adult lesions of the hippocampus produce a global impairment in serial order working memory, such that they are unable to discriminate between any two objects in a series. This finding is informative to the current study in terms of the interpretation of results obtained following neonatal lesions of the hippocampus in the rhesus monkey. If Neo-H monkeys are globally impaired on the serial order task, this would suggest a hippocampal effect on serial order memory. On the other hand, if we see an impairment that mirrors the findings of Petrides [102,103] it suggests that the Neo-H lesions have impacted the function of the dlPFC.

Thus, the main goal of this study will be to conclusively examine serial order memory in the non-human primate following a selective neonatal neurotoxic lesion of the hippocampus. This study will be the second though examination of working memory in monkeys with selective lesions of the hippocampus and should serve to independently confirm our finding of a dlPFC dependent working memory impairment.

Methods

Subjects

Eleven adult rhesus macaques (*Macaca mulatta)* between 6 to 8 years of age and weighing between 5 to 10kg were utilized in the current experiment. They were obtained as newborn monkeys from the University of Texas, M.D. Anderson Cancer Research

Center (Bastrop, TX) and were subsequently reared with age-matched peers in cohorts of 4 animals in the primate nursery of the M.D. Anderson Cancer Center (Houston, TX). At the age of 10 – 12 days, five infants received sham lesions (Neo-C, 2 males, 3 females) and five received neurotoxic lesions of the hippocampus (Neo-H-ibo, 4 males, 2 females).

Full details of their rearing experience have been previously published [160] and will be briefly summarized here. Upon arrival to the primate nursery, the infants were individually housed in cages that permitted visual, auditory and social contacts with other animals located in adjacent cages until they were one month of age. A plush surrogate (30cm in length) was provided to the animals and a principal human caregiver spent roughly 6 h/day, 5 days/week in the nursery with the infant monkeys. On weekends, the infants were handled 2-3 times per day and received a total of 2-4 hours of social interactions with familiar human experimenters. From three to nine months of age infants received in addition daily social interactions (3-4 hours/day, 5 days/week) with age- and sex-matched peers and from 1 – 3 years, each cohort was placed in a large social cage that allowed them to socialize 24-hrs per day. Finally, at approximately 3 years of age they were then moved to the Yerkes National Primate Research Center (Atlanta, GA) where they were individually housed and maintained on a continual 12 hour, light-day cycle (7am-7pm).

All animals were fed a diet of Purina Old World Monkey Chow which was supplemented with fresh fruit daily and were permitted unrestricted access to water throughout the duration of the experiment. During behavioral testing, access to food was minimally restricted to provide sufficient motivation to complete the behavioral

paradigm. Monkeys' weights were monitored weekly and maintained 85% or above their full feed weight.

All procedures were approved and used in full compliance with the Institutional Animal Care and Use Committees of both the University of Texas at Houston and Emory University, and were in line with the policies outlined in the NIH Guide for the care and use of Laboratory Animals (HHS publication 85-23, 1985).

Magnetic Resonance Imaging and Surgical Procedures

Details of all procedures were already reported in several recent publications [160,165,173,183]

Magnetic Resonance Imaging: All animals received three Magnetic Resonance Imaging scans (MRI's). The initial MRI was taken just prior to the surgery for all animals in both groups and served to select the injection sites of the neurotoxin injections in the hippocampus (see below). Two additional MR scans were performed after surgery and used to estimate the lesion location and extent. One was performed 5-8 days after the neurotoxin injections and allowed the visualization of edema caused by cell death and the other was performed one year post-surgery and permitted the measurement of shrinkage of the hippocampus that followed cell death. Both post-surgical MRI procedures provide a reasonable estimate of the lesion size as well as damage to structures adjacent to the target site [163]. Some animals in the current study had an additional adult (6-8 years of age) T1 scan taken for use in on-going studies, which was used here to illustrate the lesion extent (Figure 1).

Prior to the pre-surgical MRI procedure, the animal was sedated and maintained under isoflurane gas (1.0-3.0%, v/v, to effect) until the end of the surgical procedure.

The animal's head was secured in a non-ferromagnetic stereotaxic apparatus (Crist Instruments, Damascus, MD). The MR images were acquired with a GE Signa 1.5 Tesla Echo Speed scanner (GE Medical Systems, Milwaukee, WI) using a 5-cm surface coil. For the pre-surgical and first post-surgical scans, two types of MR images were obtained in the coronal plane. A series of high-resolution T1-weighted MR images (echo time (TE) = 11ms, repetition time (TR) = 450ms in contiguous 4mm sections, 12cm field of view (FOV), 256 x 256 matrix) followed by a series of Fluid Attenuated Inversion Recovery (FLAIR) images (Parameters: TE = 140ms, TR = 10,000ms, inversion time (TI) = 2200ms, contiguous 3mm sections, 14cm FOV, 256 x 256 matrix) images. The one-year post-surgical MR scans included only acquisition of the high-resolution T1-weighed images.

Surgical Procedures:

After the pre-surgical MRI, the infant was immediately transported to the surgical suite whilst maintaining anesthesia and its head fixed in the stereotaxic apparatus. Through the duration of the surgery the monkey received supplemental *i.v.* fluids (5% dextrose and 0.5% sodium chloride) to maintain good hydration. Prior to incision and after the procedure was completed the scalp was thoroughly disinfected. In order to minimize the potential risk of infection, all animals received Cefazolin (25mg/kg, i.m), swelling was monitored with dexamathasone sodium phosphate (0.3mg/kg, i.m.) and pain was alleviated with acetaminophen treatment.

After the skull was disinfected, Marcaine (25%, 1.5m, s.c.) was injected along the midline of the scalp and a skin incision was made to expose the underlying tissue and

skull. The subcutaneous tissue was dissected and retracted laterally to allow direct access to the skull. Two small crainiotomies were made bilaterally above the hippocampus and small cuts were made in the dura to expose the brain.

The neurotoxin injections for the hippocampal lesions were made simultaneously in both hemispheres with two 10µl Hamilton syringes attached to two Kopf manipulators (David Kopf Instruments Tujunga, CA). Ibotenic acid (Biosearch Technologies Novato, CA, 10mg/ml in PBS, pH 7.4) was injected at 7-8 sites along the axis of the hippocampus (0.4-0.6µl/site delivered at a rate of 0.2 µl/30 s and for a total of 2.8-4.2µl/hemisphere). At the end of the injection at each site, the needles were left in place for 3 minutes to allow for the ibotenic acid to diffuse and minimize it leaking back as the needle was removed. The sham surgeries followed the same procedures than those used for the hippocampal lesion with the exception that no needle was inserted into the brain.

Lesion Assessment

Extent of lesion for animals in Neo-H-ibo was estimated with the pre- and post-surgical scans since all animals are still undergoing behavioral testing. Extent of the hypersignal resulting from edema caused by cell death was evaluated using the pre- and post-surgical coronal FLAIR images which were first matched to drawings of histological coronal images of a normal 1-week-old infant monkeys (J. Bachevalier, unpublished data) onto which the extent of the hypersignal seen in each post-surgical FLAIR were drawn. Using the image analysis software program (ImageJ® http://rsb.info.nih.gov/ij) the total volume of damage on each slice for the intended target (hippocampus) and any unintended targets was calculated by measuring the surface area of the hypersignal on each slice and summing them. For a given structure, the sum of hypersignals calculated

from the left and right hemispheres was multiplied by the slice thickness, then divided by the total volume of the structure and finally multiply by 100 to provide a percent of extent of damage to each structure[164].

A second estimate of hippocampal damage was given by calculating the total hippocampal volume loss calculated using T-1 weighted scans taken 1 year post-surgery. The MR image, for each subject, through the full extent of the hippocampus was imported into the image analysis program ImageJ® (http://rsb.info.nih.gov/ij). On each image surface area of the hippocampus was recorded for the left and right hemispheres separately using the specific borders previously described [148]. The volume of the hippocampal formation included the CA fields, dentate gyrus, subicular complex an fimbria, but excluded the entorhinal, perirhinal, and parahippocampal cortices. For each hemisphere (separately), the hippocampal volume (in mm^3) was calculated by summing hippocampal surface areas on each image and multiplying by the distance between the images (i.e. 1 mm), using Cavalieri's principle (Gundersen and Jensen, 1987). For each animal in Group Neo-H-ibo, the hippocampal volume in each hemisphere was then compared to the averaged hippocampal volume from 6 normal male (n=3) and female (n = 3) monkeys of the same age (approximately 1 year of age). Percent volume reduction was then calculated using the following formula: [100-total H volume remaining/average H volume in normal subject]*100). Two trained observers measured the volume of hippocampal formation in normal animals and animals of Group Neo-H-ibo (Cronbach's alpha; $p < 0.01$ for all inter- and intra-observer reliabilities).

Behavioral Procedures

Before participating in the current investigation the subjects have had extensive, albeit identical testing histories. This testing consisted of: Item-specific Visual Paired Comparison (1.5, 6, 18 and 48 months; [165]), Oddity (3 and 15 months), Spatial Visual Paired Comparison (8, 24 and 54 months), Object discrimination reversals (48-60 months), Food Preference and Discrimination Devaluation task (60 months) , dyadic social interactions (3, 6, and 36 months), emotional reactivity to human intruder (2 and 4.5 months), social attachment to caregiver (9 months; [160]), and finally trial unique delayed non-matching-to-sample followed by session-unique DNMS and self-order task (5-6 years) [173,183].

All animals were trained on two versions of the serial order task. The initial version consisted of lists of three objects (3-SOMT) and the second one consisting of lists of four objects (4-SOMT). Both versions of the task were run in a manner identical to that described by Petrides (1991). In both the earlier study [103] and this one, animals had already been trained on the Trial-Unique Delayed Non-Matching-to-Sample prior to begin testing on the serial order task.

Apparatus and Stimuli

A Wisconsin General Testing Apparatus (WGTA) located in a dark room containing a white noise generator to mask distracting extraneous noise was used for behavioral testing. A testing board containing three recessed food wells (2cm in diameter, 1 cm deep and 13 centimeters apart, on center) served to display the stimuli, which were selected from a pool of 1000 junk objects that had been used to train all

animals in the Trial Unique-Delayed Non-Match to sample Task. Therefore, animals were familiar with all objects and care was taken to run through the entire series before re-using objects to preclude the subject from building associations to any given objects. In addition for each series of 3 or 4 objects care was taken to select objects that were easily discriminable from one another, so that task performance was not confounded by stimulus ambiguity. Rewards provided for correct choices were raisins or unsalted peanuts based on the animals' preference.

3-Object Serial Order Memory Task (3- SOMT)

Ten trials were administered in each daily session. Each trial used three objects and consisted of the successive presentations of the 3 objects one at a time over the central baited well at 10-s intervals, followed 10-s later by a recency judgment between 2 objects of the list. After a 30-s interval, a list consisted of three new objects was presented and so on for each following trials. Phase 1 of the 3-SOMT consisted of 10 trials in which recency judgments were between Object 1 and Object 3 of the list positioned on the lateral wells of the tray and the animal was rewarded for selecting the object appearing earlier in the list (i.e. Object 1 in this case). Left-right position of the rewarded object varied pseudo-randomly. After reaching a criterion of 80% correct or better in a single daily session, phase 2 was introduced in which 10 daily trials were given as for Phase 1 but the recency judgments were between Object 1 and Object 2. Once monkeys scored 80% correct or better on Phase 2, they were moved to Phase 3 in which recency judgments were now between Object 2 and Object 3) until animals again reached a criterion of 80% correct or better. A titration procedure was used throughout testing as described by Petrides (1991). Thus, if the animal scored 70% correct on any

given test day of a Phase, this Phase was repeated on the following day but if the animal scored 60% correct or poorer, they were moved back to a previous Phase. Thus, if failing Phase 3, animals were moved back to Phase 2, if they failed Phase 2, they were moved back to Phase 1 and if they failed Phase 1, they were moved back to trial-unique DNMS. This titration procedure was implemented to prevent the animal from being frustrated with continual poor performance on a Phase and to minimize their fixation on any single object in a series [102,103]. Testing was discontinued if an animal required 20 daily sessions at any phase of the task.

Each Phase was scored independently using the number of daily sessions required to achieve the criterion (80% or better in one session). It should be noted that when a phase was repeated if animal performed below 60%, this session was not included in the total number of daily sessions for that phase.

4 Object Serial Order Memory Task (4-SOMT)

The 4 Object version of the SOMT was run identically to the 3-object version with the difference that each series consisted of four objects. Parameters of the task were held constant (i.e. 10-s intervals between each object presentation as well as the recency judgments and 30-s delays between each series. The addition of a fourth stimulus added recency judgments and resulted in six training phases as follows: Phase 1 (Object 1 versus Object 4), Phase 2 (Object 1 versus Object 3), Phase 3 (Object 1 versus Object 2), Phase 4 (Object 2 versus Object 4), Phase 5 (Object 3 versus Object 4) and Phase 6 (Object 2 versus Object 3). As was the case with 3-SOMT, the animals progressed through the different phases of the task by achieving 80% or better on any one day of testing, repeated the phase if they achieved 70%, and moved back one phase if they score

60% or poorer. The number of daily sessions for each phase, excluding the repeat phase, served to measure performance.

4-SOMT Probe Trials

A novel inclusion in the application of the SOMT paradigm is a set of probe trials designed to require the animal to monitor all objects in the series. Probe trials were included in order to require the subject to actually track all objects in the series in a single session. As the SOMT is currently administered there is a possibility that over time the subject could learn that they only have to track a single object in a series, varying depending on task phase. In order to provide a test that would not allow this strategy to be successful we set up the following probe trials. The task was administered in the same way as the 4-SOMT, except that in half of the trials (5 trials) in the daily session were temporal judgments between Object 1 and Object 4 (i.e. as in Phase 1) and in the other half (5 trials) temporal judgments were between Object 2 and Object 3 (i.e. as in Phase 6). These two types of temporal judgments were randomized within a daily session so that the monkey would not know which discrimination problem that will occur, requiring them to track all stimuli in each list. Probe trials were run for three consecutive days giving a total of 30 trials, 15 of each discrimination types. To control for performance differences between animals, cumulative number of correct choices for each type of discriminations was converted to a ratio score in which the total number of correct responses on Problems 2-3 was divided by the total number of correct responses on Problems1-4. Thus, a ratio score of 1 or near 1 would indicate equivalent performance on both problem types, whereas a ratio less, or greater, than 1 would indicate better performance on one type of discrimination than the other.

Results

Lesion Extent

The results of the lesion reconstruction as evaluated with the FLAIR images are summarized in Table 3.1. Both cases Neo-H-ibo-2 and 3 had the most complete hippocampal lesions, averaging 67% and 87% damage to both hemispheres, respectively. Cases Neo-H-ibo-1, -4 and -5 had significant damage in one hemisphere (64%, 67% and 84%, respectively) but milder hippocampal damage (3%, 20.3% and 20.7%, respectively). Finally, the last case (Neo-H-ibo-6) had the smallest lesions, specifically located in the anterior portion of the hippocampus. As shown on Table 3.1, none of the cases had significant unintended damage to adjacent structures. This lesion estimate was also confirmed by measuring the percent hippocampal volume reduction as measured by the T1-W MR images taken 1 year after surgery (Table 3.2). Correlation between the two methods was $r = 0.805$, $p = 0.05$. The full extent of the hippocampal lesion in cases Neo-H-ibo-2, -3 and -5 is illustrated on axial MR images through the entire brain in Figure 3.1.

Table 3.1: Lesion Extent

Group	Intended Damage				Unintended Damage							
Subjects	Hippocampus				Amygdala				TH/TF			
Neo-H-ibo	L%	R%	X%	W%	L%	R%	X%	W%	L%	R%	X%	W%
Neo-H-ibo-1	63.8	2.9	33.2	1.8	14.0	0.0	7.0	0.0	3.1	0.5	1.8	0.0
Neo-H-ibo-2	54.4	80.9	67.6	44.0	0.0	0.0	0.0	0.0	21.4	2.7	12.1	0.6
Neo-H-ibo-3	78.5	96.3	87.4	75.6	1.7	0.0	0.8	0.0	6.1	5.5	5.8	0.3
Neo-H-ibo-4	20.3	67.3	43.8	13.6	0.0	4.7	2.4	0.0	15.3	0.0	7.6	0.0
Neo-H-ibo-5	20.7	84.0	52.6	17.5	0.0	4.9	2.5	0.0	6.1	4.0	5.1	0.2
Neo-H-ibo-6	7.9	0.0	3.9	0.0	0.0	0.0	0.0	0.0	0.0	0.0	0.0	0.0
Mean	**40.9**	**55.2**	**48.0**	**25.4**	**2.6**	**1.6**	**2.1**	**0.0**	**8.6**	**2.1**	**5.4**	**0.1**

Note: L% percent damage in the left hemisphere; R%: percent damage in the right hemisphere; X% average damage to both hemispheres; W%: weighted average damage to both hemispheres (W% = L% x R%)/100; weighted index as defined by Hodos and Bobko [168]). Mean: average damage per group; TH/TF: ventral cortical area of the temporal lobe as defined by Bonin and Bailey, 1947)

Table 3.2: Volumetric Reduction of the Hippocampus

Group	Volume Reduction			
Subjects	Hippocampus			
Neo-H-ibo	L%	R%	X%	% Remaining
Neo-H-ibo-1	27.6	10.6	19.1	80.8
Neo-H-ibo-2	61.1	72.8	67.0	33.0
Neo-H-ibo-3	54.7	47.8	51.3	48.7
Neo-H-ibo-4	33.6	61.6	47.6	52.3
Neo-H-ibo-5	49.1	64.0	56.6	43.4
Neo-H-ibo-6	21.3	8.3	14.8	85.2
Mean	**41.2**	**44.1**	**42.7**	**57.2**

L% = Percent reduction of hippocampal volume and left hemisphere, R% = Percent reduction of hippocampal volume and right hemisphere, X% = Average percent reduction in both hemispheres and % Remaining = tissue still visible in the T1 despite hippocampal lesion

Figure 3.1: Transverse MRI sections of Neo-H-ibo lesion.

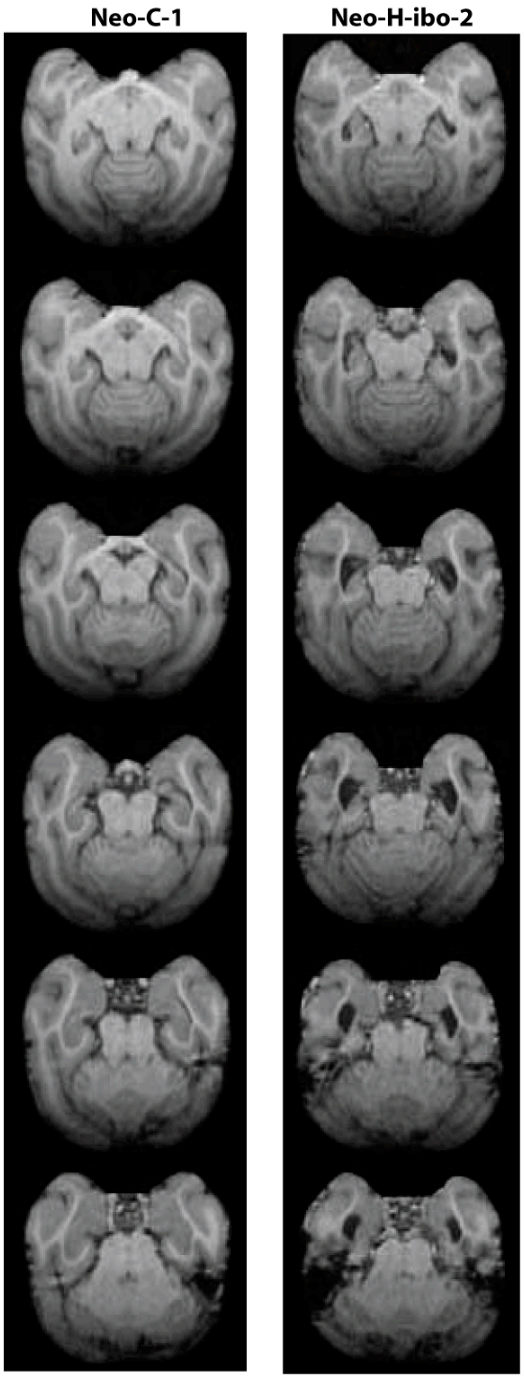

The figure depicts serial Magnetic Resonance Imaging sections (T1 weighted) in the horizontal plane of normal control monkey (Neo-C-1) and a monkey with a neonatal lesion of the hippocampus (Neo-H-ibo). In comparing the two series the lesion is clearly visible throughout all levels of the hippocampus, supporting the estimated lesion extent calculated from the FLAIR images.

Behavioral Measures

3-SOMT

The results of the 3-SOMT for monkeys with neonatal lesions of the hippocampus and sham operated controls are displayed in Figure 3.2. All subjects readily met criterion within the allotted number of sessions (20 per phase). Across the three phases of the 3-SOMT monkeys with neonatal lesions of the hippocampus and sham operated control subjects averaged 1, 5 and 2 sessions to criterion across the first three phases of the task, respectively. Pair-wise comparisons found that all subjects took more sessions to complete Phase 2 [$Z = 2.667$, $p < 0.01$] and Phase 3 [$Z = 1.983$, $p < 0.05$] than Phase 1. However, no differences in session to criterion were detected between Phase 2 and 3 [$Z = 1.548$, $p > 0.05$]. The data also demonstrated that early hippocampal lesions produced no impairment in any phase of the 3-SOMT: Phase 1 ($U= 0.833$, $p = 0.361$), Phase 2 ($U= 0.308$, $p = 0.579$) or Phase 3 ($U= 0.150$, $p = 0.698$). These results show that early lesions of the hippocampus are insufficient to impair performance on any aspect of the 3-SOMT.

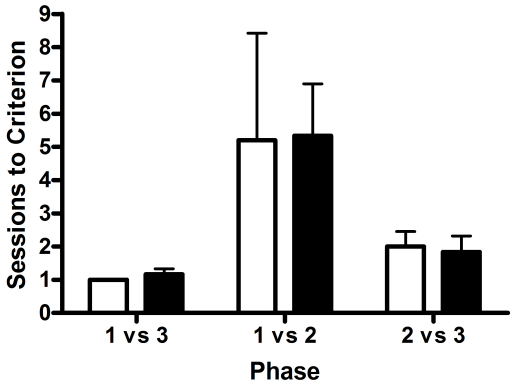

Figure 3.2: 3 Object Serial Order Memory Task-Sessions to Criterion. The graph shows the data collected on the 3-SOMT for sham operated controls (white bars) and neonatal hippocampal lesioned monkeys (black bars). As shown, no differences were detected in the number of sessions taken to achieve criterion in any phase of the task. Error bars are standard error of the mean (S.E.M.).

4-SOMT

The results of the 4-SOMT for animals with neonatal lesions of the hippocampus (Neo-H-ibo) and sham operated controls (Neo-C) are displayed in Figure 3.3. The two groups did not reliably differ in any of the Phases, except for Phase 6. Thus, both Groups Neo-H-ibo and Neo-C averaged 1 session to criterion in Phase 1 ($U= 1.20$, $p = 0.273$), 3 versus 4 sessions for Phase 2 ($U= 2.012$, $p = 0.156$) and Phase 3 ($U=1.468$, $p = 0.226$), 1 versus 2 sessions for Phase 4 ($U=0.222$, $p = 0.637$), and 2 session for both in Phase 5 ($U=3.033$, $p = 0.082$). However, for Phase 6 Group Neo-H-ibo took significantly more sessions (average: 5) as compared to Group Neo-C (average: 1 session), yielding a significant group difference ($U= 8.418$, $p = 0.004$). Thus, animals with neonatal hippocampal lesions were specifically impaired in making temporal order judgments between objects in the middle of the list (i.e. 2 vs 3) but not on those including either the first object or the last object of the list (i.e. 1-2, 1-3, 1-4, 2-4, 3-4).

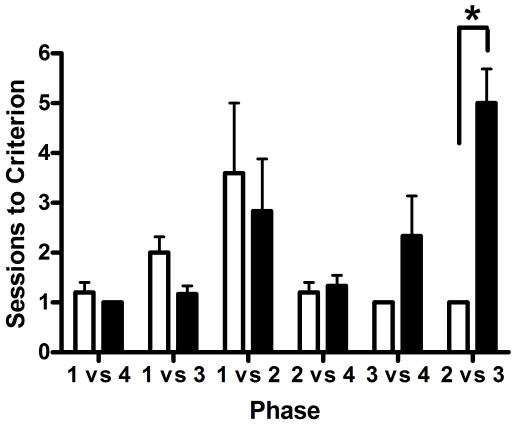

Figure 3.3: 4 Object Serial Order Memory Task- Sessions to Criterion. The graph shows the data collected on the 4-SOMT for sham operated controls (white bars) and neonatal hippocampal lesioned monkeys (black bars). Subjects performed comparably on Phases 1-5 of the task but Neo-H-ibo animals showed a severe impairment on Phase 6, (* $p = 0.004$). Error bars are standard error of the mean (S.E.M.).

4-SOMT Probe Trials

The results obtained with testing on probe trials are shown in Figure 3.4 and confirmed the specificity of the temporal order memory impairment of animals with neonatal hippocampal lesions. Ratio score for Group Neo-C averaged 1.04, suggesting that animals made as many correct choices on temporal judgments between objects 1 and 4 of the list than between objects 2-3. By contrast, Group Neo-H-ibo obtained an averaged ratio score of 0.65, indicating that the animals made more correct choices on temporal judgments between objects 1 and 4 than between objects 2 and 3. This group difference reached significance [$t(1,9) = 4.147$, $p = 0.002$).

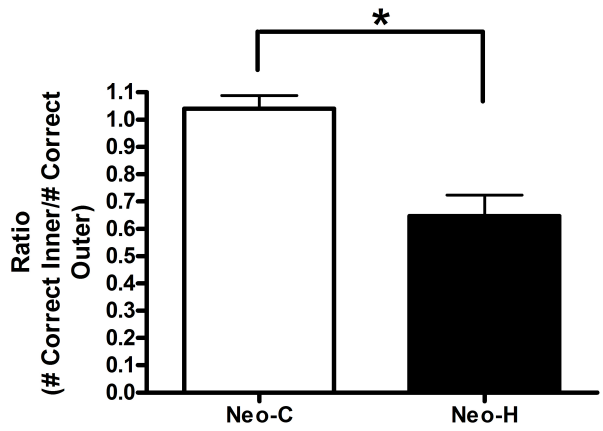

Figure 3.4: 4 Object Serial Order Memory Task Probe Trials. The graph depicts a ratio of scores for sham operated controls (white bars) and neonatal hippocampal lesioned monkeys (black bars). In this case, the cumulative correct response on the inner object discrimination (2 vs 3) was divided by the number of correct responses on the outer discrimination (1 vs 4), for the three-day probe session. A score near one indicates equivalent performance on the two trial types, whereas a score below one indicates poor performance on the inner object discrimination. As shown, monkeys with neonatal lesions of the hippocampus were severely impaired on the inner object discrimination (* $p = 0.002$), relative to controls and to their own performance on the outer object discrimination.

Correlation of Lesion and Behavior

As a way to examine the relationship between lesion extent and behavior a correlation analysis was performed using all behavioral measures and the lesion extent as measured from the FLAIR images. The only significant correlation detected was that mean bilateral damage to the hippocampus was directly related to the ratio score on the probe trials ($r = 0.820$, $p = 0.046$). However, this correlation was clearly driven by the lack of impairment as Neo-H-3 as it does not reach significance when this animal is removed from the analysis ($r = 0.698$, $p = 0.199$).

Discussion

The goal of the current investigation was to measure serial order memory in monkeys with early lesions of the hippocampus. It was determined that neonatal lesions of the hippocampus were not sufficient to impair performance on the 3-SOMT task, as expected. In contrast, Neo-H were found to be impaired on the dlPFC dependent phase of the 4-SOMT task. The impairment on the 4-SOMT task was confirmed by the 4-SOMT probe test, indicating that Neo-H monkeys are impaired in serial order memory.

In the original serial order study performed by Petrides [103] it was determined that focal dlPFC lesions but not posterior lateral PFC lesions were sufficient to severely impair performance on the 4-SOMT. These monkeys were unable to achieve criterion on Phase 6 (Object 2 vs 3) and testing was terminated after 20 sessions. The current experiment found that Neo-H monkeys were also impaired on Phase 6 of the 4-SOMT, however they eventually all achieved criterion. The difference between our animals and that of Petrides lies in that in damaging the hippocampus early in life we likely reduced dopamine transmission to the prefrontal cortex [69], which while detrimental to working memory function [135,137,138,176] is not equivalent to a prefrontal lesion. Thus, the difference in our data likely indicate that our animals eventually learned that they only had to pay attention to one object in the series, to successfully complete any discrimination and used this adaptive strategy to complete Phase 6. For this reason the probe trials became particularly valuable in demonstrating the consequences of a Neo-H lesion on serial order memory. In the probe, subjects had to attend to all objects in the series as they did not know which recency discrimination they would face on any particular trial. As a result,

while normal animals completed outer (1 vs 4) and inner (2 vs 3) object discriminations with equal accuracy, Neo-H fell to chance on inner object discriminations. Thus, this specific deficit in serial order working memory confirms our earlier finding of dlPFC dependent working memory dysfunction following early lesions of the hippocampus in the rhesus macaque.

The case of Neo-H-3 is particularly puzzling as this animal was not impaired on any component of serial order memory, in contrast to the other five animals of the lesion group. A thorough examination of the animals' lesion and behavioral data provided no potential explanation for why this single animal was so different than the rest of the lesion group. However, in the previous investigation [183] this same animal also showed no impairment on monitoring working memory, also in contrast to the rest of the lesion group. The fact that this animal showed no impairment on two independent measures of monitoring working memory suggests that the hippocampal lesion was not sufficient to impair dlPFC function in this one animal. In order to ascertain exactly what sets this one animal apart from the rest of the lesion group a post-mortem investigation into the lesion and the prefrontal cortex will be essential.

In comparing the results of the current study to rodent studies of serial order memory it is clear that the studies have addressed different cognitive functions. Previous studies by Kesner and colleagues showed that lesions of the hippocampus, in the rat, produce a global impairment temporal order judgments [95,170,188]. If the hippocampus was playing a similar role in the primate we would have seen impairments on the 3-SOMT and all phases of the 4-SOMT, would be indicative of a global impairment in working memory. However, the fact that we saw a selective impairment in working memory,

similar to what is seen following dlPFC lesions, suggests that the role of the hippocampus in serial order memory is different in rodents and primates. Also, considering that neonatal hippocampal lesions impaired only the dlPFC dependent 4-SOMT suggests that the dlPFC is likely eliciting hippocampal involvement in a top-down manner, likely through the rhinal or retrosplenial cortices [118,124].

The results of this paper support the neonatal hippocampal lesion model of schizophrenia, which has shown a great deal of promise in the rodent literature. Previous studies in the rodent schizophrenia model have shown extensive similarity to the disease state including: working memory deficits [79,80], hyper-locomotion [77,78], reduced n-acetyl-aspartate in the medial prefrontal cortex [88] and alterations in pre-pulse inhibition [72]. Cumulatively, the previous findings in the Neo-H model support the assertion that the early lesion creates a disconnect between the prefrontal cortex and the hippocampus, that mimics what is observed in schizophrenia [34,47,66]. The results of this study support the argument that the Neo-H model is tenable in the primate although further tests of prefrontal integrity should be performed prior to making any claims of certainty.

In conclusion, this study confirms our earlier finding that early lesions of the hippocampus, in the primate, are sufficient to impair working memory function dependent upon the dorsolateral prefrontal cortex. As such, future efforts should be made to characterize the nature of this impairment and its' neural substrates.

Chapter 4

Magnetic resonance spectroscopy and its' relation to working memory in adult monkeys with neonatal lesions of the hippocampus.

Introduction

In the rodent literature a preponderance of evidence suggests that early damage to the hippocampus is sufficient to impact the function of the prefrontal cortex as evidenced by impairments in the radial arm maze, continuous alternation and win-shift tasks [79-81]. Further, it has been demonstrated that early lesions of the hippocampus are sufficient to impact the functional integrity of the prefrontal cortex as assessed by neuroimaging

(reduced n-acetyl aspartate as measured by magnetic resonance spectroscopy), neurochemical (reduced GAD-67, the rate limiting enzyme in GABA synthesis) and electrophysiological measures (abnormal neuronal responsivity to dopaminergic stimulation [84-88]. However, the ability of this information to be translated to the human is inherently limited due to the differences in rodent prefrontal cortical architecture and capacity [5,90,91]. As such, it is important to determine if early hippocampal damage, in the primate, is sufficient to impact the functional integrity of the prefrontal cortex.

A recent line of work in our laboratory has focused on examining working memory processes in a cohort of adult rhesus monkeys with neonatal lesions of the hippocampus (Neo-H, and sham operated control subjects (Neo-C) [183,189]. The first study indicated that Neo-H lesions impaired monitoring working memory process dependent upon the dorsolateral prefrontal cortex (dlPFC), as measured by the Object Self Ordered task [101,102]. In contrast, maintenance working memory process dependent upon the ventrolateral prefrontal cortex [190], was unimpaired by the same neonatal lesions. To confirm these findings, the second study assessed dlPFC monitoring working memory process using the serial order memory task. The findings again demonstrated that Neo-H monkeys were impaired on the dlPFC dependent components of the 4-object serial order memory task, specifically in making recency judgments between objects in the middle of a four object series (Object 2 vs Object 3) but not on recency judgments involving the first or last items of the list. . Together, these neurobehavioral studies showed that early lesions of the hippocampus in monkeys altered working memory processes dependent upon the dorsolateral prefrontal cortex (dlPFC), but spared working memory processes dependent upon the ventrolateral prefrontal cortex (vlPFC). The data thus suggest that

the neonatal hippocampal lesions might have impacted the functional maturation of the dorsolateral prefrontal cortex. We tested this possibility using noninvasive neuroimaginig procedures. Recent advances in neuroimaging studies have highlighted the advantages of using Magnetic Resonance Spectroscopy (MRS) as a reliable and accurate *in vivo* measure of neuronal integrity. The primary metabolite obtained from ^{1}H-MRS is n-acetyl-aspartate (NAA), which is a known marker of neuronal integrity and has been utilized to study pathology associated with psychiatric diseases [191,192]. This technique is particularly attractive in translational approach because it offers a way to non-invasively measure neurochemical alterations in the brain without having to administer potentially dangerous isotopes as is the case with positron emission tomography. This technique is also advantageous for comparing the spectroscopy data from the animal model to those reported in schizophrenia [21,22,45,46,193-195]. Changes in NAA levels in the prefrontal cortex have already been reported after large neonatal medial temporal lobe lesions in monkeys [196], although these changes could not be associated with hippocampal damage since the neonatal lesions included also the amygdala and adjacent cortical areas and the prefrontal cortex voxels used for the MRS analysis were relatively large including several regions of the prefrontal cortex.

Thus, the goal of the current experiment was to examine changes in NAA lesels in the prefrontal cortex (both dorsal and ventral) that may have resulted from early damage to the hippocampus, using Magnetic resonance spectroscopy.

Methods

Subjects

Eight adult rhesus macaques (*Macaca mulatta)* between 6 to 8 years of age and weighing between 5 to 10kg were utilized in the current experiment. They were acquired as newborns from the University of Texas, M.D. Anderson Cancer Research Center (Bastrop, TX) and were subsequently surrogate-nursery-reared with age-matched peers in cohorts of four monkeys, the full details of which have been published previously [160]. Briefly, once arriving at the center the animals were individually housed but permitted social contacts with other animals in adjoining cages by one month of age. In addition, a plush surrogate was provided to the animals of approximately 30cm in length. A principal human caregiver spent roughly 6 h/day, 5 days/week in the nursery with the infant monkeys. On weekends, the infants were handled 2-3 times per day and received a total of 2-4 hours of social interactions with familiar experimenters. From the three to nine months of age infants received daily social interactions for 3-4 hours, 5 days/week with age/sexmatched peers. After arrival at the research facility, the monkeys were split into one of two groups: Sham operated control lesion (Neo-C, 2 males, 2 females) or neonatal neurotoxic lesions of the hippocampus (Neo-H-ibo, 4 males). All surgeries were performed between 10 to 15 days of age.

For the duration of the present experiment all animals were individually housed at the Yerkes National Primate Research Center (Atlanta, GA) and maintained on a continual 12 hour, light-day cycle (7am-7pm). They were fed a diet of Purina Old World Monkey Chow, which was supplemented with fresh fruit daily. All animals were

permitted unrestricted access to food and water throughout the duration of the experiment.

All procedures in the current study were approved and in full compliance with the Institutional Animal Care and Use Committees of both the University of Texas at Houston and Emory University, as well as being in line with the policies outlined in the NIH Guide for the care and use of Laboratory Animals (HHS publication 85-23, 1985).

Magnetic Resonance Imaging and Surgical Procedures

Because the MRI-guided surgical procedures were thoroughly described is several recent publications [160,165,183,189], they will be briefly summarized here. Under anesthesia (isoflurane, 1-2% to effect) and with the animal's head secured in a stereotaxic apparatus (Crist Instruments, Damascus, MD), three Magnetic Resonance Imaging scans (MRI's) were acquired with a GE Signa 1.5 Tesla Echo Speed scanner (GE Medical Systems, Milwaukee, WI) using a 3" surface coil. All scans were obtained on the coronal plane through the entire brain and included either one T1-weighed high resolution structural scans (TE/TR = 2.6 ms, 10.2 ms, 25° flip angle, contiguous 1 mm sections, 12 cm FOV, 256 x 256 matrix), three Fluid Attenuation Inversion Recovery (FLAIR) scans (TE/TR/TI = 140ms, 10,000ms, 2200ms, contiguous 3mm sections offset by 1mm posteriorly, 14cm FOV, 256 x 256 matrix) or both. The initial MRI was taken just prior to the surgery for all animals in both groups and the T1-W images served to select the injection sites through the entire length of the hippocampus and to calculate their coordinates in the anterior-posterior, medial-lateral and dorsal-ventral planes. The second scan was performed at approximately one to two weeks after surgery and T1-W and FLAIR images

were compared to those taken prior to surgery to estimate the extent of hypersignals caused by edema resulting from cell death. Finally, a third scan taken approximately one year after surgery used only the T1-W images that were compared to T1-W images of an age-matched normal animals to estimate the volume reduction of the hippocampus and was used as a second estimate of the extent of the lesions.

After the pre-surgical MRI, the infant was moved to the surgical suite whilst maintaining anesthesia and the head remaining fixed in the stereotaxic apparatus. Through the duration of the surgery, the monkey was placed on a heating pad, received supplemental *i.v.* fluids (5% dextrose and 0.5% sodium chloride) and their vital signals (heart and respiration rate, expired Co2 and temperature) were continuously monitores. The skull was disinfected and Marcaine (25%, 1.5m, s.c.) was injected along the midline incision, which was made to expose the underlying subcutaneous tissue and then the skull under aseptic conditions. Two small craniotomies were made bilaterally just above the injection sites. For the neurotoxin injections in the hippocampus, ibotenic acid (Biosearch Technologies Novato, CA, 10mg/ml in PBS, pH 7.4) was injected in 7-8 sites along the axis of the hippocampus (0.4-0.6µl/site for a total of 2.8-4.2µl/hemisphere). Injections were made simultaneously in both hemispheres using two 10µl Hamilton syringes attached to Kopf manipulators (David Kopf Instruments Tujunga, CA). After the injection at each site the needles were left in place for 3 minutes to allow for the ibotenic acid to diffuse and minimize it for leaking back in the needle track.

Sham Surgeries

The sham surgeries followed the same procedures, except that no needles were inserted into the brain.

The wound was then closed in anatomical layer and the monkey recovered in the surgical suite until it could breathe on its own. Twelve prior to surgery and 5-7 days after surgery, all animals received Cefazolin (25mg/kg, i.m) to minimize infection, dexamathasone sodium phosphate (0.3mg/kg, i.m.) to reduce swelling, and acetaminophen to manage pain.

MRI-based Lesion Extent

Extent of hippocampal lesions for each animal in Group Neo-H-ibo was estimated using the MRI images. The procedures for the lesion estimate as well as the description of the hippocampal lesion extent for the four cases used in this study have been described thoroughly in several recent reports [160,163,165,183,189] and will not be provided here. An estimate of the lesion for each case is summarized in Tables 4.1 and 4.2. Two of the four animals (Neo-H-2 and 4) had fairly extensive hippocampal lesions, averaging 68% and 44% of hypersignals, respectively and resulting in an average of 68% and 48% reduction in hippocampal volume. Neo-H-1 a fairly unilateral lesion with an estimated 64% of hypersignals (28% volume reduction) in the left hemisphere, as compared to 3% of hypersignals (11% volume reduction) in the right hemisphere. Finally, Neo-H-6 had the smallest lesion of the group, averaging 8% of hypersingals (21% volume reduction) in the left hemisphere and no visible hypersignals (8% volume reduction) in the right hemisphere.

Table 4.1: Lesion Extent

Group	Intended Damage				Unintended Damage							
Subjects	**Hippocampus**				**Amygdala**				**TH/TF**			
Neo-H-ibo	L%	R%	X%	W%	L%	R%	X%	W%	L%	R%	X%	W%
Neo-H-1	63.8	2.9	33.2	1.8	14.0	0.0	7.0	0.0	3.1	0.5	1.8	0.0
Neo-H-2	54.4	80.9	67.6	44.0	0.0	0.0	0.0	0.0	21.4	2.7	12.1	0.6
Neo-H-4	20.3	67.3	43.8	13.6	0.0	4.7	2.4	0.0	15.3	0.0	7.6	0.0
Neo-H-6	7.9	0.0	3.9	0.0	0.0	0.0	0.0	0.0	0.0	0.0	0.0	0.0
Mean	**36.6**	**37.8**	**37.1**	**14.8**	**3.5**	**1.2**	**2.4**	**0.0**	**9.9**	**0.8**	**5.3**	**0.1**

Note: L% percent damage in the left hemisphere; R%: percent damage in the right hemisphere; X% average damage to both hemispheres; W%: weighted average damage to both hemispheres (W% = L% x R%)/100; weighted index as defined by Hodos and Bobko [168]). Mean: average damage per group; TH/TF: ventral cortical area of the temporal lobe as defined by Bonin and Bailey, 1947)

Table 4.2: Volumetric Reduction of the Hippocampus

Group	Volume Reduction		
Subjects	**Hippocampus**		
Neo-H-ibo	L%	R%	X%
Neo-H-1	27.6	10.6	19.1
Neo-H-2	61.1	72.8	67.0
Neo-H-4	33.6	61.6	47.6
Neo-H-6	21.3	8.3	14.8
Mean	**35.9**	**38.3**	**37.1**

L% = Percent reduction of hippocampal volume and left hemisphere, R% = Percent reduction of hippocampal volume and right hemisphere, X% = Average percent reduction in both hemispheres

Magnetic Resonance Spectroscopy (MRS)

Pre-Imaging Preparation:

The animal was sedated with telazol (3 mg/kg *i.m.*), intubated with an endotracheal cathether and maintained on isoflurane (1-2% to effect) anesthesia during the entire neuroimaging procedure. An *i.v.* line containing 0.9% physiological saline was placed in the sural vein to maintain the animal hydrated through the procedure and ELMA cream was given to the eye sockets and inside the ears as an analgesic. The animal's head was then secured into a non-ferromagnetic stereotaxic apparatus (Crist Instruments, Damascus, MD) and the animal was transferred to the scanner. All vital signs were continuously monitored including: heart rate, blood pressure, core temperature and expired CO_2.

Each scanning session lasted approximately six hours, during which a high-resolution structural scan (T1) followed by single-voxel, localized proton MR spectroscopy to identify robust relative changes in metabolite concentrations for a total of five volumes of interest, i.e. left and right dorsolateral prefrontal cortex (dlPFC), left and right ventrolateral prefrontal cortex (vlPFC) and right primary somatosensory cortex (S1).

Image Acquisition and Analysis:

All MRI scans were acquired on a 3.0T Siemens Clinical Scanner using a 2-channel surface coil. Initially, a high-resolution T1 whole-brain structural scan was collected using the same parameters as the 1-year post-surgical scan (see above). This scan allowed to reliably placing the voxels for spectroscopy.. All volumes of interest (VOI's) were comprised of a three dimensional volume of 5mm x 5mm x 5mm. The T1 coronal sections were used to position the voxel in each VOI. The dlPFC VOI (Fig.

4.1A) was placed dorsal to the principal sulcus, within the middle of its rostral-caudal extent, defined as the mid-dlPFC by Petrides [5]. The vlPFC VOI (Fig. 4.1B) was placed ventral to the principal sulcus and lateral to the lateral orbital sulcus. The S1 VOI (Fig. 4.1C) was placed ventral-lateral to the central sulcus. Given the inherent individual variability in brain surface, all efforts were made to ensure that the voxel for a given VOI was not overlying a sulcus to maximize tissue sampling and minimize signal from cerebrospinal fluid.

Localized volume shimming was performed manually to minimize the local field-inhomogeneity and achieve efficient water suppression with the CHESS method. Spectra with and without water suppression was obtained for correction of eddy current-induced spectral distortion. Water-suppressed proton MR spectra parameters: TE = 30 ms, TR = 1.5 s, VOI = 0.2 μL, spectral bandwidth = 2000 Hz, points per FID = 1024, number of averages = 300 with phase cycling. Spectra without water suppression were acquired with similar parameters but with 10 averages. Acquired spectra were processed and analyzed with LC-Model (http://s-provencher.com), a software platform specifically designed for *in vivo* MRS analysis.

The focus of this work was placed onto absolute concentrations of n-acetyl-aspartate (NAA), a known marker of neuronal integrity and functionality [191]. Although previous studies have utilized ratios of NAA to creatine, LC-Model permits absolute quantification of NAA via a comparison with the water signal. For each VOI, NAA data were then compared between groups and then correlated with behavioral data obtained from the same animals on the serial temporal order working memory task [189]. The serial

order memory task assesses dlPFC dependent and dlPFC independent working memory processes, using variations of the same paradigm [102,103].

Statistical Analysis

Group differences in NAA levels for each region of interest were analyzed with independent samples t-tests corrected for multiple comparisons. Correlations between NAA levels, lesion extent and behavior were assessed using a correlation matrix (Pearson's r).

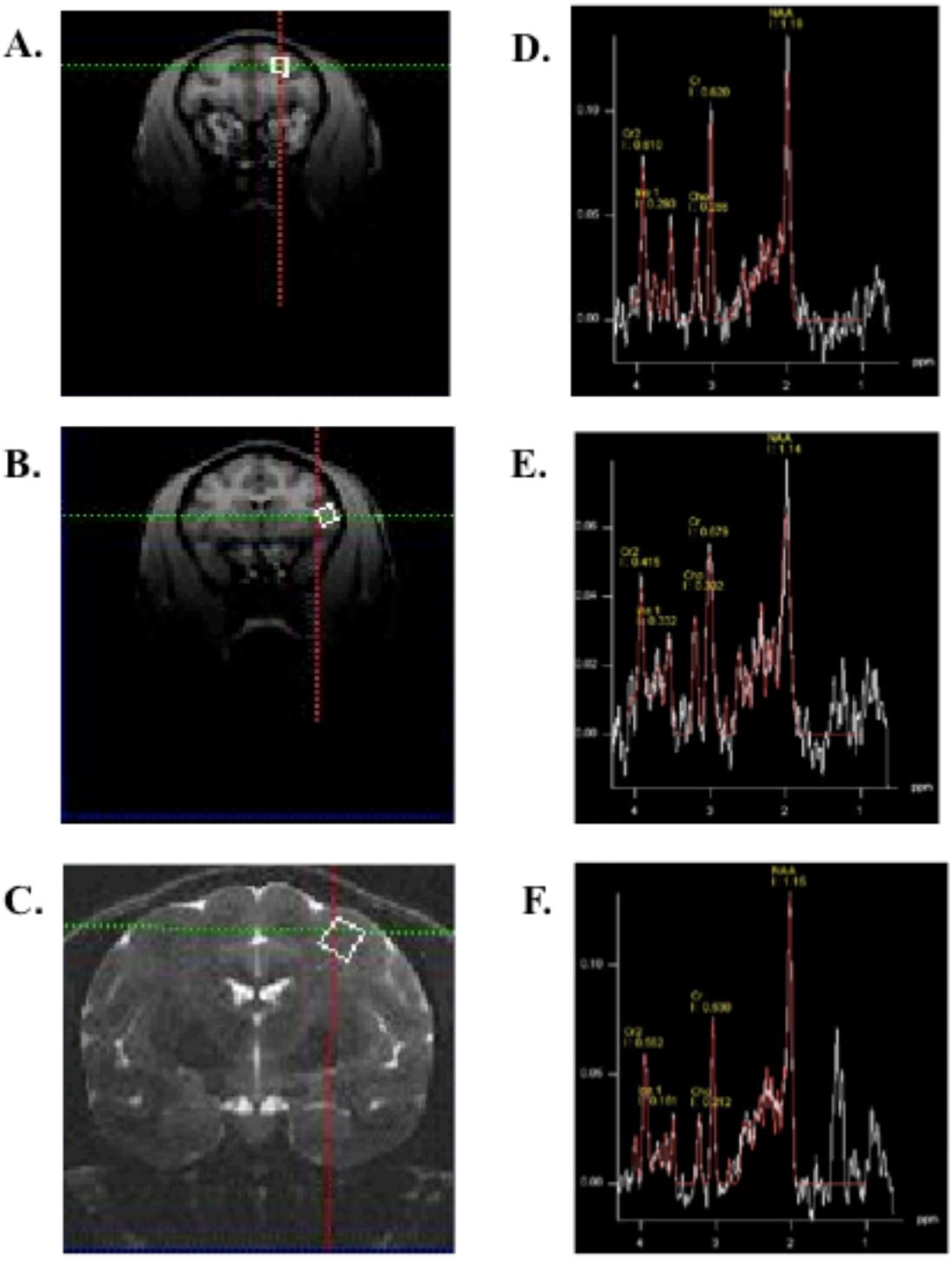

Figure 4.1: Sample MRS Spectra and Voxel Placement. This figure shows the placement of voxels (left column) and raw uncorrected spectra from a representative case (Neo-C-1) for the dlPFC (A and D), vlPFC (B and E) and S1 (C and F). Note: The voxel placments for A and B were performed on a T1 weighted image, whereas voxel placement for C was performed on a T2 weighted image.

Results

NAA was quantified (mmol/L) within five regions of interest in all animals, except case Neo-H-ibo-1 for which the right vlPFC spectra could not be reliably obtained due to the limited amount of vlPFC tissue just lateral to the lateral orbital sulcus. Examples of NAA spectra obtained for each region of interest are shown in Figure 4.1 (D, E, and F) in a representative case (Neo-C-1).

NAA in the Dorsolateral prefrontal cortex

Figure 4.2 shows absolute NAA levels within the left and right dlPFC of animals in both groups. Animals with neonatal hippocampal lesions obtained NAA levels similar to those of the sham-operated controls for both the right [X: Neo-C = 8.19 ± 0.794 and Neo-H = 7.08 ± 1.378; $t(1, 6) = 1.403$, $p = 0.210$] or left [X: Neo-C = 8.72 ± 0.790 and Neo-H = 7.09 ± 2.512; $t(1,6) = 1.240$, $p = 0.261$] dlPFC . However, it should be noticed that, in the left hemisphere, NAA levels in Group Neo-H-ibo showed a greater variability than those of sham-operated controls, with one animal showing NAA levels below and another one showing NAA levels above the controls' NAA levels. To examine whether this variability may have resulted from variations in lesion extent and/or task performance, correlations were made between NAA levels and these two parameters. NAA levels in the left [$r = - 0.132$, $p = 0.868$] or right [$r = 0.244$, $p = 0.756$] dlPFC did not correlate with hippocampal lesion extent estimated from the post-surgical FLAIR MRI (see Table 4.1). However, as shown in Figure 4.3A, NAA levels in the left hemisphere of animals with neonatal lesions correlated with performance on the 4-SOMT working memory task (2 vs 3 pairings, see Table 4.3). Thus, the NAA individual

variations in the left dlPFC for Group Neo-H-ibo indicated that lower NAA levels were related with better performance on the task. No such relationship was observed between dlPFC NAA levels and task performance in control subjects (Figure 4.3B). In contrast, no relationship was found between right dlPFC NAA and performance on the 4-SOMT (2 vs 3 discriminations) for either Neo-H-ibo [r = 0.490, p = 0.510] or Neo-C [not calculated because performance on 2 vs 3 was identical for all 4 sham-operated controls].

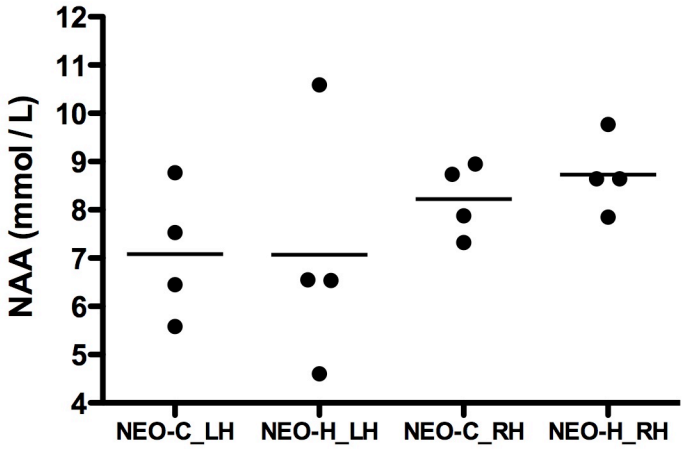

Figure 4.2: NAA within the dlPFC. The above graph shows n-acetyl-aspartate levels for the right and left hemispheres dlPFC for groups Neo-C and Neo-H. No differences in NAA levels were detected between groups in either hemisphere. However, in the left hemisphere group Neo-H seems to show more variability in NAA, with one subject below and one subject above control NAA levels. To examine the variability of NAA, correlations between NAA, lesion extent and behavior were performed. Bars indicate group means.

Table 4.3: Serial Order Memory Task

Subjects	4-SOMT						4-SOMT Probe	
Neo-C	**1vs4**	**1vs3**	**1vs2**	**2vs4**	**3vs4**	**2vs3**	**Outer**	**Inner**
Neo-C-1	2	2	9	1	1	1	12	13
Neo-C-3	1	1	3	1	1	1	11	11
Neo-C-5	1	1	3	1	1	1	10	12
Neo-C-6	1	2	3	1	1	1	12	12
Mean	**1.2**	**1.5**	**4.5**	**1**	**1**	**1**	**11.2**	**12**
Neo-H-ibo								
Neo-H-ibo-1	1	1	1	1	1	8	13	7
Neo-H-ibo-2	1	1	7	1	6	5	13	8
Neo-H-ibo-4	1	1	1	1	1	3	15	8
Neo-H-ibo-6	1	1	1	1	2	5	12	6
Mean	**4**	**4**	**2.5**	**4**	**2.5**	**5.2**	**13.2**	**7.2**

Session to criterion are shown for the 4-Object Serial Order Memory Task (SOMT) and the 4-Object Serial Order Memory Task Probe Trials (4-SOMT Probe) for all subjects in the current investigation.

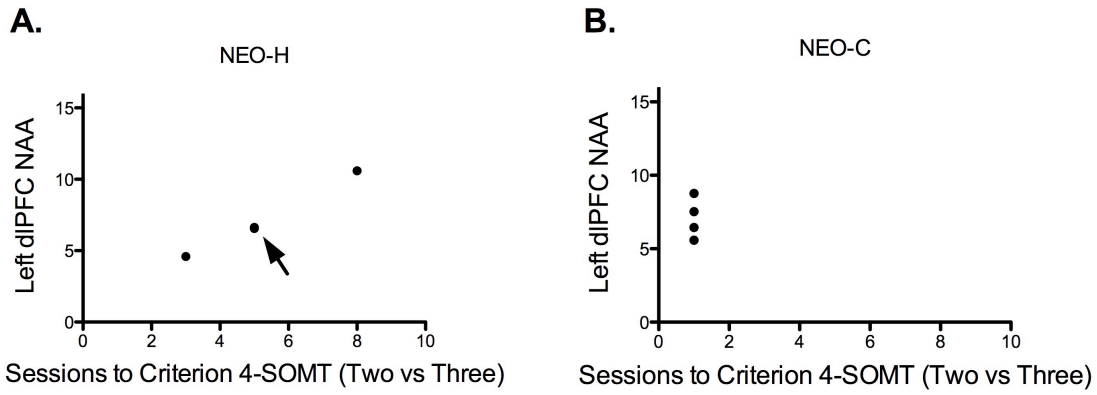

Figure 4.3: Correlation between Left dlPFC NAA and 4-SOMT Performance. The above figure shows correlations between NAA in the left dlPFC of Neo-H (A.) and sham-operated control subjects (B). As shown (A), a direct relationship between NAA levels in the dlPFC and performance on the dlPFC dependent NAA exists following neonatal lesions of the hippocampus ($r = 0.996$, $p = 0.004$). In contrast, no relationship was observed between dlPFC NAA in control subjects (correlation not performed because sessions to criterion was constant). In comparing the two data sets it is clear that the NAA levels have been altered, such that Neo-H animals with levels of NAA comparable to controls are impaired on the dlPFC dependent behavioral task. The arrow indicates two overlapping data points.

NAA in the ventrolateral prefrontal cortex

Figure 4.4 shows absolute NAA levels (mmol/L) for the left and right ventrolateral prefrontal cortex. Within the left vlPFC, Group Neo-H-ibo obtained NAA levels ($X = 8.67 \pm 0.854$) greater than those of Group Neo-C ($X = 7.52 \pm 0.166$), as revealed by a significant group difference [$t(1,6) = 2.650$, $p = 0.03$] . By contrast, no group differences were detected in the right hemisphere [$X = 7.54, \pm 1.528$ and $X = 7.43, \pm 0.320$, for groups Neo-H-ibo and Neo-C, respectively; $t(1,5) = 0.120$, $p = 0.909$]. To determine whether the lack of group differences in the right vlPFC may have resulted from an outlier value in Group Neo-C, correlations were performed between the right and the left NAA levels in the vlPFC of both Groups Neo-H and Neo-C. There was a positive correlation between the left and right vlPFC NAA levels for animals with neonatal hippocampal lesions ($r = 0.998$, $p = 0.037$, see Figure 5.5A) but not for the sham-operated controls($r = - 0.252$, $p = 0.748$, see Figure 5C).

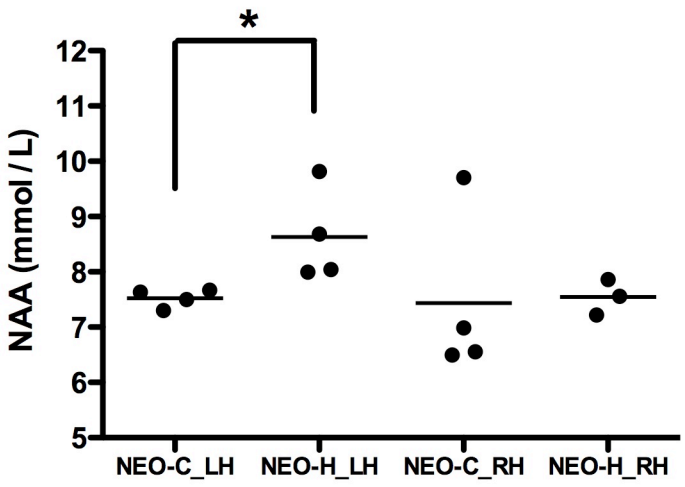

Figure 4.4: NAA within the vlPFC. The above graphs show correlations between NAA levels of the left and right hemisphere for groups Neo-H (A) and Neo-C (B). As show, NAA levels in the vlPFC correlate highly with one another in group Neo-H [r = 0.998, p = 0.037] but not in group Neo-C [r = 0.252, p = 0.748].

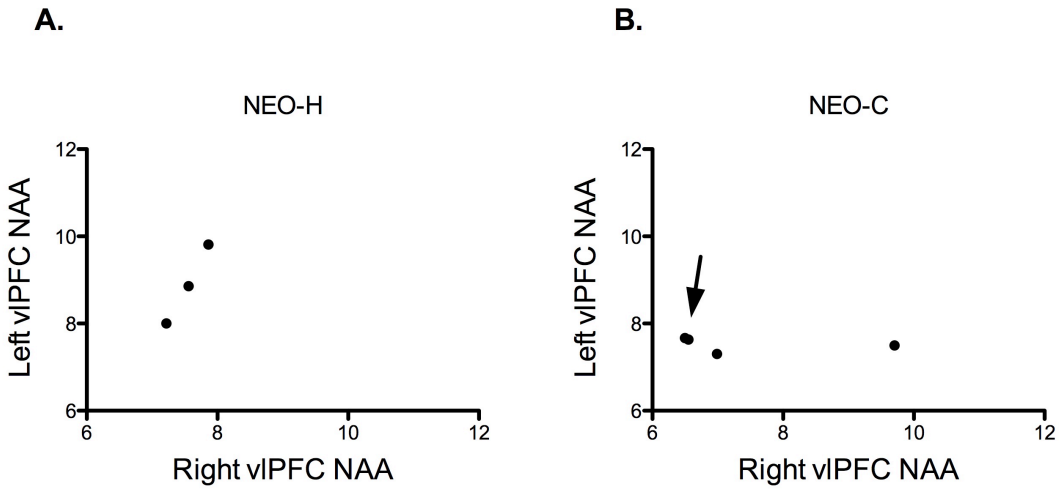

Figure 4.5: Correlations between left and right vlPFC NAA. The above graphs show correlations between NAA levels of the left and right hemisphere for groups Neo-H (A) and Neo-C (B). As show, NAA levels in the vlPFC correlate highly with one another in group Neo-H [r = 0.998, p = 0.037] but not in group Neo-C [r = 0.252, p = 0.748].

Correlations between NAA levels in the vlPFC and performance on the serial order task for animals with neonatal hippocampal lesions (Figure 4.6A and 4.6C) revealed a negative correlation in both the left and right hemispheres [$r = 0.999$, $p = 0.001$ and $r = 0.999$, $p = 0.021$, respectively], increases in vlPFC NAA were associated with poorer performance on the serial order task. No correlations were found for the sham-operated controls in either the left ($r = 0.334$, $p = 0.666$, see Figure 4.6B) or right ($r = 0.842$, $p = 0.158$, see Figure 4.6D) hemispheres.

NAA in primary somatosensory cortex (S1)

Figure 4.7 shows absolute NAA levels (mmol/L) for the primary somatosensory cortex (S1) in the right hemisphere for both groups. NAA levels for Group Neo-H-ibo ($X = 9.68, \pm 0.484$) were similar to those of Group Neo-C ($X = 9.57, \pm 1.129$) as revealed by no significant group difference [$t(1,6) = 0.185$, $p = 0.860$].

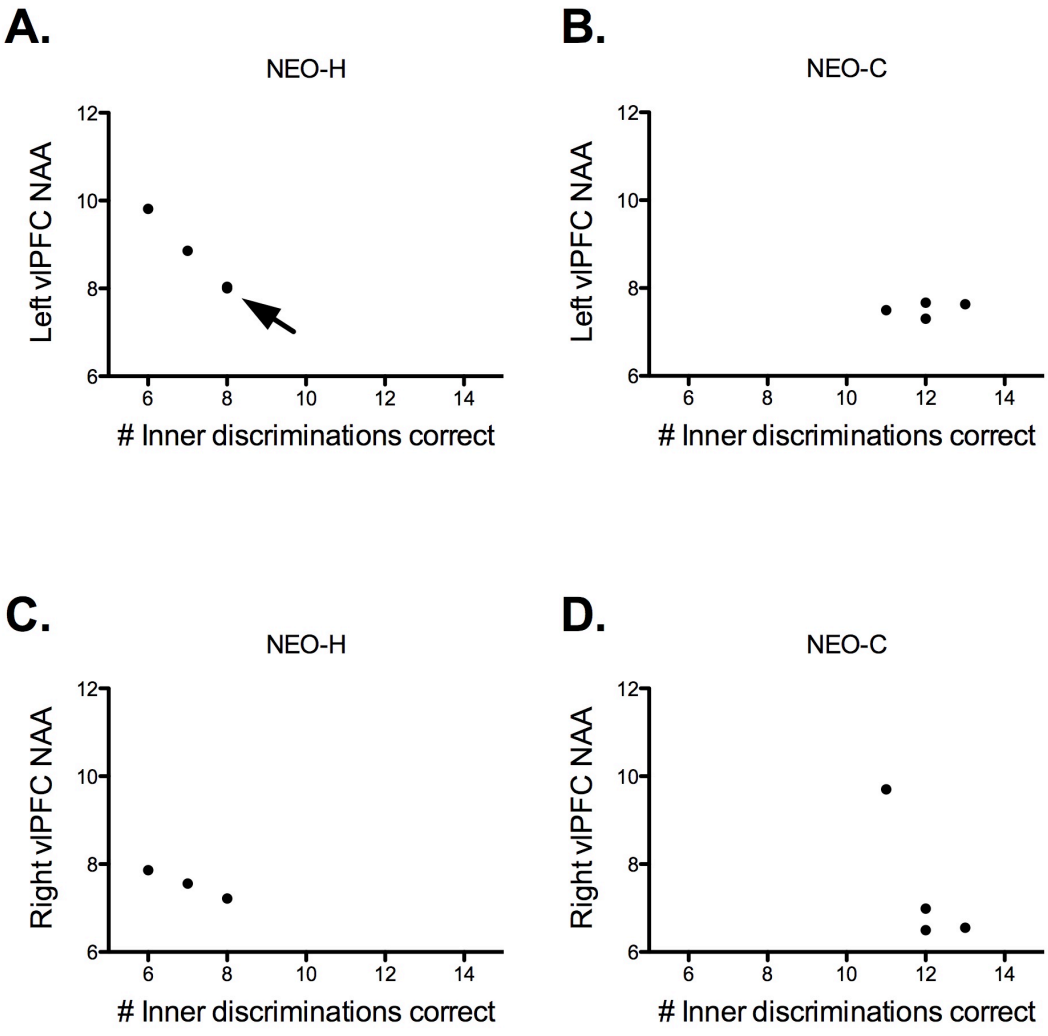

Figure 4.6: Correlations between vlPFC NAA and performance on the SOMT Probe. The above graphs show correlations between performance on the 4-SOMT probe and NAA levels within left (A and B) and right (C and D) vlPFC. NAA levels in left (A: [r = - 0.999, r = 0.001]) and right (C: [r = - 0.999, r = 0.021]) vlPFC of group Neo-H inversely correlate with performance on the 4-SOMT probe trials. In contrast, no relationship between task performance and vlPFC NAA was observed in either the left (B: [r = 0.334, p = 0.666]) or right hemisphere (D: [r = 0.842, p = 0.158]) of the sham operated control subjects. (Arrow indicates two overlapping data points).

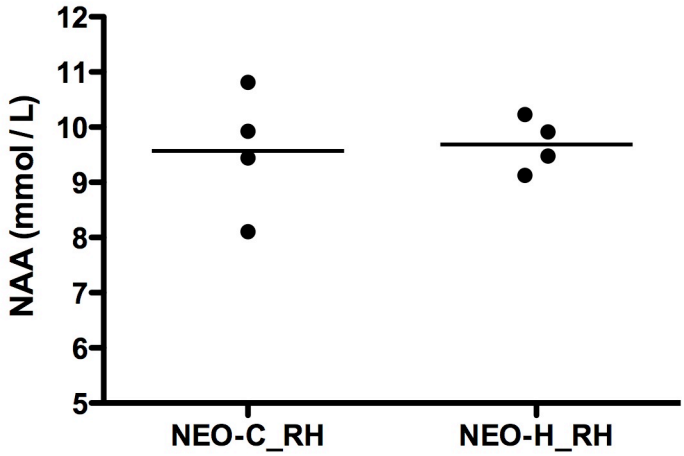

Figure 4.7: NAA within S1. The above figure shows NAA levels for the right hemisphere somatosensory cortex of Neo-H and sham operated control subjects. This region was selected as an additional control area as there would be no reason to think that early lesions of the hippocampus would impact the function of S1. As seen in the graph no differences in NAA were detected between the two groups, confirming that alterations in NAA of the frontal cortex represent a focal functional alteration between functionally connected structures, as opposed to a global neurochemical change. Bars indicate group means.

Discussion

This study investigated the effects of neonatal hippocampal lesions in monkeys on functioning of the lateral prefrontal cortex, using Magnetic Resonance Spectroscopy. The results indicate that neonatal lesions of the hippocampus did not significantly alter the NAA levels within the dlPFC, although it did increase the variability of NAA levels in the dlPFC of the left hemisphere. By contrast, the same neonatal lesions resulted in a significant increase in NAA levels within the vlPFC of the left hemisphere relative to sham-operated controls. Lastly, these effects of neonatal hippocampal lesions on NAA levels in the lateral prefrontal cortex do not reflect non-specific alterations resulting from

the early lesions since NAA levels in the somatosensory cortex of animals with neonatal hippocampal lesions were comparable to those of controls. These results will be discussed in turn.

Neonatal hippocampal lesions and malfunctioning of the lateral prefrontal cortex

These results indicate that the early hippocampal lesions have impacted the functional integrity of the lateral prefrontal cortex. Although NAA levels in the left dlPFC in Group Neo-H did not differ significantly from those of Group Neo-C, they correlated significantly with performance on the task such that lower NAA levels were associated with poorer performance scores. Thus, a thorough post-mortem investigation of the integrity of the dlPFC is warranted to examine how dlPFC function may have changed as a result of the early hippocampal lesion. Additionally, as we have consistently found impairments on behavioral tasks related to the function of the dlPFC in is unlikely that the early hippocampal lesion did not effect the functional maturation of this structure. Conversely, NAA levels of Group Neo-H in the left vlPFC were greater than those of Group Neo-C and correlated inversely with performance on the task, such that lower NAA levels were associated with better performance on the task. Thus, although neonatal hippocampal lesions affected more NAA levels in the left hemisphere than in the right hemisphere, there was also a clear distinction on the NAA changes in the dlPFC and vlPFC. That is, following neonatal hippocampal lesions, lower NAA levels were associated with poorer performance for the dlPFC but with better performance for the vlPFC, suggesting that the vlPFC may have unsuccessfully compensated for a dysfunctional dlPFC. This assertion is in line with earlier results from Goldman and

colleagues demonstrating that, following neonatal lesions of the dlPFC, its functions are supported by the vlPFC and orbital frontal cortex, although task performance never reached normal adult levels [104,143]. How could this functional substitution result in increased vlPFC NAA levels? Presumably, in the presence of a dysfunctional dlPFC, vlPFC could have been recruited more extensively during working memory performance and could at long-term have resulted in morphological changes in the vlPFC since NAA levels are associated with general activity levels of a given structure [191] and with increased morphological/ultra-structural changes across development [197].

In addition to lesion extent and task performance, it is also worth considering the potential impact the rearing conditions may have had on the integrity of the prefrontal cortex. A previous study demonstrated that infant monkeys reared in social isolation showed significantly reduced volume of posterior corpus callosum, which was associated with deficits in learning the Trial Unique Delayed Non-Matching-to-Sample paradigm [171]. However, all subjects of the current study, which were raised in an enriched nursery environment with both human and peer contacts, daily, learned the DNMS task as rapidly as normal adult animals raised in a semi-naturalistic setting [173]. Further, the sham-operated controls learned the SOMT working memory task comparably or better than the adult animals raised in a semi-naturalistic setting reported in Petrides's studies [103]. In total, the combined behavioral data indicate that our rearing conditions did not play a significant factor in the outcome of the current study.

NAA levels and normal brain function

In examining the interpretation of NAA MRS studies it is important to consider the role of NAA in normal brain function. Recent studies have shown that NAA, a precursor to NAAG, is created in neurons and trafficked to glia where it is subsequently cleaved to release the glutamate molecule [198,199]. This glutamate release created by NAAG cleavage is responsible for triggering the release of calcium waves by glial cells, suggesting a critical role for NAA in the regulation of synchrony within a region, which if disrupted would be detrimental to normal brain function. Thus, the increased levels of NAA seen in the vlPFC may reflect a chronic over-activity of this region, presumably due to a dysfunctional dlPFC. In contrast, the increased variability of NAA in the dlPFC may reflect a state of dysfunction that may vary depending on the locus and/or extent of the hippocampal lesion, and on individual variability.

Relationships to the rodent literature and schizophrenia

In parallel to these results, a previous study in rodents examined the effects of early ventral hippocampal lesions on prefrontal cortical NAA [88]. The study showed that early lesions of the hippocampus reduced levels of NAA within the medial prefrontal cortex of adult rats. This finding mirrors what is found in schizophrenia, however the homology of the frontal cortex between rodents and primates is still largely debated [90,91]. An alternative explanation for the observed differences in the current study in the rodent model may have to do with the time at which the lesion occurred. As the rat brain is

more developed at birth our lesion may have missed the developmental window whereby early lesions of the hippocampus are sufficient to effect the development of the dlPFC.

Lastly, in comparing our results to those of the schizophrenia literature several considerations must be made. First, quite a few studies have shown reduced NAA within the prefrontal cortex of schizophrenia patients [22,23,193], however other studies have found no differences in NAA of the frontal cortex [195,200]. These discrepancies may be related to a variety of factors including: large voxel sizes, loci of the volume of interest and variability of the patient group. What is important to note from the schizophrenia literature is that alterations in the NAA within the prefrontal cortex correlates with frontal cortical dysfunction, mirroring the findings of the current manuscript.

Thus, the current study demonstrated that early lesions of the hippocampus were sufficient to alter prefrontal cortical integrity as evidenced by increased NAA in the vlPFC and a more highly variable NAA in the dlPFC, which both correlated in a different way with performance on the dlPFC-dependent task. Thus, early lesions of the hippocampus in primates impact the normal development of the frontal cortex.

Chapter 5

Pre-pulse inhibition deficits in adult monkeys with neonatal lesions of the hippocampus or orbital frontal cortex, but not amygdala.

Introduction

Sensory-motor gating, the autonomous process of filtering extraneous stimuli, has been extensively studied in rodents and humans using the pre-pulse inhibition paradigm (PPI)[48,59]. PPI measures the individuals' natural ability to reduce their startle response when presented with a preceding stimulus of lesser magnitude and close temporal proximity. Further, the magnitude of inhibition is inversely correlated with the pre-pulse

interval, such that pre-pulses in closer temporal proximity to the startle pulse result in greater inhibition.

Previous studies in rodents have elucidated the neural circuitry of this system, which involves a number of brain stem nuclei, the medial prefrontal cortex, amygdala, hippocampus, and the olfactory cortex for a review see, [48]. A large body of work has successfully shown that neonatal, but not adult, lesions of the hippocampus impair PPI [71-74,82,201]. It has been proposed that early lesions of the hippocampus alter the circuitry of the ventral striatum, a region, which is known to cause a similar impairment in pre-pulse inhibition if damaged [202,203]. In turn, this malfunctioning of the ventral striatum may yield further disruption of the prefrontal cortex, thus resulting in the working memory deficits often associated with neonatal ventral hippocampal lesions in rodents. Thus, a malfunctioning of the ventral striatum following neonatal hippocampal lesions may impact both PPI and working memory abilities [68].

Despite a large body of evidence in the rodent literature describing the behavioral syndrome associated with early lesions of the ventral hippocampus, little to no evidence exists in the non-human primate. Aseries of recent studies in our laboratory have illustrated that early lesions of the hippocampus in the non-human primate severely altered the function of the prefrontal cortex[183,189]. Specifically, these studies showed that monitoring working memory, a memory process known to be mediated by the dorsolateral prefrontal cortex[101-103], is impaired in adult monkeys with neonatal hippocampal lesions. Further, a magnetic resonance spectroscopy study of these same animals[204] demonstrated that the functional integrity of the prefrontal cortex has been altered, and more importantly correlated with the magnitude of working memory deficits

observed in these animals. Insofar as the rodent literature has demonstrated that working memory impairments and sensory-motor gating processes are both found following neonatal lesions of the hippocampus, it is imperative to determine whether the same could also be true for the non-human primate.

Thus, the goal of the present study was three folds. First, given the paucity of PPI studies in monkeys, it was important to replicate the acoustic startle and PPI curves reported in an earlier study of sensory-motor gating in the normal rhesus monkey [205]. Second, to make comparisons with the rodent literature, acoustic startle and pre-pulse inhibition were investigated in adult monkeys with neonatal lesions of the hippocampus. We predicted that, if neonatal hippocampal lesions in monkeys will also impact the functioning of the ventral striatum, significant deficits in PPI should be observed. Finally, given that lesions of the amygdala[206-208], but not those of the medial prefrontal cortex [209-212], yielded PPI deficits in rodents, we also measured PPI in adult monkeys that had received either neonatal neurotoxic acid lesions of the amygdala or neonatal aspiration lesions of the orbital frontal cortex.

Methods

Subjects

Twenty-two rhesus macaques (*Macaca mulatta)* between 6 to 8 years of age and weighing between 5 to 10 kg were utilized in the current experiment. They were acquired as newborns from the breeding colony of the University of Texas, M.D. Anderson Cancer Center Science Park (Bastrop, TX) and brought to the nursery at M.D. Anderson Cancer Center where they were surrogate nursery raised in age- and sex-matched cohorts of 4 animals each [160]. Infant monkeys were individually housed but permitted social contacts

with other animals in adjoining cages until one month of age. In addition, a plush surrogate was provided to the animals of approximately 30 cm in length. A principal human caregiver spent roughly 6 h/day, 5 days/week in the nursery with the infant monkeys. On weekends, the infants were handled 2-3 times per day and received a total of 2-4 hours of social interactions with familiar experimenters. From one to nine months of age, infants received daily social interactions for 3-4 hours, 5 days/week with age/sex matched peers and by 1 year of age, each cohort was socially housed until approximately 3 years of age. They were then moved to the Yerkes National Primate Research Center at Emory University (Atlanta, GA) where they were housed individually in rooms with a 12 hour light/dark cycle (7AM:7PM). All monkeys were fed Purina Old World Primate chow supplemented with fresh fruit and during behavioral testing.

At the ages of 10-15 days, all monkeys had received brain surgeries that consisted of either neurotoxic lesions of the hippocampus (Group Neo-H: 4 males, 2 females), neurotoxic lesions of the amygdala (Group Neo-A: 3 males, 3 females), aspiration lesions of the orbital frontal cortex (Group Neo-O: 2 males, 3 females) or sham-operations (Group Neo-C, 2 males, 3 females). From infancy through adulthood, they also received extensive behavioral training to measure the effects of the lesions on learning and memory abilities, decision making skills and regulation of emotional reactivity (see details below in Behavioral Procedures).

All experimental procedures were approved by the Institutional Animal Care and Use Committee at the University of Texas at Houston and Emory University and were conformed to the NIH Guide for the care and use of Laboratory Animals (HHS publication 85-23, 1985).

Neuroimaging and Surgical Procedures

All neuroimaging and surgical procedures have been described extensively in an earlier report [160] and will be briefly summarized below.

Pre-surgical MRI scans

On the day of surgery, the infant monkeys were placed in an induction box saturated with isoflurane gas (1.0-3.0%, v/v, to effect), intubated and maintained under isoflurane gas throughout the procedure. They were then placed in a non-ferromagnetic stereotaxic apparatus (Crist Instruments, Damascus, MD) and centered in the scanner. Two types of MR images were acquired with a GE Signa 1.5 Tesla Echo Speed scanner (GE Medical Systems, Milwaukee, WI) using a 5-inch surface coil. A series included a 3D T1-weighted fast spoiled gradient (FSPGR)-echo MR images (TE = 2.6 ms, TR = 10.2 ms, 25° flip angle, contiguous 1 mm sections, 12 cm FOV, 256 x 256 matrix) . and was performed for all four groups. The other series included three sets of Fluid-Attenuated Inversion Recovery (FLAIR) images (TE/TR/TI = 140 ms/10,000 ms/, 2200ms, in contiguous 3mm sections, 14cm FOV, 256 x 256 matrix) offset by 1 mm posteriorly and was performed on Groups Neo-H-ibo and Neo-A-ibo only. The pre-surgical T1W images were used to select stereotaxic coordinates for the neurotoxin injection sites for Groups Neo-H and Neo-A [161] and to identify the sulcal pattern on the orbital surface in Group Neo-O-asp since the sulci serve to identify borders of areas 11 and 13 of the orbital frontal cortex.

At completion of the pre-surgical MRI, the animal was maintained under gas anesthesia and immediately transported to the surgical suite. The scalp was disinfected with Nolvasan solution and an intravenous drip containing 5% dextrose and 0.5% sodium

chloride was infused to maintain hydration. The animal was maintained on a heating pad to maintain core temperature, and all vital signs (core temperature, pulse, blood pressure and expired CO_2) were continuously monitored until the end of the procedure.

Neurotoxic Lesion of the hippocampus and amygdala

After the skull was disinfected, Marcaine (25%, 1.5m, s.c.) was injected along the midline of the scalp and an incision was made to expose the underlying tissue and skull. Small craniotomies were made above the injection sites and cuts were made in the dura to expose the brain and permit the penetration of the injection needles. Injections of ibotenic acid (Biosearch Technologies Novato, CA, 10mg/ml in PBS, pH 7.4) were made simultaneously in both hemispheres with two 10µl Hamilton syringes attached to Kopf manipulators (David Kopf Instruments Tujunga, CA). For the hippocampal lesions, 7-8 sites along the axis of the hippocampus were injected (0.4-0.6µl/site at a rate of 0.2 µl/30 sec for a total of 2.8-4.2µl/hemisphere). For the amygdala lesions, 15 sites targeting the center of the amygdala on each hemisphere and spaced 2 mm apart in all directions were injected (0.2-0.4 µl/site at a rate of 0.2 µl/30 sec for a total of 0.8-1.6 µl).

After the injection at each site, the needles were left in place for 3 minutes to allow for the ibotenic acid to diffuse and minimize it leaking back as the needle was removed. Additionally, each time the needle was removed from the brain, it was swabbed with cotton-tipped applicators to assure that any tissue or residual neurotoxin on the surface of the needle was removed prior to reinsertion at another site.

Orbital Frontal Cortex Aspiration Lesion

The orbital frontal cortex aspiration procedure were performed using surgical procedures described by Machado and Bachevalier (2006) and were reported before [213,214]. Briefly, to gain access to the orbital frontal cortex, a bone opening was performed just above the orbit and the dura was cut. The edge of the frontal lobe was gently elevated to visualize the orbital surface and to delineate the borders of areas 11 and 13, which are mostly confined between the lateral orbital frontal sulcus laterally and the strial olfactory medially. These two landmarks were used to delineate the medio-lateral extent of the orbital lesions. Anteriorly, the border of the lesion was an imaginary line joining the anterior tip of the medial orbital frontal sulcus to the tip of the lateral orbital frontal sulcus. Posteriorly, the border of the lesion was a line joining the medial bank of the lateral orbital sulcus to the olfactory stria just anterior to its division into the medial and lateral olfactory tracts. Aspiration of the cortical tissue between these borders was performed with 21 and 23 gauge, aspirating probes in combination with an electro-cautery tool with the aid of a surgical microscope. Care was specifically given to not inflict damage to the white matter under the cortical mantle.

Sham surgeries

The surgical procedures for the sham surgeries were identical to those of the hippocampal and amygdala lesions and included the opening of the skin, bone and dura but no needles were inserted into the brain.

Post-Operative Care

Following the completion of the surgical procedures, animals were placed in incubators to maintain core body temperature. Post-operative care included a seven-day regimen of dexamethasone sodium phosphate (0.3mg/kg i.m.) to reduce swelling,

Cefazolin (25mg/kg i.m.) to minimize infection, and acetaminophen for pain management.

MRI-based Lesion Assessment

Post-surgical MRI scans were given to all animals, except the sham-operated animals, 6-8 days after the surgical procedures. Animals of Groups Neo-H-ibo and Neo-A-ibo received a series of T1-W images and FLAIR images, whereas only the T1-W was performed on Group Neo-O-asp. The post-surgical FLAIR images for Groups Neo-H-ibo and Neo-A-ibo indicated areas of high water density caused by the cell death and were matched with both the pre-surgical T1W and FLAIR images to verify the location and extent of lesions to the targeted area as well as to evaluate any inadvertent damage to adjacent structures [162,163]. For Group Neo-O-asp, the post-surgical T1 images were compared to the pre-surgical T1 images to estimate the amount of orbital frontal cortex removed by the aspiration lesions and that to any adjacent cortical areas.

For animals of Groups Neo-H-ibo and Neo-A-ibo, post-surgical FLAIR coronal images through the hippocampus or amygdala were matched to drawing of coronal sections of a normal one-week-old rhesus monkey template brain (J. Bachevalier, unpublished data). The extent of hypersignals seen on each FLAIR image was then plotted onto the corresponding template using the pre-surgical T1-W and FLAIR images to maximize accuracy. The drawings were then imported into an image analysis software program (ImageJ® http://rsb.info.nih.gov/ij) to calculate the total volume of damage on each image for both the intended target (hippocampus or amygdala) and any adjacent structures. The percentage of total volume damaged for a given structure was obtained by adding the surface area of each slice, multiplying the total surface by the slice

thickness (1 mm), dividing by the total volume of the structure in the normal brain and multiplying by 100 [164]. This process of *in vivo* lesion reconstruction has been described, documented and validated previously [163].

For animals in Group Neo-O, pre- and post-surgical T1-weighted images were used to estimate total volume of tissue aspirated from the orbital frontal cortex (Areas 11 and 13) and adjacent cortical regions. The post-surgical images were matched to corresponding coronal drawings from the normal one-week-old rhesus monkey template brain and extent of tissue damaged on the T1-W images was drawn onto the corresponding template images. Within each hemisphere, the total volume of aspirated tissue from the orbital frontal cortex and adjacent regions was measured using ImageJ® and again expressed as a percentage of the normal volume for that region as for the estimation of hippocampal and amygdala damage, see above [163].

Behavioral Procedures

Before participating in the current investigation the subjects have had extensive, albeit identical testing histories. For simplicity, a brief description of their testing history will be listed with the ages at which this testing occurred: Visual Paired Comparison (1.5, 6, 18 and 48 months) [165], Oddity (3 and 15 months), Visual Paired Comparison-Spatial (8 and 24 months), Object discrimination reversals (48-60 months), Food Preference (60 months), Social Dyad Testing (3, 6 and 36 months), Human Intruder (2 and 4.5 months), Social Attachment (9 months)[20], Trial Unique-Delayed Non-Match to Sample (60-72 months) [173], Object and Spatial Memory Span Tasks (60-72 months), Session Unique

Delayed Non-Match to Sample (72-84 months) and Object Self Ordered Task (72-84 months) [183], Serial Order Memory task (84-96 months) [189].

Apparatus

Startle and pre-pulse inhibition testing was performed on the Primate Startle Reflex System (Med Associates: St. Albans, VT) as illustrated in Figure 4. The system is equipped with two speakers (frequency- 4000-20,000 Hz, Amplitude 70-120dB with an error of ± 0.5dB), one emits startle noise and pre-pulses and the other emits a background noise frequency used as a cue. In all experiments, the acoustic noises (background, startle pulses and pre-pulses) were compromised of white noise, which by definition includes all frequencies. Whole body startle was measured via a load cell, mounted to the platform that supports the restraint chair. The load cell is a force transducer that is calibrated to the weight of each animal prior to a startle session and allows to measure startle responses irrespective of animal's body size and weight.

Habituation

All subjects had already been habituated to being seated in a standard primate restraint chair (Crist Instruments: Damascus, MD) during previous testing and required only a few days to accustom to the primate chair used for startle training. Thus, prior to the initiation of the startle and pre-pulse inhibition experiments, they received three sessions, spaced by a minimum of two days apart. In each session a background noise of 65dB was constantly emitted to drown out extraneous noise. Pulses were emitted for a duration of 200 msec, with pulse intensities of: 90, 100, 110, 115 and 120dB, at 30s intervals. Within a session, each pulse intensity was administered 10 times (50 total

pulses/session) and the order of pulse intensity was randomized in a Latin square design to minimize the impact of increased pulses on startle response.

Baseline Startle

Baseline startle testing was conducted to determine any effects of the neonatal lesions on baseline startle response. Similar to the habituation condition, baseline startle sessions consisted of 50 total pulses (at intensities of 90, 100 110, 115 and 120dB), administered at variable intervals (average 30s) to reduce anticipatory behavior by the animal. As was the case with the habituation sessions, the order of pulses was randomized in a Latin square design. Each animal received two baseline startle sessions, which were averaged to generate a mean startle response for each animal.

Pre-pulse Inhibition

Pre-pulse inhibition (PPI) for all four groups of animals was evaluated in two sessions using varied pre-pulse intervals. The parameters were as follows: 65dB background noise, 120dB acoustic startle noise (duration 200ms), and 69dB pre-pulse (duration 20ms). The interval between the onset of the pre-pulse and pulse was tested at 60, 120, 240, 480, 1000 and 5000 msec intervals. Additionally, a pre-pulse only condition was examined. The two PPI sessions included pulse only, pre-pulse only and 60 msec, 120 msec and 1000 msec pre-pulse intervals for Session 1, and pulse only and 120 msec, 240 msec, 480 msec and 5000 msec pre-pulse intervals in Session 2 with all trials randomized in a Latin square design.

Statistical Analysis

Startle amplitudes are expressed as arbitrary units and inhibition is expressed as a percentage of startle response in the absence of a pre-pulse (Percent inhibition = Startle

Magnitude in the absence of pre-pulse-Startle Magnitude in presence of pre-pulse/Startle Magnitude in the absence of pre-pulse x 100). Baseline startle and PPI were analyzed separately using Two-way Repeated measures ANOVA's. The main factors were Groups (2, i.e. Group Neo-C and one of the experimental groups) and Startle Intensities (5) or Pre-pulse Intervals (6) with repeated measures for the last two factors. Group and interaction differences were analyzed with t-tests. Finally, a correlation matrix was performed for each lesions group using the startle at each intensity, the PPI at each pre-pulse and lesion extent data to determine any relationships between lesion extent or extent of unintended damage and behavioral performance.

Results

Lesion Extent

Estimate of extent of hippocampal damage as well as unintended damage to adjacent structures is given in Table 5.1 and a representative case is illustrated in Figure 5.1. Two animals (Neo-H-2 and Neo-H-3) received extensive damage to the hippocampus bilaterally, averaging 67.6 and 87.4%, respectively. Three others (cases Neo-H-1, -4 and -5) had asymmetrical lesions with extensive damage on one hemisphere (average: 72%), but moderate damage on the other hemisphere (average: 15%). Only, case Neo-H-ibo-6 had relatively small hippocampal damage bilaterally (7.9 and 0% for the left and right hemispheres, respectively). Unintended damage in each case was almost non-existent, except for slight encroachment to the posterior amygdala (Cases Neo-H-ibo-1,- 3,- 4, and -)5 and to areas TH/TF (cases Neo-H-ibo-1 to -5).

Table 5.1: Estimate of intended hippocampal damage and unintended damage

Group	**Intended Damage**				**Unintended Damage**							
Subjects	**Hippocampus**				**Amygdala**				**TH/TF**			
Neo-H-ibo	L%	R%	X%	W%	L%	R%	X%	W%	L%	R%	X%	W%
Neo-H-ibo-1	63.8	2.9	33.2	1.8	14.0	0.0	7.0	0.0	3.1	0.5	1.8	0.0
Neo-H-ibo-2	54.4	80.9	67.6	44.0	0.0	0.0	0.0	0.0	21.4	2.7	12.1	0.6
Neo-H-ibo-3	78.5	96.3	87.4	75.6	1.7	0.0	0.8	0.0	6.1	5.5	5.8	0.3
Neo-H-ibo-4	20.3	67.3	43.8	13.6	0.0	4.7	2.4	0.0	15.3	0.0	7.6	0.0
Neo-H-ibo-5	20.7	84.0	52.6	17.5	0.0	4.9	2.5	0.0	6.1	4.0	5.1	0.2
Neo-H-ibo-6	7.9	0.0	3.9	0.0	0.0	0.0	0.0	0.0	0.0	0.0	0.0	0.0
Mean	**40.9**	**55.2**	**48.0**	**25.4**	**2.6**	**1.6**	**2.1**	**0.0**	**8.6**	**2.1**	**5.4**	**0.1**

Note: L% percent damage in the left hemisphere; R%: percent damage in the right hemisphere; X% average damage to both hemispheres; W%: weighted average damage to both hemispheres (W% = L% x R%)/100 as defined by Hodos and Bobko [168]).
Abbreviation: TH/TF - ventral cortical area of the temporal lobe as defined by Bonin and Bailey, 1947)

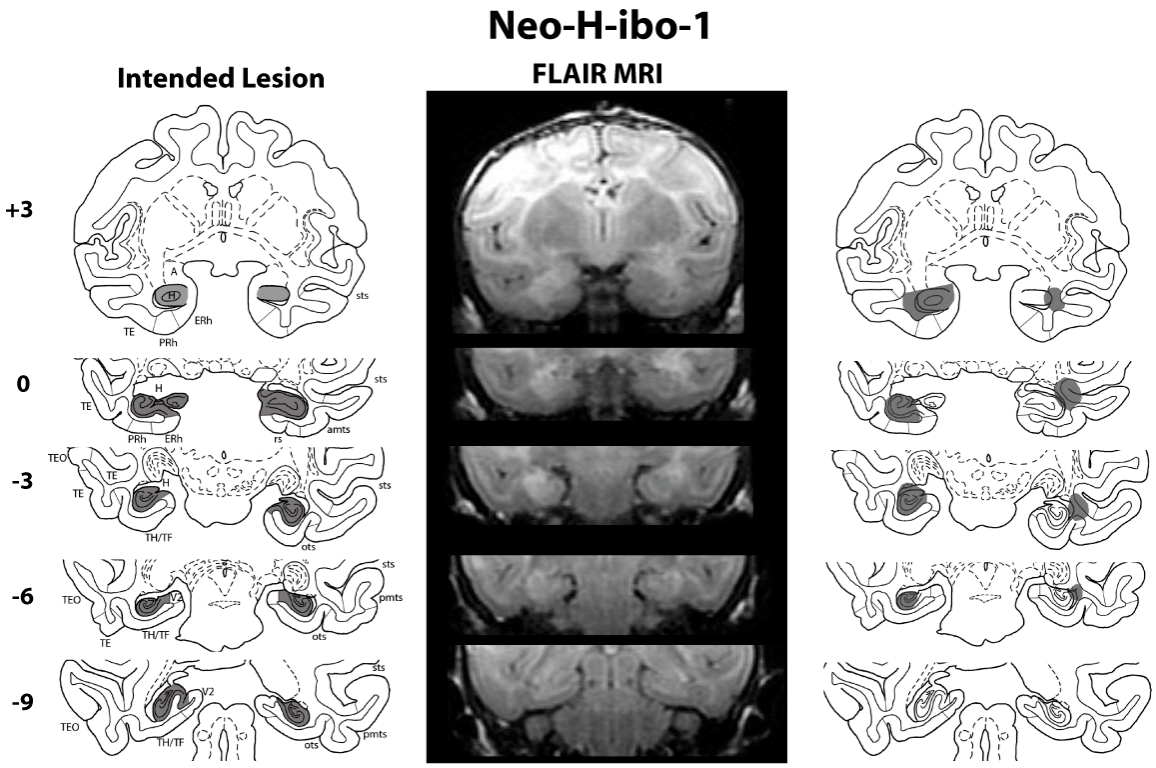

Figure 5.1: Example Neonatal Neurotoxic Hippocampal lesion: Neo-H-ibo-1. This figure shows the intended amygdala lesions (left), post surgical FLAIR MRI (middle) and reconstructed lesion (right). Abbreviations: Erh-entorhinal cortex, Prh-perirhinal cortex, A-amygdala, H-hippocampus, TE-temporal area TE, rs-rhinal sulcus, sts-superior temporal sulcus, and amts-anterior medial temporal sulcus.

Estimate of extent of amygdala damage and of unintended damage to adjacent structures is given in Table 5.2 and one representative case is illustrated in Figure 5.2. Extent of amygdala damage varied from 47.1% to 86.8%. In all cases, except one (Neo-A-ibo-1), the amygdala damage was at least 20% greater in the right hemisphere than in the left hemisphere. Unintended damage to the anterior hippocampus was minimal in all cases (Average 8.0%) and only one (Neo-A-1) had slight damage to the temporal cortical areas TE and TG (20.7% bilaterally), entorhinal cortex (2.4% bilaterally) and perirhinal cortex (6.0% bilaterally).

Table 5.2: Estimate of intended amygdala damage and unintended damage

Group	Intended Damage				Unintended Damage			
Neo-A-ibo	Amygdala				Hippocampus			
	L%	R%	X%	W%	L%	R%	X%	W%
Neo-A-ibo-1	80.5	90.7	86.8	74.7	5.1	3.1	4.1	0.2
Neo-A-ibo-2	43.0	77.6	59.8	32.6	0.0	0.8	0.4	0.0
Neo-A-ibo-3	33.0	61.1	47.1	20.2	0.0	0.0	0.0	0.0
Neo-A-ibo-4	62.1	90.0	76.0	55.9	1.9	3.0	2.4	0.1
Neo-A-ibo-5	41.2	66.6	53.9	27.5	0.0	0.0	0.0	0.0
Neo-A-ibo-6	52.1	75.6	63.8	39.3	5.6	10.3	8.0	0.5
Mean	**52.1**	**71.8**	**63.5**	**38.1**	**2.1**	**2.9**	**2.5**	**0.1**

Note: L% percent damage in the left hemisphere; R%: percent damage in the right hemisphere; X% average damage to both hemispheres; W%: weighted average damage to both hemispheres (W% = L% x R%)/100 as defined by Hodos and Bobko [168]).

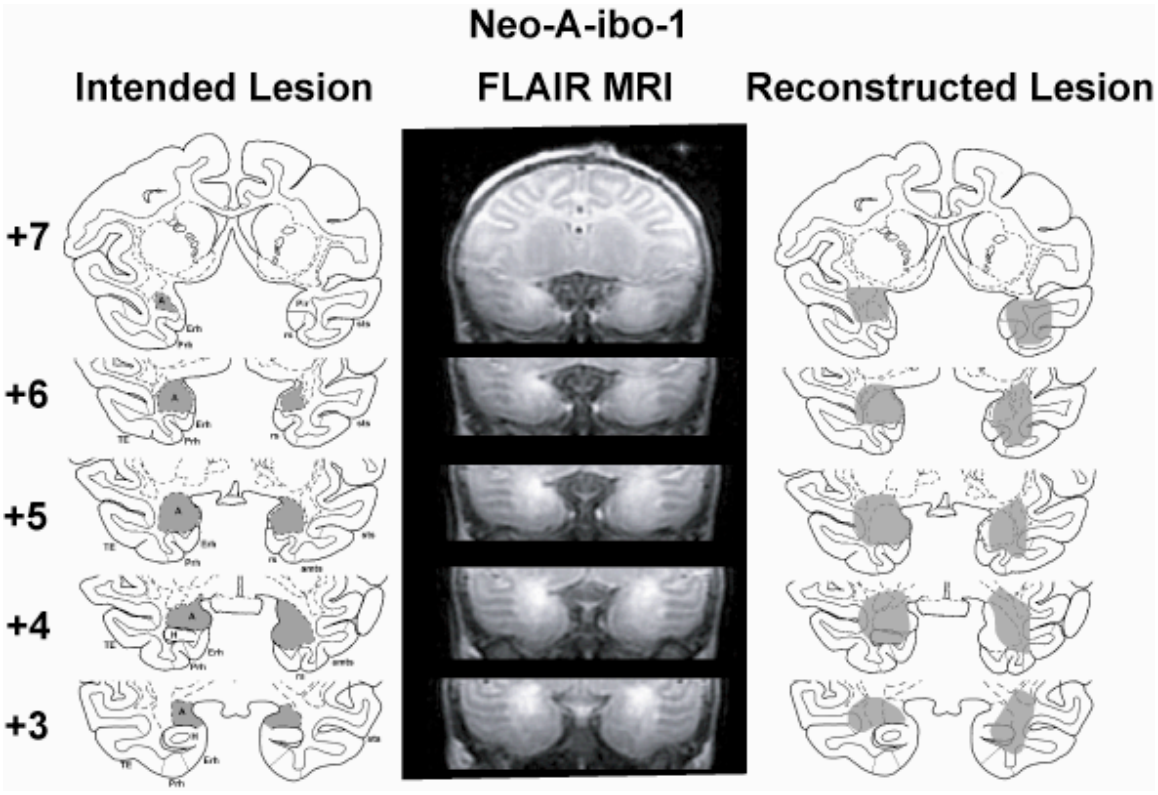

Figure 5.2: Example Neonatal Neurotoxic Amygdala lesion: Neo-A-ibo-1. This figure shows the intended amygdala lesions (left), post surgical FLAIR MRI (middle) and reconstructed lesion (right). Abbreviations: Erh-entorhinal cortex, Prh-perirhinal cortex, A-amygdala, H-hippocampus, TE-temporal area TE, rs-rhinal sulcus, sts-superior temporal sulcus, and amts-anterior medial temporal sulcus.

Extent of damage to orbital frontal cortical areas 11 and 13 and of unintended damage to adjacent cortical areas is given for each animal in Group Neo-O in Tables 5.3 and 5.4, respectively, and one representative case is illustrated in Figure 5.3. All animals sustained symmetrical and fairly complete lesions of areas 11 and 13 with an average damage of 84.2% and 90.0%, respectively. Unintended damage was mostly found within the insular area (Ia) in four out of the six animals (Neo-O-2, 4, 5 and 6) averaging 65% bilateral damage, although two animals had only minimal damage to this area (Neo-O-1 X: 7.5% and Neo-O-3 X: 15.1%, bilaterally). Other unintended damage was far less extensive and limited bilaterally to areas 12 (X: 14.3%) laterally and 14 (X: 12.3%), medially.

Table 5.3: Estimate of intended damage to orbital frontal areas 11 and 13

Group	**Intended Damage**							
Neo-O-asp	**Area 11**				**Area 13**			
	L%	R%	X%	W%	L%	R%	X%	W%
Neo-O-asp-1	80.5	92.7	86.8	74.7	93.0	73.5	83.3	68.4
Neo-O-asp-2	62.6	95.6	79.1	59.9	99.3	100	99.6	99.3
Neo-O-asp-3	98.7	100	99.4	98.7	94.0	82.4	88.2	77.4
Neo-O-asp-4	84.1	93.9	89.0	79.0	87.3	95.6	91.4	83.4
Neo-O-asp-5	84.0	98.9	91.5	83.1	96.8	97.2	97.0	94.1
Mean	**81.9**	**96.2**	**89.1**	**79.0**	**94.0**	**89.7**	**87.5**	**84.5**

Note: L% percent damage in the left and R%: percent damage right hemisphere, respectively; X% average damage to both hemispheres; W%: weighted average damage to both hemispheres (W% = L% x R%)/100 as defined by Hodos and Bobko [168]). . Areas 11 and 13 are frontal cortical areas as defined by Carmichael and Price [215].

Table 5.4: Estimate of Unintended Damage Resulting from the Neo-O-asp lesion.

Group	**Unintended Damage**											
Neo-O-asp	**Area 12**				**Area 14**				**Ia**			
	L%	**R%**	**X%**	**W%**	**L%**	**R%**	**X%**	**W%**	**L%**	**R%**	**X%**	**W%**
Neo-O-asp-1	49.2	11.0	25.6	4.4	8.0	10.2	9.1	4.4	11.6	3.4	7.5	0.4
Neo-O-asp-2	9.3	1.4	5.4	0.1	31.9	6.8	19.4	2.2	78.5	57.7	68.1	45.3
Neo-O-asp-3	22.3	21.6	22.0	4.8	18.7	11.6	15.1	2.2	16.5	13.8	15.1	2.3
Neo-O-asp-4	2.8	4.0	3.4	0.1	9.7	12.6	11.2	1.2	82.5	64.6	73.6	53.3
Neo-O-asp-5	18.5	22.8	20.6	4.2	6.5	11.0	8.8	0.7	87.0	68.7	77.4	59.0
Mean	**20.4**	**12.6**	**15.4**	**2.7**	**14.9**	**10.4**	**12.7**	**2.1**	**55.2**	**41.6**	**48.3**	**32.0**

Note: L% percent damage in the left and R%: percent damage right hemisphere, respectively; X% average damage to both hemispheres; W%: weighted average damage to both hemispheres (W% = L% x R%)/100as defined by Hodos and Bobko [168]). Areas 12, 14 and ia are frontal cortical areas as defined by Carmichael and Price [215].

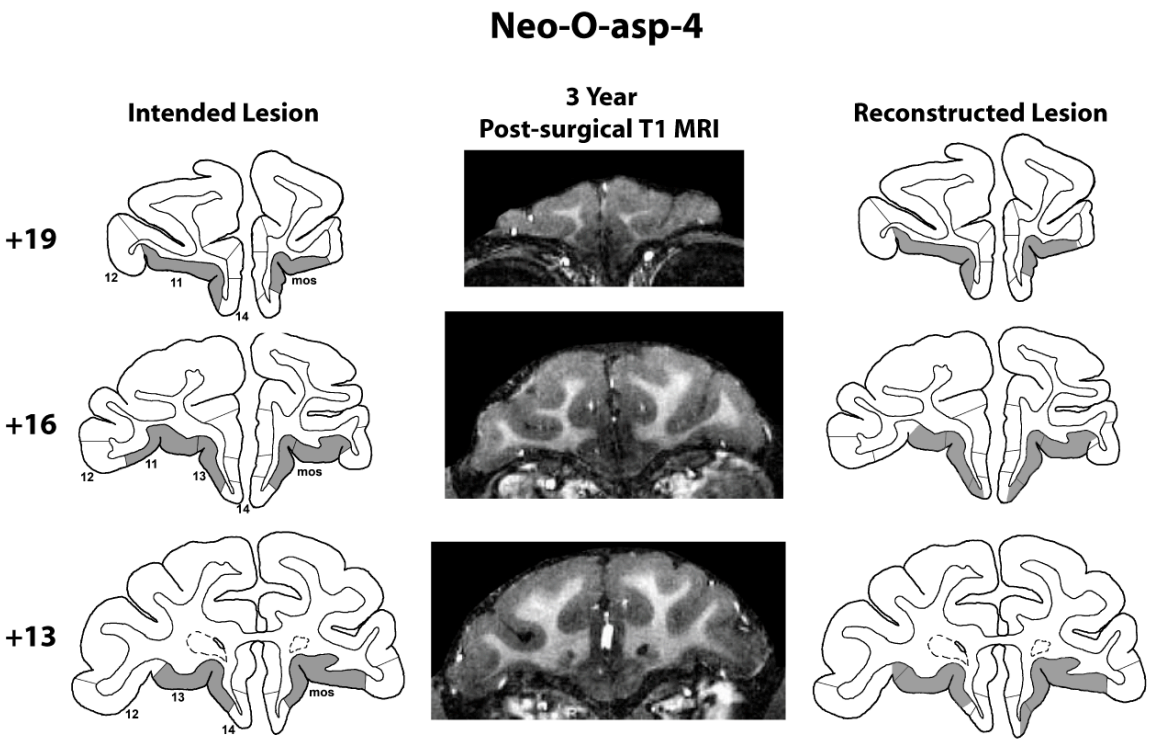

Figure 5.3: Example Neonatal Aspiration Lesion of the Orbital Frontal cortex (areas 11 and 13): Neo-O-asp-4. The figure shows the intended lesion (left), 3 year-post surgical MRI (middle) and reconstructed lesion (right). Numbers indicate cortical areas according to Carmichael and Price [215] and mos: medial orbital sulcus.

Baseline Startle and PPI in Groups Neo-C and Neo-H-ibo

Figure 5.5 (A and D) illustrates baseline startle curves, at each pulse intensity, and PPI curves at each pre-pulse interval for monkeys with neonatal neurotoxic lesions of the hippocampus (Neo-H-ibo) and sham-operated controls (Neo-C).

As shown in Figure 5.5A, Group Neo-C exhibited increases in startle magnitude relative to the increase in acoustic startle noise amplitude (baseline: 0.153 ± 0.027,

95dB: 0.516 ± 0.095, 100dB: 0.613 ± 0.113, 110dB: 1.193 ± 0.367, 115dB: 1.295 ± 0.390 and 120dB 3.320 ± 1.162). An intensity effect was found within control subjects [$F(5,20) = 5.926$, $p < 0.01$]. Further analysis revealed that startle magnitude was greater at all pulse intensities, as compared to baseline: 95db [$t(1,4 = -3.982$, $p = 0.01$], 100dB [$t(1,4) = -4.302$, $p = 0.01$], 110dB [$t(1,4) = -2.807$, $p = 0.04$], 115dB [$t(1,4) = -2.851$, $p = -2.851$, $p = 0.04$] and 120dB [$t(1,4) = -2.701$, $p = 0.05$]. However, no difference in startle magnitude was detected between any of the pre-pulse intensities ($p > 0.05$). A similar increase in startle magnitude with increasing startle noise intensities (Fig. 5.5A) was found in animals with neonatal hippocampal lesions baseline: 0.151 ± 0.023, 95dB: 0.768 ± 0.191, 100dB: 0.802 ± 0.256), 110dB: 1.752 ± 0.583, 115dB: 2.115 ± 0.804 and 120dB: 2.678 ± 0.929). Although the increase in startle amplitude in Group Neo-H-ibo was slightly blunted as compared to that of Group Neo-C, this group difference was not significant [$F(1,9) = 0.124$, $p = 0.732$]. Similarly to control subjects, Group Neo-H also showed an intensity effect [$F(1,9) = 13.255$, $p = 0.005$]. Lastly, no group differences were detected as a function of pulse intensity [$F(1,9) = 0.013$, $p > 0.05$].

Sham-operated control monkeys demonstrated an inhibitory response (Fig. 5.5D), which was maximal when the pre-pulse occurred 120-240 msec prior to pulse onset (60 msec: 55.5% ± 9.1, 120 msec: 65.2% ± 8.7, 240 msec: 65.4% ± 8.9, 480 msec: 55.9% ± 16.5, 1000 msec 37.5% ± 17.8 and 5000 msec: 29.9% ± 16.6). Analysis of the effect of pre-pulse interval revealed a significant difference in inhibition [$F(5,20) = 3.161$, $p < 0.05$]. A further examination of this effect revealed that inhibition generated by the 120 msec pre-pulse was significantly greater than a pre-pulse interval of 1000 msec [$t(1,4) = 2.727$, $p < 0.05$] and approached significance as compared to pre-pulses at 5000 msec

[t(1,4) = 2.476, p = 0.06]. Also, pre-pulses at 240 msec [t(1,4) = 3.754, p < 0.05] and 480 msec [t(1,4) = 4.986, p < 0.01] generated significantly more inhibition as compared to pre-pulses at 5000 msec. In comparison to sham-operated controls, animals with Neo-H-ibo lesions showed comparable inhibition at the short pre-pulse intervals of 60 msec (54.5% ± 11.4), 120 msec (58.6% ± 14.0) and 240 msec (48.6% ± 6.0), but reduced inhibition with longer pre-pulse intervals (480 msec: 31.1% ± 14.5, 1000 msec: -21.4% ± 11.9 and 5000 msec: -57.1% ± 44.3). Analysis of variable interval PPI following neonatal hippocampal lesions reveled a significant effect of pre-pulse interval [F(5,45) = 7.336, p < 0.001]. Average PPI, irrespective of pre-pulse interval was significantly reduced in Neo-H [F(1,9) = 18.876, p < 0.01], as compared to sham-operated controls. The interaction of lesion and pre-pulse interval approached significance [F(5,45) = 2.171, p = 0.07]. Further, analysis of this effect that the current study lacked sufficient to detect interaction differences (power = 0.658). As such, pre-planned comparisons between Neo-H and Neo-C were made to determine if PPI differed at any specific interval. The post-hoc analysis revealed that Neo-H showed reduced PPI at the 1000 msec interval [t(1,9) = 2.829, p < 0.05]. In sum, these results indicated that Neo-H lesions impair PPI without altering baseline startle in rhesus macaques.

Baseline amplitudes and percent inhibition in Group Neo-H-ibo did not correlate with extent of hippocampal damage or extent of inadvertent damage to adjacent structures.

Baseline Startle and PPI in Groups Neo-C and Neo-A-ibo

Figure 5.5 (B and E) illustrates baseline startle curves at each pulse intensity and PPI curves at each pre-pulse interval for monkeys with neonatal neurotoxic lesions of the amygdala (Neo-A-ibo) and sham-operated controls (Neo-C).

Animals in Group Neo-A-ibo showed an increase in startle amplitude (Fig. 5.5B) at almost all startle noise intensities, although individual variability was greater in this group (baseline: 0.154 ± 0.019, 95dB: 1.560 ± 0.802, 100dB: 2.087 ±0.960), 110dB: 3.870 ±1.499, 115dB: 3.866 ± 1.369 and 120dB: 6.816 ±: 2.416). Analysis of the data revealed an effect of pulse intensity [$F(5,40) = 12.221$, $p < 0.001$]. It was subsequently determined that Neo-A-ibo showed in increased startle response, relative to sham operated controls [$F(1,8) = 12.822$, $p < 0.01$]. As was the case with Neo-H-ibo, no interaction was observed between pulse intensity and lesion group [$F(5,40) = 1.687$, $p = 0.160$], but the design lacked sufficient power (0.241) to detect any potential observed change. As such, pre-planned comparisons were made to determine if startle was increased at any particular pulse intensity in Neo-A-ibo. The comparisons revealed no significant difference at pulse intensity, although the difference in the magnitude of startle in Neo-A-ibo as compared to sham-operated controls approached significance at 115dB [$t(1,8) = -1.805$, $p = 0.109$].

Interestingly, neonatal lesions of the amygdala did not alter the inhibitory response at any pre-pulse intervals (Fig. 5.5E). Animals in this group obtained inhibitory responses that were similar to those of sham-operated controls at all pre-pulse intervals (60 msec: 74.6% ± 4.5, 120 msec: 65.3% ± 10.4, 240 msec: 70.7% ± 8.2, 480 msec: 48.7% ± 10.2, 1000 msec: 13.3% ± 24.2 and 5000 msec: 13.7% ± 6.4). Thus, the factor Group did not reach significance [$F(1,8) = 0.102$, $p = 0.758$] but an effect of pre-pulse

interval was found [$F(5,40) = 17.402$, $p < 0.001$]. No interaction effect of amygdala lesion and and pre-pulse interval was detected [$F(1,8) = 2.422$, $p = 0.158$]. Pre-planned comparisons confirmed that neonatal amygdala lesions did not impair PPI at any pre-pulse interval ($p > 0.05$), however Neo-A-ibo subjects showed greater inhibition at the 60 msec pre-pulse interval that approached significance [$t(1,8) = -1.864$, $p = 0.09$]. These results demonstrate that neonatal amygdala lesions, in the rhesus monkey, are not sufficient to impair PPI.

Baseline amplitudes and percent inhibition in Group Neo-A-ibo did not correlate with extent of amygdala damage or extent of inadvertent damage to adjacent structures.

Baseline Startle and PPI in Groups Neo-C and Neo-O-asp

Figure 5.5 (C and F) illustrates baseline startle curves at each pulse intensity and PPI curves at each pre-pulse interval for monkeys with neonatal aspiration lesions of the orbital frontal cortex (Neo-O-asp) and sham-operated controls (Neo-C).

Group Neo-O-asp showed a flattened startle response curve (Fig. 5.5C), with low startle magnitude at all amplitudes (baseline: 0.158 ± 0.028, 95dB: 0.322 ± 0.121, 100dB: 0.398 ± 0.135, 110dB: 0.405 ± 0.141, 115dB 560 ± 0.167 and 120dB: 1.110 ± 0.437). This shallow increase in startle amplitude did not differ significantly from the more substantial increase in startle amplitude found in Group Neo-C, although it approached significance [$F(1,8) = 3.959$, $p = 0.082$]. In parallel, to findings in Neo-H-ibo and Neo-A-ibo, Neo-O-asp showed an effect of startle magnitude of pulse intensity [$F(5,40) = 8.754$, $p < 0.001$]. In contrast to the other two lesion groups an interaction of orbital frontal lesion and pulse intensity was detected [$F(5,40] = 2.699$, $p < 0.05$]. The

interaction effect was not significant at any pulse intensity ($p > 0.05$), although it did approach significance at 110dB pulse intensity [$t(1,8) = 2.001$, $p = 0.08$]. These findings indicate that early lesions of the orbital frontal cortex are sufficient to produce a minor reduction of startle magnitude to acoustic stimuli.

However, as compared to controls, neonatal lesions of the orbital frontal cortex have severely reduced pre-pulse inhibition at all pre-pulse intervals (60 msec: 26.5% ± 19.4, 120 msec: 31.8% ± 11.4, 240 msec: 27.7% ± 12.0, 480 msec: -64.1% ± 82.5, 1000 msec: 20.4% ± 13.1 and 5000 msec: 21.9% ± 10.1). This group difference became significant only at the 120 and 240 msec pre-pulse intervals (Fig. 5.5F). Analysis of the data revealed that Neo-O-asp showed reduced inhibition [$F(1,8) = 6.971$, $p < 0.05$]. However, Neo-O-asp did not show an effect of pre-pulse interval [$F(5,40) = 1.387$, $p = 0.250$], indicating a severe disruption of the sensory-motor gating circuitry. No interaction of pre-pulse intensity and lesion was detected [$F(5,40] = 1.472$, $p = 0.221$], however pre-planned comparisons revealed deficits at specific pre-pulse intervals. Neo-O-asp was found to show impaired inhibitory responses at pre-pulse intervals of 120 [$t(1,8) = 2.309$, $p = 0.05$] and 240 msec [$t(1,8) = 2.512$, $p < 0.05$] pre-pulse intervals. These results demonstrate that neonatal aspiration lesions of the orbital frontal cortex (areas 11 and 13) are sufficient to impair sensory-motor gating.

Although there were no correlations between baseline startle amplitude and extent of orbital frontal lesions or unintended adjacent damage, PPI was positively correlated to mean bilateral unintended damage to area 14 at pre-pulse intervals of 60 msec ($r = 0.960$, $p < 0.05$), 120 msec ($r = 0.960$, $p < 0.01$) and 240 msec ($r = 0.988$, $p < 0.01$). At each of this interval, the greater the damage to area 14 the lesser inhibition observed.

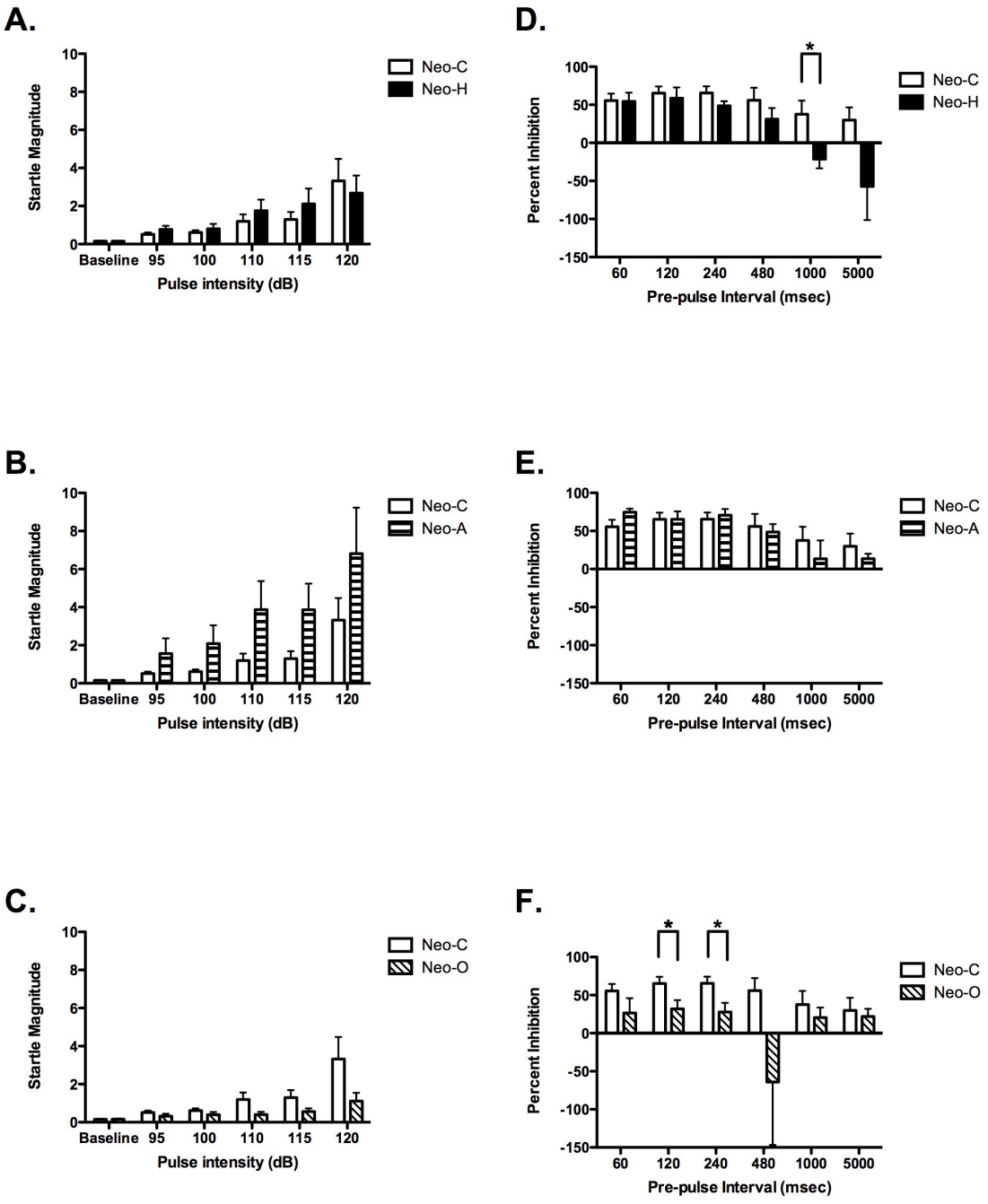

Figure 5.5: Startle and PPI. Baseline startle responses (graphs in the left column) to pulse intensities of 90, 100, 110, 115 and 120dB across two startle sessions in sham-

operated controls (Group Neo-C) as compared to animals with neonatal hippocampal lesions (Group Neo-H-ibo inA), animals with neonatal amygdala lesions (Group Neo-A in B) and animals with neonatal orbital frontal lesions (Group Neo-O-asp in C). Pre-pulse inhibition (graphs in the right column) to pre-pulse intervals of 60, 120, 240, 480, 1000 and 5000 msec in Group Neo-C vs Group Neo-H-ibo (D), Group Neo-C vs. Group Neo-A-ibo (E) and Group Neo-C vs. Group-Neo-O-asp (F). * ($p < 0.05$).

Discussion

The current study yielded several important results. First, it replicates data from an earlier study of acoustic startle and PPI curves in rhesus monkeys [205]. Second, the results demonstrated for the first time that neonatal lesions of the hippocampus in the rhesus monkey altered the neural circuitry necessary for the filtering of acoustic stimuli. Third, whereas neonatal amygdala lesions did not alter the startle amplitude response or pre-pulse inhibition, neonatal lesions of the orbital frontal cortical areas 11 and 13 reduced baseline startle amplitudes and blunted PPI at short intervals. These results will be discussed in turn.

The hippocampus and sensory motor gating

Neonatal lesions of the hippocampus in monkeys reduced prepulse inhibition and more specifically at the longer intervals of 480 msec, 1000 msec and 5000 msec, indicating that the hippocampus plays a role in sensory motor gating. Although these findings in monkeys concur with those reported in rodents with neonatal hippocampal lesions [5, 7], one important difference between the primates and the rodents data relies on the pre-pulse intervals at which these changes occurred. Thus, reduced PPI in the monkeys were found mostly at the long pre-pulse intervals (i.e. 1000 msec), whereas reduced PPI in rodents were found at shorter prepulse intervals (i.e. between 60-240 msec)[72,74]. Although the reasons for such species differences are at present not clear,

several possibilities exist. One potential explanation relates to the size of the lesions. The animals of the present study had far greater hippocampal lesion (including both posterior and anterior regions), as opposed to rodents in which the neonatal lesions targeted specifically the ventral hippocampus (anterior hippocampus of primate)[68,70]. Thus, the neonatal hippocampal lesions in primate could have had more widespread effects on brain maturation than the rodent lesions, resulting in a change in the temporal effect on sensory-motor gating. A second possibility may be linked to the developmental age at which the neonatal lesion occurred in the two species. Thus, although in both species the hippocampal lesions occurred only few days after birth, brain maturation at the time of lesion differed significantly between the two species, being more mature in the primates than in the rodents hence resulting in different effects on the maturation of the remaining neural networks [216]. Regardless, subsequent histological investigations of the brain of the monkeys with neonatal lesions should examine the ventral striatum for alterations in gamma-aminobutyric acid-a receptors (GABA), which have been shown to be critical in regulating PPI [217], and were potentially impacted by the early lesion. Additional measures of PPI using different sensory modalities (vision or touch) could confirm and substantiate the current findings. Nevertheless, we feel confident that the effects noticed after neonatal lesions are genuine given that different outcomes resulted from lesions of the amygdala and orbital frontal cortex (see below).

The orbital frontal cortex, but not the amygdala, regulates sensory motor gating

The second interesting finding of this paper is that early lesions of the amygdala do not impair pre-pulse inhibition. A series of previous studies in rodents have

demonstrated that damage to the amygdala, in infancy or adulthood, severely disrupts PPI [201,206,207]. This species difference is reminiscent to that observed with the same monkeys when tested on object reversal learning. Thus, although amygdala lesions in monkeys, either in infancy or adulthood, fail to disrupt the abilities to switch choice selection when the reward contingency of the stimuli has changed,[218,219] similar lesions in rodents result in significant impairment.[220] One potential explanation for this species difference is related to the significant expansion of the orbital frontal cortex in the monkeys, which may support some of the functions normally mediated by the amygdala in the [221]. This possibility has received support from the findings we obtained in the animals with neonatal orbital cortex lesions. Thus, contrary to the sparing of PPI after neonatal amygdala lesions, neonatal lesions of the orbital frontal cortex resulted in severe reduction in PPI, more specifically at the short pre-pulses of 120 and 240 msec.

The last interesting finding of the current study is the significant correlation obtained between unintended damage to area 14 (medial frontal cortex) and magnitude of inhibition at pre-pulse intervals of 60, 120 and 240 msec following neonatal aspiration lesions of the orbital frontal cortex. Thus, greater damage to the medial prefrontal cortex was associated with more inhibition, despite the fact that Group Neo-O was impaired at intervals of 120 and 240 msec relative to control subjects. Interestingly, the monkey with the greatest bilateral damage to area 14 (Case Neo-O-asp-2, 19.4% bilateral) did no differ from controls at any of the aforementioned intervals: 60 msec (80.0%), 120 msec (70.7%) and 240 msec (71.1%). This result is intriguing but may indicate that in monkeys, as in rodents, neonatal lesions of the medial prefrontal cortex enhanced PPI [211,212]. The fact that we still saw decreased startle in the remainder of the group may be due to the limited

extent of damage to area 14 and its' ability to counteract the effects of damage to areas 11 and 13. Future studies with selective lesions of each of these areas are needed to delineate the specific roles each of these areas plays in sensory-motor gating.

Conclusions

Impaired sensory-motor gating after neonatal hippocampal lesions parallel and extend findings reported in rodents with neonatal ventral hippocampal lesions [72-74,208]. In addition, the effects of early lesions of the hippocampus in monkeys on pre-pulse inhibition are consistent with the deficit in PPI reported in schizophrenia literature [49,51,56-58,222], which is acknowledged as a core symptom of the disorder. Thus, in both rodents and primates, the early lesions of the hippocampus not only impaired sensory-motor gating but also working memory processes and are associated with prefrontal malfunction [72,80,183,189], which recapitulate a number of neuropathological changes and symptoms reported in schizophrenia [24,34,39,58,60,62,223-225]. However, although the neonatal hippocampal model in rodents and primates could be used as important tool to shed light on the etiology of schizophrenia and test new therapeutic strategies, they do not re-create the human syndrome in its entirety.

Chapter 6

Overall Discussion

This general discussion will begin with an overall review of the behavioral and neuroimaging data. Subsequently, the current findings will be discussed in light of what is known about working memory, n-acetyl-aspartate, and the rodent model of schizophrenia. Lastly, the limitations and future directions of this line of research will be highlighted.

Summary

The first set of experiments was designed to examine monitoring and maintenance working memory following neonatal lesions of the hippocampus, by

employing two behavioral tasks that measure these processes. Adult monkeys with neonatal lesions of the hippocampus and sham-operated controls were tested on the Session Unique Delayed Non-Match-to-Sample and Object Self Ordered tasks that assess maintenance and monitoring working memory processes, respectively. The results of this first experiment indicated that early lesions of the hippocampus impaired monitoring but not maintenance working memory processes. As monitoring working memory has been consistently found to be dependent upon the dlPFC [92,93,101-103,157,158], these findings provided the first evidence that early lesions of the hippocampus in the non-human primate impact the functional integrity of this structure.

In order to independently confirm our preliminary finding of a functional deficit of dlPFC dependent working memory following early lesions of the hippocampus, the same group of monkeys and their controls were tested on the serial order memory task. The serial order memory task also measures monitoring, much like the Object-Self Ordered task, but has the advantage to test both maintenance and monitoring working memory processes, in a single behavioral task [102,103]. The results of this second experiment also showed that neonatal lesions of the hippocampus were sufficient to impair working memory processes (monitoring) dependent upon the dlPFC, but spare working memory processes (maintenance) dependent upon the vlPFC. The results of these two studies, in sum, provide strong evidence that early damage to the hippocampus can impact the function of the dlPFC in later life.

The third experiment employed Magnetic Resonance Spectroscopy (MRS) to examine integrity of the prefrontal cortex. n-acetly-asparte (NAA) levels were measured in the dlPFC, vlPFC and primary somatosensory cortex of these same animals. The

results of this experiment demonstrated no overall changes in the NAA levels within the dlPFC after the neonatal hippocampal lesions, although individual variability of NAA levels within this region was greatly increased and correlated with behavioral performance on the monitoring working memory tasks. In contrast, NAA levels in the vlPFC increased bilaterally and were inversely correlated with their performance on the working memory tasks. Lastly, no difference of NAA levels was detected in the primary somatosensory cortex, suggesting the NAA changes in the prefrontal cortex were genuine and did not result from non-specific global NAA alterations after the early hippocampal lesion.

In the fourth, and final experiment we sought to examine the impact of neonatal hippocampal lesions in the primate on sensory-motor gating. Sensory-motor gating was assessed using the pre-pulse inhibition paradigm, which measures inhibitory modulation of whole body startle to acoustic stimuli [205]. The results of the PPI experiment showed that neonatal lesions of the hippocampus in the rhesus monkey, disrupted sensory-motor gating at long pre-pulse intervals. Given that sensory-motor gating depends upon the same ventral striatal neural circuitry as working memory [202,203,217], overall the behavioral and cognitive findings support the hypothesis that early lesions of the hippocampus impact the functioning of the dlPFC through the ventral striatum.

Symptom Category	Measure	Result
Cognitive (Working Memory)	SU-DNMS	No impairment
	Obj-SO	Impairment
	3-SOMT	No Impairment
	4-SOMT	Impairment
	4-SOMT Probe	Impairment
Pathology (NAA levels)	dlPFC NAA	No Change
	vlPFC NAA	Increased
	S1 NAA	No Change
Sensory-Motor Gating	Startle	No Change
	Pre-pulse Inhibition	Impairment

Table 6.1: *Data Summary Table.* The table outlines the effects of early hippocampal lesions in the rhesus monkey as it pertains to schizophrenia.

Prefrontal cortical function in Neo-H, as it relates to working memory

One of the primary goals of this thesis was to thoroughly evaluate the consequence of early hippocampal lesions on prefrontal cortical function in the primate, employing a battery of working memory tasks. The strength of employing multiple measures of working memory is that it provides independent confirmation of the working memory impairment associated with neonatal lesions of the hippocampus. The conceptualization of the original design of the experiment focused on providing essentially four measures of working memory: 2 measures of vlPFC function (SU-DNMS and 3-SOMT) and 2 measures of dlPFC function (Obj-SO and 4-SOMT). This was modified at a later date to include the 4-SOMT probe trials to provide one last examination of both vlPFC and dlPFC function, simultaneously.

The results of the current investigation demonstrated no impairment on SU-DNMS or 3-SOMT tasks, indicating consistent data between the two independent

measures of maintenance working memory. This result confirms that early lesions of the hippocampus are not sufficient to impair the function of the maintenance working memory [102,103,156,167]. In a similar manner, the Obj-SO and 4-SOMT tasks both showed that Neo-H monkeys were severely impaired on monitoring working memory, highlighting a selective deficit in working memory performance, related to the dlPFC. Lastly, the 4-SOMT probe trials confirmed these findings and demonstrated that dlPFC-dependent working memory processes are impaired but vlPFC-dependent processes are intact following selective lesions of the hippocampus in the rhesus monkey.

Hippocampal versus prefrontal effects on working memory

In discussing the findings of the current experiments it is also important to discuss how these findings relate to a prefrontal-mediated impairment. Previous studies in the human initially characterized the nature of working memory impairments resulting from prefrontal cortical lesions [157,186]. Sequential investigations in the monkeys with focal lesions of the prefrontal cortex vastly improved our understanding of prefrontal contributions to working memory for order [101-103], such that lesions of the prefrontal cortex result in subtle impairments in performance. In the case of serial order, dlPFC lesions render the animal unable to discriminate serial items that do not include an endpoint, (i.e. in a four item series a recency discrimination between objects 2 and 3). In contrast, studies of temporal order in rats have consistently shown that hippocampal lesions globally impair memory for temporal order [95,170], regardless of the temporal location of the object. Our results demonstrated that neonatal hippocampal lesions in the

monkey, produces a behavioral profile that is consistent with a prefrontal deficit, and not an hippocampal deficit, as they showed no global impairment in serial order memory.

MRS, What exactly is NAA and what does the current finding really mean?

The magnetic resonance spectroscopy study was aimed at examining, *in vivo*, the functional architecture of the prefrontal cortex, following neonatal lesions of the hippocampus. The primary measure obtained from ^{1}H-MRS is levels of n-acetyl-aspartate (NAA), an amino acid that has consistently been linked with normal nervous system function [198]. NAA levels, as measured by MRS, have been associated with brain dysfunction in a wide variety of psychiatric diseases including schizophrenia, autism and bi-polar disorder [192]. In particular MRS has been widely used to study regional brain abnormalities in schizophrenia [21-23,46,193,195], although the observed decreased levels in NAA were originally thought to reflect reduced neuronal numbers in the brain. However, recent studies have shown that reduced NAA levels are associated with more subtle alterations, such as changes in spine density alterations of synaptic releasing proteins [16-18,20,226]. In addition, recent research has shown that successful neuroleptic treatment, which is thought to alter spine densities and synaptic release, can actually increase the levels of NAA within the dlPFC of schizophrenia patients [194], suggesting that NAA is more indicative of functional integrity. In light of this, a discussion of recent research in to the neural mechanisms associated with changes in NAA may aid in interpreting the current findings.

Initially, NAA was characterized by Tallan, as the second most abundant amino acid in the brain, after glutamate, in mammalian species [227]. While it was first thought

that NAA was synthesized in the periphery, it was later discovered that it could not cross the blood brain barrier [228] and is, in fact, synthesized in the mitochondria of neurons [229,230]. Following synthesis in neurons, NAA then has a variety of functions, although it is typically coupled to glutamate (n-acetyl-aspartyl-glutamate, NAAG) and released from vesicles, as all other neurotransmitters in the brain. NAAG then has two primary mechanisms of action: 1. As an endogenous NMDA in neurons, reducing overall excitability of the system [198] and 2. As an agonist at the glutamate receptor (mGluR3), an auto-receptor, which regulates calcium fluxes released from astrocytes [231,232]. These studies support NAA as a critical mediator of neuronal function within the central nervous system, in general, and more specifically a homeostatic peacekeeper. Inadequate production of NAA could lead to calcium imbalances in the system, creating an environment of excitotoxicity and general dysfunction, which has been found in certain types of epilepsy [233]. In general, decreases in NAA would be associated with decreased overall activation of a structure as it is produced as a product of activity. Conversely, brain areas with increased NAA are likely indicative of increased overall activity, as increased NAA production would be required to balance increased excitability. Consequently, brain areas showing increased NAA would be associated with increased spine densities and synaptic release machinery.

The current study reported increased NAA within the vlPFC following neonatal lesions of the hippocampus. Further, the NAA levels in the vlPFC were inversely proportional to the performance on the dlPFC dependent working memory tasks, such that greater NAA levels were associated with poorer performance on the dlPFC dependent working memory tasks. One interpretation of these findings is that, as dlPFC

becomes less functional, performance may depend more heavily on the vlPFC and presumably may result in increased NAA levels. However, given that the vlPFC cannot completely substitute for all of dlPFC functions, the increase in NAA levels in the vlPFC may help maintenance memory processes dependent upon the vlPFC, but may not support monitoring memory processes mediated by the dlPFC. This scenario will explain the pattern of working memory performance deficit seen in animals with Neo-H lesions. Presumably, as the vlPFC is activated more frequently and to a greater degree than normal, more NAA is produced to control excitability that will likely result in morphological changes (spine densities, synaptic release proteins etc) in the vlPFC.

Implications

The primary goal of this thesis was to determine if the rodent model of schizophrenia, employing neonatal lesions of the hippocampus [68] was in fact tenable in the primate. While considerable work has been performed in this model, the questionable homology of the prefrontal cortex, between rodents and primates [91,234], raises the questions of how this model will apply in a primate. As such, the rhesus monkey affords an opportunity to examine the consequence of early hippocampal damage to a prefrontal cortex that is more homologous to the human condition [4,5,92]. The results of these series of studies support the application of the rodent schizophrenia model in the primate, with certain subtle differences. In general the rodent model has demonstrated impairments in maintenance working memory [79-81,152-154]. In contrast, we found maintenance working memory (vlPFC dependent) to be intact, but monitoring working memory (dlPFC dependent) to be impaired following selective neonatal hippocampal lesions in the non-human primate. In addition, we found sensory-motor gating impairments in Neo-H

monkeys, similar to the findings in rats [72-74], although the impairment was at longer pre-pulse intervals rather than at the short pre-pulse intervals as shown in the previous rodent studies. Lastly, MRS studies in the Neo-H rats reported reduced NAA in the medial prefrontal cortex (presumed rodent homolog of the dlPFC) [88]. In contrast, the MRS study found no overall reduction in NAA within the dlPFC, although it did seem to increase the variability of the NAA levels, which correlated with the behavioral performance dlPFC dependent tasks. Thus, these results indicate that the neonatal hippocampal lesion model of schizophrenia is tenable in the non-human primate.

Limitations

As is the case with any method, certain limitations apply in the ability of the current investigation to generalize to the human condition in general and to schizophrenia, specifically. While we sought to investigate the consequence of early hippocampal damage as a potential non-human primate "model" of schizophrenia, this in no way means that we were attempting to recreate the full-blown disease in a monkey. In contrast, I would argue that schizophrenia is a uniquely human disease that is not possible without the expansive human neocortex. In this case, the focus is an attempt to understand how two structures (hippocampus and dlPFC) that have been consistently implicated in schizophrenia interact across the developmental window in a non-human primate. Thus, the early lesion model of studying functional interactions has allowed us to demonstrate that early damage to the hippocampus results in a dysfunctional dlPFC in adulthood, providing the first causal evidence for this connection, in the primate.

A second limitation of the study, in its ability to generalize to schizophrenia, is the extent of hippocampal damage in our animals. A meta-analysis of hippocampal volume

reduction, in over 500 schizophrenia patients, found the average bilateral reduction to be approximately 4 percent [40]. In contrast, we estimated the average bilateral damage to the hippocampus to be 48% for the monkeys in the current study. The difference in mean lesion size may contribute significantly to behavioral phenotypes, especially considering some studies have noted an inverse relationship between extent of hippocampal damage and impairments on behavioral tasks [235].

Future Directions

The series of experiments described in this thesis have successfully shown that early lesions of the hippocampus are sufficient to impact the functional integrity of the prefrontal cortex. However, these experiments have raised a series of questions. The first line of questioning has to do with the nature of the effect that we are seeing following early lesions of the hippocampus. Is the adult hippocampus necessary for monitoring working memory? The current study showed that neonatal lesions are sufficient to impair working memory and that the integrity of the prefrontal cortex seems to be altered as a consequence, as measured by MRS. However, no study to date has examine the consequence of adult hippocampal lesions on monitoring working memory in the primate. These studies are needed in order to determine if the effect we are seeing is a developmental, functional or mixed developmental/functional affect on the prefrontal cortical function.

A second level of future studies should be aimed at histological studies of Neo-H monkeys to examine changes at the cellular, receptor and molecular level that can explain the nature of changes seen at the behavioral level. Years of work in rodents and monkeys have elucidated the extent of dopaminergic regulation of working memory [135-

[138,176,234,236,237] and pre-pulse inhibition [225,238,239] in the prefrontal cortex and ventral striatum, respectively. In addition, several other studies have reported alterations in GABAergic and dopaminergic markers following neonatal lesions of the hippocampus in the rat [83,85,86,154,240]. Given the behavioral profile we have documented following neonatal hippocampal lesions in the monkeys it naturally follows that future investigations would seek to investigate the molecular changes associated with the dopamine and GABA in the prefrontal cortex and ventral striatum/nucleus accumbens.

Finally, it will be also very important to investigate the time course of the behavioral and cognitive changes that we have described. Thus, will the dysfunction of the dlPFC occurs immediately after the neonatal lesions or did the lesion have impacted remodeling within the dlPFC that emerges during adolescence? Are the deficits in working memory processes also emerging at the same time point? Answers to those questions are critical to validate this primate model that could provide important tool to test new therapeutic agents to alleviate the devastating cognitive impairments seen in schizophrenia.

References

1 Floresco, S. B., Geyer, M. A., Gold, L. H. & Grace, A. A. Developing predictive animal models and establishing a preclinical trials network for assessing treatment effects on cognition in schizophrenia. *Schizophr Bull* **31**, 888-894, (2005).

2 Geyer, M. A. & Heinssen, R. New approaches to measurement and treatment research to improve cognition in schizophrenia. *Schizophr Bull* **31**, 806-809, (2005).

3 Nuechterlein, K. H., Robbins, T. W. & Einat, H. Distinguishing separable domains of cognition in human and animal studies: what separations are optimal for targeting interventions? A summary of recommendations from breakout group 2 at the measurement and treatment research to improve cognition in schizophrenia new approaches conference. *Schizophr Bull* **31**, 870-874, (2005).

4 Levy, R. & Goldman-Rakic, P. S. Association of storage and processing functions in the dorsolateral prefrontal cortex of the nonhuman primate. *J Neurosci* **19**, 5149-5158, (1999).

5 Petrides, M. Lateral prefrontal cortex: architectonic and functional organization. *Philos Trans R Soc Lond B Biol Sci* **360**, 781-795, (2005).

6 (American Psychiatric Association, Washington, D.C., 2000).

7 Fombonne, E. Epidemiology of pervasive developmental disorders. *Pediatr Res* **65**, 591-598, (2009).

8 McGrath, J. J. & Susser, E. S. New directions in the epidemiology of schizophrenia. *Med J Aust* **190**, S7-9, (2009).

9 Susser, E. S. & Lin, S. P. Schizophrenia after prenatal exposure to the Dutch Hunger Winter of 1944-1945. *Arch Gen Psychiatry* **49**, 983-988, (1992).

10 Kendell, R. E. & Kemp, I. W. Maternal influenza in the etiology of schizophrenia. *Arch Gen Psychiatry* **46**, 878-882, (1989).

11 Barr, C. E., Mednick, S. A. & Munk-Jorgensen, P. Exposure to influenza epidemics during gestation and adult schizophrenia. A 40-year study. *Arch Gen Psychiatry* **47**, 869-874, (1990).

12 Malaspina, D. *et al.* Advancing paternal age and the risk of schizophrenia. *Arch Gen Psychiatry* **58**, 361-367, (2001).

13 Wu, E. Q. *et al.* The economic burden of schizophrenia in the United States in 2002. *J Clin Psychiatry* **66**, 1122-1129, (2005).

14 Caqueo-Urizar, A., Gutierrez-Maldonado, J. & Miranda-Castillo, C. Quality of life in caregivers of patients with schizophrenia: a literature review. *Health Qual Life Outcomes* **7**, 84, (2009).

15 Manschreck, T. C. & Boshes, R. A. The CATIE schizophrenia trial: results, impact, controversy. *Harv Rev Psychiatry* **15**, 245-258, (2007).

16 Selemon, L. D., Rajkowska, G. & Goldman-Rakic, P. S. Abnormally high neuronal density in the schizophrenic cortex. A morphometric analysis of prefrontal area 9 and occipital area 17. *Arch Gen Psychiatry* **52**, 805-818; discussion 819-820, (1995).

17 Garey, L. J. *et al.* Reduced dendritic spine density on cerebral cortical pyramidal neurons in schizophrenia. *J Neurol Neurosurg Psychiatry* **65**, 446-453, (1998).

18 Glantz, L. A. & Lewis, D. A. Decreased dendritic spine density on prefrontal cortical pyramidal neurons in schizophrenia. *Arch Gen Psychiatry* **57**, 65-73, (2000).

19 Isseroff, A., Rosvold, H. E., Galkin, T. W. & Goldman-Rakic, P. S. Spatial memory impairments following damage to the mediodorsal nucleus of the thalamus in rhesus monkeys. *Brain Res* **232**, 97-113, (1982).

20 Glantz, L. A. & Lewis, D. A. Reduction of synaptophysin immunoreactivity in the prefrontal cortex of subjects with schizophrenia. Regional and diagnostic specificity. *Arch Gen Psychiatry* **54**, 943-952, (1997).

21 Bertolino, A. *et al.* Regionally specific pattern of neurochemical pathology in schizophrenia as assessed by multislice proton magnetic resonance spectroscopic imaging. *Am J Psychiatry* **153**, 1554-1563, (1996).

22 Deicken, R. F., Zhou, L., Corwin, F., Vinogradov, S. & Weiner, M. W. Decreased left frontal lobe N-acetylaspartate in schizophrenia. *Am J Psychiatry* **154**, 688-690, (1997).

23 Tanaka, Y. *et al.* Quantitative magnetic resonance spectroscopy of schizophrenia: relationship between decreased N-acetylaspartate and frontal lobe dysfunction. *Psychiatry Clin Neurosci* **60**, 365-372, (2006).

24 Ardekani, B. A., Nierenberg, J., Hoptman, M. J., Javitt, D. C. & Lim, K. O. MRI study of white matter diffusion anisotropy in schizophrenia. *Neuroreport* **14**, 2025-2029, (2003).

25 Buchsbaum, M. S. *et al.* MRI white matter diffusion anisotropy and PET metabolic rate in schizophrenia. *Neuroreport* **9**, 425-430, (1998).

26 Caan, M. W. *et al.* Shaving diffusion tensor images in discriminant analysis: a study into schizophrenia. *Med Image Anal* **10**, 841-849, (2006).

27 Federspiel, A. *et al.* Alterations of white matter connectivity in first episode schizophrenia. *Neurobiol Dis* **22**, 702-709, (2006).

28 Hao, Y. *et al.* White matter integrity of the whole brain is disrupted in first-episode schizophrenia. *Neuroreport* **17**, 23-26, (2006).

29 Hubl, D. *et al.* Pathways that make voices: white matter changes in auditory hallucinations. *Arch Gen Psychiatry* **61**, 658-668, (2004).

30 Kubicki, M. *et al.* DTI and MTR abnormalities in schizophrenia: analysis of white matter integrity. *Neuroimage* **26**, 1109-1118, (2005).

31 Kubicki, M., Westin, C. F., McCarley, R. W. & Shenton, M. E. The application of DTI to investigate white matter abnormalities in schizophrenia. *Ann N Y Acad Sci* **1064**, 134-148, (2005).

32 Jansma, J. M., Ramsey, N. F., van der Wee, N. J. & Kahn, R. S. Working memory capacity in schizophrenia: a parametric fMRI study. *Schizophr Res* **68**, 159-171, (2004).

33 Snitz, B. E. *et al.* Lateral and medial hypofrontality in first-episode schizophrenia: functional activity in a medication-naive state and effects of short-term atypical antipsychotic treatment. *Am J Psychiatry* **162**, 2322-2329, (2005).

34 Barch, D. M., Sheline, Y. I., Csernansky, J. G. & Snyder, A. Z. Working memory and prefrontal cortex dysfunction: specificity to schizophrenia compared with major depression. *Biol Psychiatry* **53**, 376-384, (2003).

35 Steen, R. G., Mull, C., McClure, R., Hamer, R. M. & Lieberman, J. A. Brain volume in first-episode schizophrenia: systematic review and meta-analysis of magnetic resonance imaging studies. *Br J Psychiatry* **188**, 510-518, (2006).

36 Altshuler, L. L., Conrad, A., Kovelman, J. A. & Scheibel, A. Hippocampal pyramidal cell orientation in schizophrenia. A controlled neurohistologic study of the Yakovlev collection. *Arch Gen Psychiatry* **44**, 1094-1098, (1987).

37 Conrad, A. J., Abebe, T., Austin, R., Forsythe, S. & Scheibel, A. B. Hippocampal pyramidal cell disarray in schizophrenia as a bilateral phenomenon. *Arch Gen Psychiatry* **48**, 413-417, (1991).

38 Eastwood, S. L. & Harrison, P. J. Decreased synaptophysin in the medial temporal lobe in schizophrenia demonstrated using immunoautoradiography. *Neuroscience* **69**, 339-343, (1995).

39 Szeszko, P. R. *et al.* Neuropsychological correlates of hippocampal volumes in patients experiencing a first episode of schizophrenia. *Am J Psychiatry* **159**, 217-226, (2002).

40 Nelson, M. D., Saykin, A. J., Flashman, L. A. & Riordan, H. J. Hippocampal volume reduction in schizophrenia as assessed by magnetic resonance imaging: a meta-analytic study.[see comment]. *Arch Gen Psychiatry* **55**, 433-440, (1998).

41 Bogerts, B. *et al.* Reduced temporal limbic structure volumes on magnetic resonance images in first episode schizophrenia. *Psychiatry Res* **35**, 1-13, (1990).

42 Bogerts, B., Meertz, E. & Schonfeldt-Bausch, R. Basal ganglia and limbic system pathology in schizophrenia. A morphometric study of brain volume and shrinkage. *Arch Gen Psychiatry* **42**, 784-791, (1985).

43 Hirayasu, Y. *et al.* Lower left temporal lobe MRI volumes in patients with first-episode schizophrenia compared with psychotic patients with first-episode affective disorder and normal subjects. *Am J Psychiatry* **155**, 1384-1391, (1998).

44 Velakoulis, D. *et al.* Hippocampal volume in first-episode psychoses and chronic schizophrenia: a high-resolution magnetic resonance imaging study. *Arch Gen Psychiatry* **56**, 133-141, (1999).

45 Bertolino, A. *et al.* Reproducibility of proton magnetic resonance spectroscopic imaging in patients with schizophrenia. *Neuropsychopharmacology* **18**, 1-9, (1998).

46 Renshaw, P. F., Yurgelun-Todd, D. A., Tohen, M., Gruber, S. & Cohen, B. M. Temporal lobe proton magnetic resonance spectroscopy of patients with first-episode psychosis. *Am J Psychiatry* **152**, 444-446, (1995).

47 Meyer-Lindenberg, A. S. *et al.* Regionally specific disturbance of dorsolateral prefrontal-hippocampal functional connectivity in schizophrenia. *Arch Gen Psychiatry* **62**, 379-386, (2005).

48 Swerdlow, N. R., Geyer, M. A. & Braff, D. L. Neural circuit regulation of prepulse inhibition of startle in the rat: current knowledge and future challenges. *Psychopharmacology (Berl)* **156**, 194-215, (2001).

49 Braff, D. *et al.* Prestimulus effects on human startle reflex in normals and schizophrenics. *Psychophysiology* **15**, 339-343, (1978).

50 Hazlett, E. A. *et al.* Prefrontal cortex glucose metabolism and startle eyeblink modification abnormalities in unmedicated schizophrenia patients. *Psychophysiology* **35**, 186-198, (1998).

51 Braff, D. L., Grillon, C. & Geyer, M. A. Gating and habituation of the startle reflex in schizophrenic patients. *Arch Gen Psychiatry* **49**, 206-215, (1992).

52 Perry, W. & Braff, D. L. Information-processing deficits and thought disorder in schizophrenia. *Am J Psychiatry* **151**, 363-367, (1994).

53 Karper, L. P. *et al.* Preliminary evidence of an association between sensorimotor gating and distractibility in psychosis. *J Neuropsychiatry Clin Neurosci* **8**, 60-66, (1996).

54 Ford, J. M., Roth, W. T., Menon, V. & Pfefferbaum, A. Failures of automatic and strategic processing in schizophrenia: comparisons of event-related brain potential and startle blink modification. *Schizophr Res* **37**, 149-163, (1999).

55 Bender, S. *et al.* A topographic event-related potential follow-up study on 'prepulse inhibition' in first and second episode patients with schizophrenia. *Psychiatry Res* **90**, 41-53, (1999).

56 Perry, W., Geyer, M. A. & Braff, D. L. Sensorimotor gating and thought disturbance measured in close temporal proximity in schizophrenic patients. *Arch Gen Psychiatry* **56**, 277-281, (1999).

57 Braff, D. L., Swerdlow, N. R. & Geyer, M. A. Symptom correlates of prepulse inhibition deficits in male schizophrenic patients. *Am J Psychiatry* **156**, 596-602, (1999).

58 Parwani, A. *et al.* Impaired prepulse inhibition of acoustic startle in schizophrenia. *Biol Psychiatry* **47**, 662-669, (2000).

59 Swerdlow, N. R., Weber, M., Qu, Y., Light, G. A. & Braff, D. L. Realistic expectations of prepulse inhibition in translational models for schizophrenia research. *Psychopharmacology (Berl)* **199**, 331-388, (2008).

60 Park, S. & Holzman, P. S. Schizophrenics show spatial working memory deficits. *Arch Gen Psychiatry* **49**, 975-982, (1992).

61 Perlstein, W. M., Dixit, N. K., Carter, C. S., Noll, D. C. & Cohen, J. D. Prefrontal cortex dysfunction mediates deficits in working memory and prepotent responding in schizophrenia. *Biol Psychiatry* **53**, 25-38, (2003).

62 Chey, J., Lee, J., Kim, Y. S., Kwon, S. M. & Shin, Y. M. Spatial working memory span, delayed response and executive function in schizophrenia. *Psychiatry Res* **110**, 259-271, (2002).

63 Lee, J. & Park, S. Working memory impairments in schizophrenia: A Meta-Analysis. *Journal of Abnormal Psychology* **114**, 599-611, (2005).

64 Honey, G. D. *et al.* Differences in frontal cortical activation by a working memory task after substitution of risperidone for typical antipsychotic drugs in patients with schizophrenia.[see comment]. *Proc Natl Acad Sci U S A* **96**, 13432-13437, (1999).

65 Lehrer, D. S. *et al.* Thalamic and prefrontal FDG uptake in never medicated patients with schizophrenia. *Am J Psychiatry* **162**, 931-938, (2005).

66 Cannon, T. D. *et al.* Dorsolateral prefrontal cortex activity during maintenance and manipulation of information in working memory in patients with schizophrenia. *Arch Gen Psychiatry* **62**, 1071-1080, (2005).

67 Meyer-Lindenberg, A. *et al.* Evidence for abnormal cortical functional connectivity during working memory in schizophrenia. *Am J Psychiatry* **158**, 1809-1817, (2001).

68 Lipska, B. K. Using animal models to test a neurodevelopmental hypothesis of schizophrenia. *J Psychiatry Neurosci* **29**, 282-286, (2004).

69 Lodge, D. J. & Grace, A. A. The hippocampus modulates dopamine neuron responsivity by regulating the intensity of phasic neuron activation. *Neuropsychopharmacology* **31**, 1356-1361, (2006).

70 Tseng, K. Y., Chambers, R. A. & Lipska, B. K. The neonatal ventral hippocampal lesion as a heuristic neurodevelopmental model of schizophrenia. *Behav Brain Res* **204**, 295-305, (2009).

71 Rueter, L. E. *et al.* Chronic low dose risperidone and clozapine alleviate positive but not negative symptoms in the rat neonatal ventral hippocampal lesion model of schizophrenia. *Psychopharmacology (Berl)* **176**, 312-319, (2004).

72 Lipska, B. K. *et al.* Neonatal excitotoxic hippocampal damage in rats causes post-pubertal changes in prepulse inhibition of startle and its disruption by apomorphine. *Psychopharmacology (Berl)* **122**, 35-43, (1995).

73 Le Pen, G. *et al.* Prepulse inhibition deficits of the startle reflex in neonatal ventral hippocampal-lesioned rats: reversal by glycine and a glycine transporter inhibitor. *Biol Psychiatry* **54**, 1162-1170, (2003).

74 Le Pen, G. & Moreau, J. L. Disruption of prepulse inhibition of startle reflex in a neurodevelopmental model of schizophrenia: reversal by clozapine, olanzapine and risperidone but not by haloperidol. *Neuropsychopharmacology* **27**, 1-11, (2002).

75 Laplante, F., Nakagawasai, O., Srivastava, L. K. & Quirion, R. Alterations in behavioral responses to a cholinergic agonist in post-pubertal rats with neonatal ventral hippocampal lesions: relationship to changes in muscarinic receptor levels. *Neuropsychopharmacology* **30**, 1076-1087, (2005).

76 Pouzet, B., Zhang, W. N., Weiner, I., Feldon, J. & Yee, B. K. Latent inhibition is spared by N-methyl-D-aspartate (NMDA)-induced ventral hippocampal lesions, but is attenuated following local activation of the ventral hippocampus by intracerebral NMDA infusion. *Neuroscience* **124**, 183-194, (2004).

77 Sams-Dodd, F., Lipska, B. K. & Weinberger, D. R. Neonatal lesions of the rat ventral hippocampus result in hyperlocomotion and deficits in social behaviour in adulthood. *Psychopharmacology (Berl)* **132**, 303-310, (1997).

78 Al-Amin, H. A., Weinberger, D. R. & Lipska, B. K. Exaggerated MK-801-induced motor hyperactivity in rats with the neonatal lesion of the ventral hippocampus. *Behav Pharmacol* **11**, 269-278, (2000).

79 Chambers, R. A., Moore, J., McEvoy, J. P. & Levin, E. D. Cognitive effects of neonatal hippocampal lesions in a rat model of schizophrenia. *Neuropsychopharmacology* **15**, 587-594, (1996).

80 Lipska, B. K., Aultman, J. M., Verma, A., Weinberger, D. R. & Moghaddam, B. Neonatal damage of the ventral hippocampus impairs working memory in the rat. *Neuropsychopharmacology* **27**, 47-54, (2002).

81 Levin, E. D. & Christopher, N. C. Effects of clozapine on memory function in the rat neonatal hippocampal lesion model of schizophrenia. *Prog Neuropsychopharmacol Biol Psychiatry* **30**, 223-229, (2006).

82 Lipska, B. K., Lerman, D. N., Khaing, Z. Z. & Weinberger, D. R. The neonatal ventral hippocampal lesion model of schizophrenia: effects on dopamine and GABA mRNA markers in the rat midbrain. *Eur J Neurosci* **18**, 3097-3104, (2003).

83 Goto, Y. & O'Donnell, P. Delayed mesolimbic system alteration in a developmental animal model of schizophrenia. *J Neurosci* **22**, 9070-9077, (2002).

84 Tseng, K. Y. *et al.* A neonatal ventral hippocampal lesion causes functional deficits in adult prefrontal cortical interneurons. *J Neurosci* **28**, 12691-12699, (2008).

85 Francois, J. *et al.* Selective reorganization of GABAergic transmission in neonatal ventral hippocampal-lesioned rats. *Int J Neuropsychopharmacol* **12**, 1097-1110, (2009).

86 Endo, K., Hori, T., Abe, S. & Asada, T. Alterations in GABA(A) receptor expression in neonatal ventral hippocampal lesioned rats: comparison of prepubertal and postpubertal periods. *Synapse* **61**, 357-366, (2007).

87 O'Donnell, P., Lewis, B. L., Weinberger, D. R. & Lipska, B. K. Neonatal hippocampal damage alters electrophysiological properties of prefrontal cortical neurons in adult rats. *Cereb Cortex* **12**, 975-982, (2002).

88 Bertolino, A. *et al.* Reduced N-acetylaspartate in prefrontal cortex of adult rats with neonatal hippocampal damage. *Cereb Cortex* **12**, 983-990, (2002).

89 Lipska, B. K., Halim, N. D., Segal, P. N. & Weinberger, D. R. Effects of reversible inactivation of the neonatal ventral hippocampus on behavior in the adult rat. *J Neurosci* **22**, 2835-2842, (2002).

90 Seamans, J. K., Lapish, C. C. & Durstewitz, D. Comparing the prefrontal cortex of rats and primates: insights from electrophysiology. *Neurotox Res* **14**, 249-262, (2008).

91 Uylings, H. B., Groenewegen, H. J. & Kolb, B. Do rats have a prefrontal cortex? *Behav Brain Res* **146**, 3-17, (2003).

92 Petrides, M. The role of the mid-dorsolateral prefrontal cortex in working memory. *Exp Brain Res* **133**, 44-54, (2000).

93 Petrides, M., Alivisatos, B. & Frey, S. Differential activation of the human orbital, mid-ventrolateral, and mid-dorsolateral prefrontal cortex during the processing of visual stimuli. *Proc Natl Acad Sci U S A* **99**, 5649-5654, (2002).

94 Keefe, R. S. *et al.* One-year double-blind study of the neurocognitive efficacy of olanzapine, risperidone, and haloperidol in schizophrenia. *Schizophr Res* **81**, 1-15, (2006).

95 Kesner, R. P., Gilbert, P. E. & Barua, L. A. The role of the hippocampus in memory for the temporal order of a sequence of odors. *Behav Neurosci* **116**, 286-290, (2002).

96 Jacobsen, C. F., Wolfe, J. B. & Jackson, T. A. An experimental analysis of the functions of the frontal association areas in primates. *Journal of Nervous Mental Disease* **82**, 1014, (1935).

97 Pribram, K. H., Mishkin, M., Rosvold, H. E. & Kaplan, S. J. Effects on delayed-response performance of lesions of dorsolateral and ventromedial frontal cortex of baboons. *J Comp Physiol Psychol* **45**, 565-575, (1952).

98 Goldman, P. S. & Rosvold, H. E. Localization of function within the dorsolateral prefrontal cortex of the rhesus monkey. *Exp Neurol* **27**, 291-304, (1970).

99 Goldman, P. S., Rosvold, H. E., Vest, B. & Galkin, T. W. Analysis of the delayed-alternation deficit produced by dorsolateral prefrontal lesions in the rhesus monkey. *J Comp Physiol Psychol* **77**, 212-220, (1971).

100 Levy, R. & Goldman-Rakic, P. S. Segregation of working memory functions within the dorsolateral prefrontal cortex. *Exp Brain Res* **133**, 23-32, (2000).

101 Petrides, M. Monitoring of selections of visual stimuli and the primate frontal cortex. *Proc Biol Sci* **246**, 293-298, (1991).

102 Petrides, M. Impairments on nonspatial self-ordered and externally ordered working memory tasks after lesions of the mid-dorsal part of the lateral frontal cortex in the monkey. *J Neurosci* **15**, 359-375, (1995).

103 Petrides, M. Functional specialization within the dorsolateral frontal cortex for serial order memory. *Proc Biol Sci* **246**, 299-306, (1991).

104 Goldman, P. S. Functional development of the prefrontal cortex in early life and the problem of neuronal plasticity. *Exp Neurol* **32**, 366-387, (1971).

105 Baddeley, A. Working memory. *Science* **255**, 556-559, (1992).

106 Jacobsen, C. F. Functions of the frontal association area in primates. *Archives of Neurology and Psychiatry* **45**, 565-575, (1935).

107 Jacobsen, C. F. & Nissen, H. W. Studies of cerebral function in primates. *J Comp Physiol Psychol* **23**, 101-112, (1937).

108 Mishkin, M. & Pribram, K. H. Analysis of the effects of frontal lesions in monkey. I. Variations of delayed alternation. *J Comp Physiol Psychol* **48**, 492-495, (1955).

109 Mishkin, M. & Pribram, K. H. Analysis of the effects of frontal lesions in monkey. II. Variations of delayed response. *J Comp Physiol Psychol* **49**, 36-40, (1956).

110 Pribram, K. H. A further experimental analysis of the behavioral deficit that follows injury to the primate frontal cortex. *Exp Neurol* **3**, 432-466, (1961).

111 Mishkin, M. Effects of small frontal lesions on delayed alternation in monkeys. *J Neurophysiol* **20**, 615-622, (1957).

112 Gross, C. G. & Weiskrantz, L. Evidence for dissociation of impairment on auditory discrimination and delayed response following lateral frontal lesions in monkeys. *Exp Neurol* **5**, 453-476, (1962).

113 Fuster, J. M., Bauer, R. H. & Jervey, J. P. Cellular discharge in the dorsolateral prefrontal cortex of the monkey in cognitive tasks. *Exp Neurol* **77**, 679-694, (1982).

114 Niki, H. Prefrontal unit activity during delayed alternation in the monkey. I. Relation to direction of response. *Brain Res* **68**, 185-196, (1974).

115 Friedman, H. R. & Goldman-Rakic, P. S. Coactivation of prefrontal cortex and inferior parietal cortex in working memory tasks revealed by 2DG functional mapping in the rhesus monkey. *J Neurosci* **14**, 2775-2788, (1994).

116 Pinto-Hamuy, T. & Linck, P. Effect of Frontal Lesions on Performance of Sequential Tasks by Monkeys. *Exp Neurol* **12**, 96-107, (1965).

117 Hasegawa, R. P., Blitz, A. M. & Goldberg, M. E. Neurons in monkey prefrontal cortex whose activity tracks the progress of a three-step self-ordered task. *J Neurophysiol* **92**, 1524-1535, (2004).

118 Goldman-Rakic, P. S., Selemon, L. D. & Schwartz, M. L. Dual pathways connecting the dorsolateral prefrontal cortex with the hippocampal formation and parahippocampal cortex in the rhesus monkey. *Neuroscience* **12**, 719-743, (1984).

119 Curtis, C. E. & D'Esposito, M. The effects of prefrontal lesions on working memory performance and theory. *Cogn Affect Behav Neurosci* **4**, 528-539, (2004).

120 Owen, A. M. The role of the lateral frontal cortex in mnemonic processing: the contribution of functional neuroimaging. *Exp Brain Res* **133**, 33-43, (2000).

121 Petrides, M. & Pandya, D. N. Dorsolateral prefrontal cortex: comparative cytoarchitectonic analysis in the human and the macaque brain and corticocortical connection patterns. *Eur J Neurosci* **11**, 1011-1036, (1999).

122 Tobias, T. J. Afferents to prefrontal cortex from the thalamic mediodorsal nucleus in the rhesus monkey. *Brain Res* **83**, 191-212, (1975).

123 Pribram, K. H., Chow, K. L. & Semmes, J. Limit and organization of the cortical projection from the medial thalamic nucleus in monkey. *J Comp Neurol* **98**, 433-448, (1953).

124 Morris, R., Pandya, D. N. & Petrides, M. Fiber system linking the mid-dorsolateral frontal cortex with the retrosplenial/presubicular region in the rhesus monkey. *J Comp Neurol* **407**, 183-192, (1999).

125 Pandya, D. N., Dye, P. & Butters, N. Efferent cortico-cortical projections of the prefrontal cortex in the rhesus monkey. *Brain Res* **31**, 35-46, (1971).

126 Johnson, T. N., Rosvold, H. E. & Mishkin, M. Projections from behaviorally-defined sectors of the prefrontal cortex to the basal ganglia, septum, and diencephalon of the monkey. *Exp Neurol* **21**, 20-34, (1968).

127 Suzuki, W. A. & Amaral, D. G. Perirhinal and parahippocampal cortices of the macaque monkey: cortical afferents. *J Comp Neurol* **350**, 497-533, (1994).

128 Rockland, K. S. & Van Hoesen, G. W. Some temporal and parietal cortical connections converge in CA1 of the primate hippocampus. *Cereb Cortex* **9**, 232-237, (1999).

129 Amaral, D. G. & Cowan, W. M. Subcortical afferents to the hippocampal formation in the monkey. *J Comp Neurol* **189**, 573-591, (1980).

130 Suzuki, W. A. & Amaral, D. G. Cortical inputs to the CA1 field of the monkey hippocampus originate from the perirhinal and parahippocampal cortex but not from area TE. *Neurosci Lett* **115**, 43-48, (1990).

131 Saunders, R. C. & Rosene, D. L. A comparison of the efferents of the amygdala and the hippocampal formation in the rhesus monkey: I. Convergence in the entorhinal, prorhinal, and perirhinal cortices. *J Comp Neurol* **271**, 153-184, (1988).

132 Rosene, D. L. & Van Hoesen, G. W. Hippocampal efferents reach widespread areas of cerebral cortex and amygdala in the rhesus monkey. *Science* **198**, 351-317, (1977).

133 Carmichael, S. T. & Price, J. L. Limbic connections of the orbital and medial prefrontal cortex in macaque monkeys. *J Comp Neurol* **363**, 615-641, (1995).

134 Friedman, D. P., Aggleton, J. P. & Saunders, R. C. Comparison of hippocampal, amygdala, and perirhinal projections to the nucleus accumbens: combined

anterograde and retrograde tracing study in the Macaque brain. *J Comp Neurol* **450**, 345-365, (2002).

135 Castner, S. A. & Goldman-Rakic, P. S. Enhancement of working memory in aged monkeys by a sensitizing regimen of dopamine D1 receptor stimulation. *J Neurosci* **24**, 1446-1450, (2004).

136 Abi-Dargham, A. *et al.* Prefrontal dopamine D1 receptors and working memory in schizophrenia. *J Neurosci* **22**, 3708-3719, (2002).

137 Watanabe, M., Kodama, T. & Hikosaka, K. Increase of extracellular dopamine in primate prefrontal cortex during a working memory task. *J Neurophysiol* **78**, 2795-2798, (1997).

138 Wang, M., Vijayraghavan, S. & Goldman-Rakic, P. S. Selective D2 receptor actions on the functional circuitry of working memory. *Science* **303**, 853-856, (2004).

139 Kwon, H., Reiss, A. L. & Menon, V. Neural basis of protracted developmental changes in visuo-spatial working memory. *Proc Natl Acad Sci U S A* **99**, 13336-13341, (2002).

140 Zald, D. H. & Iacono, W. G. The development of spatial working memory abilities. *Developmental Neuropsychology* **14**, 563-578, (1998).

141 Luciana, M. & Nelson, C. A. The functional emergence of prefrontally-guided working memory systems in four- to eight-year-old children. *Neuropsychologia* **36**, 273-293, (1998).

142 Goldman, P. S., Rosvold, H. E. & Mishkin, M. Selective sparing of function following prefrontal lobectomy in infant monkeys. *Exp Neurol* **29**, 221-226, (1970).

143 Goldman, P. S., Rosvold, H. E. & Mishkin, M. Evidence for behavioral impairment following prefrontal lobectomy in the infant monkey. *J Comp Physiol Psychol* **70**, 454-463, (1970).

144 Alexander, G. E. & Goldman, P. S. Functional development of the dorsolateral prefrontal cortex: an analysis utlizing reversible cryogenic depression. *Brain Res* **143**, 233-249, (1978).

145 Anderson, S. A., Classey, J. D., Conde, F., Lund, J. S. & Lewis, D. A. Synchronous development of pyramidal neuron dendritic spines and parvalbumin-immunoreactive chandelier neuron axon terminals in layer III of monkey prefrontal cortex. *Neuroscience* **67**, 7-22, (1995).

146 Zeamer, A. E., Heuer, E. & Bachevalier, J. Developmental trajectory of object recognition memory in infant rhesus macaques with and without neonatal hippocampal lesions. *J Neurosci*, (Submitted).

147 Zeamer, A. E. & Bachevalier, J. Neonatal lesions of the perirhinal cortex alter the development of object recognition abilities in monkeys. *Neuroscience Meeting Planner. Washington DC: Society for Neuroscience Online* **98.6**, (2009).

148 Payne, C., Machado, C. J., Bliwise, N. G. & Bachevalier, J. Maturation of the hippocampal formation and amygdala in Macaca mulatta: A volumetric magnetic resonance imaging study. *Hippocampus*, (2009).

149 Eckenhoff, M. F. & Rakic, P. A quantitative analysis of synaptogenesis in the molecular layer of the dentate gyrus in the rhesus monkey. *Brain Res Dev Brain Res* **64**, 129-135, (1991).

150 Berger, B., De Grissac, N. & Alvarez, C. Precocious development of parvalbumin-like immunoreactive interneurons in the hippocampal formation and entorhinal cortex of the fetal cynomolgus monkey. *J Comp Neurol* **403**, 309-331, (1999).

151 Lavenex, P., Banta Lavenex, P. & Amaral, D. G. Postnatal development of the primate hippocampal formation. *Dev Neurosci* **29**, 179-192, (2007).

152 Marquis, J. P., Goulet, S. & Dore, F. Y. Neonatal ventral hippocampus lesions disrupt extra-dimensional shift and alter dendritic spine density in the medial prefrontal cortex of juvenile rats. *Neurobiol Learn Mem* **90**, 339-346, (2008).

153 Brady, A. M. Neonatal ventral hippocampal lesions disrupt set-shifting ability in adult rats. *Behav Brain Res* **205**, 294-298, (2009).

154 Beninger, R. J. *et al.* Neonatal ventral hippocampal lesions in male and female rats: effects on water maze, locomotor activity, plus-maze and prefrontal cortical GABA and glutamate release in adulthood. *Behav Brain Res* **202**, 198-209, (2009).

155 Tseng, K. Y., Lewis, B. L., Lipska, B. K. & O'Donnell, P. Post-pubertal disruption of medial prefrontal cortical dopamine-glutamate interactions in a developmental animal model of schizophrenia. *Biol Psychiatry* **62**, 730-738, (2007).

156 Stern, C. E. *et al.* Activity in ventrolateral and mid-dorsolateral prefrontal cortex during nonspatial visual working memory processing: evidence from functional magnetic resonance imaging. *Neuroimage* **11**, 392-399, (2000).

157 Petrides, M. & Milner, B. Deficits on subject-ordered tasks after frontal- and temporal-lobe lesions in man. *Neuropsychologia* **20**, 249-262, (1982).

158 Petrides, M., Alivisatos, B., Evans, A. C. & Meyer, E. Dissociation of human mid-dorsolateral from posterior dorsolateral frontal cortex in memory processing. *Proc Natl Acad Sci U S A* **90**, 873-877, (1993).

159 Heuer, E. D. & Bachevalier, J. Modulation of working memory by neonatal lesions of the hippocampus in the rhesus macaque. . *Society for Neuroscience Abstracts Online Washington DC* **305.17**, On Line, (2007).

160 Goursaud, A. P. & Bachevalier, J. Social attachment in juvenile monkeys wth neonatal lesion of the hippocampus, amygdala and orbitofrontal cortex. *Behav Brain Res* **176**, 75-93, (2007).

161 Saunders, R. C., Aigner, T. G. & Frank, J. A. Magnetic resonance imaging of the rhesus monkey brain: use for stereotactic neurosurgery. *Exp Brain Res* **81**, 443-446, (1990).

162 Malkova, L., Lex, C. K., Mishkin, M. & Saunders, R. C. MRI-Based evaluation of locus and extent of neurotoxic lesions in monkeys.[erratum appears in Hippocampus 2001;11(5):614]. *Hippocampus* **11**, 361-370, (2001).

163 Nemanic, S., Alvarado, M. C., Price, R. E., Jackson, E. F. & Bachevalier, J. Assessment of locus and extent of neurotoxic lesions in monkeys using

neuroimaging techniques: a replication. *J Neurosci Methods* **121**, 199-209, (2002).

164 Gundersen, H. J. & Jensen, E. B. The efficiency of systematic sampling in stereology and its prediction. *J Microsc* **147**, 229-263, (1987).

165 Zeamer, A. E., Heuer, E. & Bachevalier, J. Developmental trajectory of object recognition memory in infant rhesus macaques with and without neonatal hippocampal lesions. *J Neurosci*, (In Press).

166 Bachevalier, J., Beauregard, M. & Alvarado, M. C. Long-term effects of neonatal damage to the hippocampal formation and amygdaloid complex on object discrimination and object recognition in rhesus monkeys (Macaca mulatta). *Behav Neurosci* **113**, 1127-1151, (1999).

167 Mishkin, M. & Delacour, J. An analysis of short-term visual memory in the monkey. *J Exp Psychol Anim Behav Process* **1**, 326-334, (1975).

168 Hodos, W. & Bobko, P. A weighted index of bilateral brain lesions. *J Neurosci Methods* **12**, 43-47, (1984).

169 Diamond, A., Zola-Morgan, S. & Squire, L. R. Successful performance by monkeys with lesions of the hippocampal formation on AB and object retrieval, two tasks that mark developmental changes in human infants. *Behav Neurosci* **103**, 526-537, (1989).

170 Kesner, R. P., Hunsaker, M. R. & Ziegler, W. The role of the dorsal CA1 and ventral CA1 in memory for the temporal order of a sequence of odors. *Neurobiol Learn Mem* **93**, 111-116, (2010).

171 Sanchez, M. M., Hearn, E. F., Do, D., Rilling, J. K. & Herndon, J. G. Differential rearing affects corpus callosum size and cognitive function of rhesus monkeys. *Brain Res* **812**, 38-49, (1998).

172 Sackett, G. P., Ruppenthal, G. C. & Davis, A. E. Survival, growth, health, and reproduction following nursery rearing compared with mother rearing in pigtailed monkeys (Macaca nemestrina). *Am J Primatol* **56**, 165-183, (2002).

173 Heuer, E. & Bachevalier, J. Tests of recognition memory: Effects of selective lesions of the hippocampus in infancy or adulthood. (In Preperation).

174 Haber, S. N., Lynd, E., Klein, C. & Groenewegen, H. J. Topographic organization of the ventral striatal efferent projections in the rhesus monkey: an anterograde tracing study. *J Comp Neurol* **293**, 282-298, (1990).

175 Haber, S. N., Lynd-Balta, E. & Mitchell, S. J. The organization of the descending ventral pallidal projections in the monkey. *J Comp Neurol* **329**, 111-128, (1993).

176 Murphy, B. L., Arnsten, A. F., Goldman-Rakic, P. S. & Roth, R. H. Increased dopamine turnover in the prefrontal cortex impairs spatial working memory performance in rats and monkeys. *Proc Natl Acad Sci U S A* **93**, 1325-1329, (1996).

177 Machado, C. J., Snyder, A. Z., Cherry, S. R., Lavenex, P. & Amaral, D. G. Effects of neonatal amygdala or hippocampus lesions on resting brain metabolism in the macaque monkey: a microPET imaging study. *Neuroimage* **39**, 832-846, (2008).

178 Cirilli, L., Payne, C. & Bachevalier, J. Neonatal hippocampal and amygdala lesions alter the development of the corpus callosum: An MRI study in adult monkeys. *Neuroscience Meeting Planner. Washington DC: Society for Neuroscience Online* **536.20**, (2009).

179 Belger, A. *et al.* Dissociation of mnemonic and perceptual processes during spatial and nonspatial working memory using fMRI. *Hum Brain Mapp* **6**, 14-32, (1998).

180 Kim, J. J. *et al.* Functional disconnection between the prefrontal and parietal cortices during working memory processing in schizophrenia: a[15(O)]H2O PET study. *Am J Psychiatry* **160**, 919-923, (2003).

181 Schmahmann, J. D. & Pandya, D. N. *Fiber pathways of the brain*. (Oxford University Press, 2006).

182 Kievit, J. & Kuypers, H. G. Organization of the thalamo-cortical connexions to the frontal lobe in the rhesus monkey. *Exp Brain Res* **29**, 299-322, (1977).

183 Heuer, E. & Bachevalier, J. Monitoring, but not maintenance, working memory processes are impaired following selective neonatal lesions of the hippocampus in rhesus macaque., (In Preperation).

184 Friedman, H. R. & Goldman-Rakic, P. S. Activation of the hippocampus and dentate gyrus by working-memory: a 2-deoxyglucose study of behaving rhesus monkeys. *J Neurosci* **8**, 4693-4706, (1988).

185 Olson, I. R., Page, K., Moore, K. S., Chatterjee, A. & Verfaellie, M. Working memory for conjunctions relies on the medial temporal lobe. *J Neurosci* **26**, 4596-4601, (2006).

186 Kesner, R. P., Hopkins, R. O. & Fineman, B. Item and order dissociation in humans with prefrontal cortex damage. *Neuropsychologia* **32**, 881-891, (1994).

187 Ergorul, C. & Eichenbaum, H. Essential role of the hippocampal formation in rapid learning of higher-order sequential associations. *J Neurosci* **26**, 4111-4117, (2006).

188 Lee, I., Jerman, T. S. & Kesner, R. P. Disruption of delayed memory for a sequence of spatial locations following CA1- or CA3-lesions of the dorsal hippocampus. *Neurobiol Learn Mem* **84**, 138-147, (2005).

189 Heuer, E. & Bachevalier, J. Dorsolateral prefrontal working memory processes are impaired after selective neonatal lesions of the hippocampus in adult rhesus macaques. (In Preperation).

190 Mishkin, M. & Manning, F. J. Non-spatial memory after selective prefrontal lesions in monkeys. *Brain Res* **143**, 313-323, (1978).

191 Baslow, M. H. & Guilfoyle, D. N. Using proton magnetic resonance imaging and spectroscopy to understand brain "activation". *Brain Lang* **102**, 153-164, (2007).

192 Dager, S. R., Corrigan, N. M., Richards, T. L. & Posse, S. Research applications of magnetic resonance spectroscopy to investigate psychiatric disorders. *Top Magn Reson Imaging* **19**, 81-96, (2008).

193 Cecil, K. M., Lenkinski, R. E., Gur, R. E. & Gur, R. C. Proton magnetic resonance spectroscopy in the frontal and temporal lobes of neuroleptic naive patients with schizophrenia. *Neuropsychopharmacology* **20**, 131-140, (1999).

194 Bertolino, A. *et al.* The effect of treatment with antipsychotic drugs on brain N-acetylaspartate measures in patients with schizophrenia. *Biol Psychiatry* **49**, 39-46, (2001).

195 O'Neill, J. *et al.* 1H MRSI evidence of metabolic abnormalities in childhood-onset schizophrenia. *Neuroimage* **21**, 1781-1789, (2004).

196 Bertolino, A. *et al.* Altered development of prefrontal neurons in rhesus monkeys with neonatal mesial temporo-limbic lesions: a proton magnetic resonance spectroscopic imaging study. *Cereb Cortex* **7**, 740-748, (1997).

197 Kreis, R., Ernst, T. & Ross, B. D. Development of the human brain: in vivo quantification of metabolite and water content with proton magnetic resonance spectroscopy. *Magn Reson Med* **30**, 424-437, (1993).

198 Baslow, M. H. Functions of N-acetyl-L-aspartate and N-acetyl-L-aspartylglutamate in the vertebrate brain: role in glial cell-specific signaling. *J Neurochem* **75**, 453-459, (2000).

199 Neale, J. H., Bzdega, T. & Wroblewska, B. N-Acetylaspartylglutamate: the most abundant peptide neurotransmitter in the mammalian central nervous system. *J Neurochem* **75**, 443-452, (2000).

200 Galinska, B. *et al.* Duration of untreated psychosis and proton magnetic resonance spectroscopy (1H-MRS) findings in first-episode schizophrenia. *Med Sci Monit* **15**, CR82-88, (2009).

201 Pouzet, B. *et al.* The effects of hippocampal and fimbria-fornix lesions on prepulse inhibition. *Behav Neurosci* **113**, 968-981, (1999).

202 Kodsi, M. H. & Swerdlow, N. R. Prepulse inhibition in the rat is regulated by ventral and caudodorsal striato-pallidal circuitry. *Behav Neurosci* **109**, 912-928, (1995).

203 Kodsi, M. H. & Swerdlow, N. R. Quinolinic acid lesions of the ventral striatum reduce sensorimotor gating of acoustic startle in rats. *Brain Res* **643**, 59-65, (1994).

204 Heuer, E., Zhang, X. & Bachevalier, J. Magnetic resonance spectroscopy and its' relation to working memory in adult monkeys with neonatal lesions of the hippocampus., (In preperation).

205 Winslow, J. T., Parr, L. A. & Davis, M. Acoustic startle, prepulse inhibition, and fear-potentiated startle measured in rhesus monkeys. *Biol Psychiatry* **51**, 859-866, (2002).

206 Wan, F. J. & Swerdlow, N. R. The basolateral amygdala regulates sensorimotor gating of acoustic startle in the rat. *Neuroscience* **76**, 715-724, (1997).

207 Decker, M. W., Curzon, P. & Brioni, J. D. Influence of separate and combined septal and amygdala lesions on memory, acoustic startle, anxiety, and locomotor activity in rats. *Neurobiol Learn Mem* **64**, 156-168, (1995).

208 Daenen, E. W., Wolterink, G., Van Der Heyden, J. A., Kruse, C. G. & Van Ree, J. M. Neonatal lesions in the amygdala or ventral hippocampus disrupt prepulse inhibition of the acoustic startle response; implications for an animal model of neurodevelopmental disorders like schizophrenia. *Eur Neuropsychopharmacol* **13**, 187-197, (2003).

209 Lacroix, L., Spinelli, S., White, W. & Feldon, J. The effects of ibotenic acid lesions of the medial and lateral prefrontal cortex on latent inhibition, prepulse inhibition and amphetamine-induced hyperlocomotion. *Neuroscience* **97**, 459-468, (2000).

210 Salazar, R. F., White, W., Lacroix, L., Feldon, J. & White, I. M. NMDA lesions in the medial prefrontal cortex impair the ability to inhibit responses during reversal of a simple spatial discrimination. *Behav Brain Res* **152**, 413-424, (2004).

211 Schwabe, K., Enkel, T., Klein, S., Schutte, M. & Koch, M. Effects of neonatal lesions of the medial prefrontal cortex on adult rat behaviour. *Behav Brain Res* **153**, 21-34, (2004).

212 Schneider, M. & Koch, M. Behavioral and morphological alterations following neonatal excitotoxic lesions of the medial prefrontal cortex in rats. *Exp Neurol* **195**, 185-198, (2005).

213 Machado, C. J. & Bachevalier, J. The impact of selective amygdala, orbital frontal cortex, or hippocampal formation lesions on established social relationships in rhesus monkeys (Macaca mulatta). *Behav Neurosci* **120**, 761-786, (2006).

214 Meunier, M., Bachevalier, J. & Mishkin, M. Effects of orbital frontal and anterior cingulate lesions on object and spatial memory in rhesus monkeys. *Neuropsychologia* **35**, 999-1015, (1997).

215 Carmichael, S. T. & Price, J. L. Architectonic subdivision of the orbital and medial prefrontal cortex in the macaque monkey. *J Comp Neurol* **346**, 366-402, (1994).

216 Clancy, B., Finlay, B. L., Darlington, R. B. & Anand, K. J. Extrapolating brain development from experimental species to humans. *Neurotoxicology* **28**, 931-937, (2007).

217 Kodsi, M. H. & Swerdlow, N. R. Ventral pallidal GABA-A receptors regulate prepulse inhibition of acoustic startle. *Brain Res* **684**, 26-35, (1995).

218 Izquierdo, A. & Murray, E. A. Selective bilateral amygdala lesions in rhesus monkeys fail to disrupt object reversal learning. *J Neurosci* **27**, 1054-1062, (2007).

219 Kazama, A. & Bachevalier, J. Selective aspiration or neurotoxic lesions of orbital frontal areas 11 and 13 spared monkeys' performance on the object discrimination reversal task. *J Neurosci* **29**, 2794-2804, (2009).

220 Schoenbaum, G., Setlow, B., Nugent, S. L., Saddoris, M. P. & Gallagher, M. Lesions of orbitofrontal cortex and basolateral amygdala complex disrupt acquisition of odor-guided discriminations and reversals. *Learn Mem* **10**, 129-140, (2003).

221 Murray, E. A. The amygdala, reward and emotion. *Trends Cogn Sci* **11**, 489-497, (2007).

222 Weike, A. I., Bauer, U. & Hamm, A. O. Effective neuroleptic medication removes prepulse inhibition deficits in schizophrenia patients. *Biol Psychiatry* **47**, 61-70, (2000).

223 Perlstein, W. M., Carter, C. S., Noll, D. C. & Cohen, J. D. Relation of prefrontal cortex dysfunction to working memory and symptoms in schizophrenia. *Am J Psychiatry* **158**, 1105-1113, (2001).

224 Tan, H. Y., Choo, W. C., Fones, C. S. & Chee, M. W. fMRI study of maintenance and manipulation processes within working memory in first-episode schizophrenia.[see comment]. *Am J Psychiatry* **162**, 1849-1858, (2005).

225 Swerdlow, N. R. & Geyer, M. A. Clozapine and haloperidol in an animal model of sensorimotor gating deficits in schizophrenia. *Pharmacol Biochem Behav* **44**, 741-744, (1993).

226 Akbarian, S. *et al.* Gene expression for glutamic acid decarboxylase is reduced without loss of neurons in prefrontal cortex of schizophrenics. *Arch Gen Psychiatry* **52**, 258-266, (1995).

227 Tallan, H. H. Studies on the distribution of N-acetyl-L-aspartic acid in brain. *J Biol Chem* **224**, 41-45, (1957).

228 Berlinguet, L. & Laliberte, M. Metabolism of N-acetyl-L-aspartic acid in mice. *Can J Biochem* **44**, 783-789, (1966).

229 Knizley, H., Jr. The enzymatic synthesis of N-acetyl-L-aspartic acid by a water-insoluble preparation of a cat brain acetone powder. *J Biol Chem* **242**, 4619-4622, (1967).

230 Patel, T. B. & Clark, J. B. Synthesis of N-acetyl-L-aspartate by rat brain mitochondria and its involvement in mitochondrial/cytosolic carbon transport. *Biochem J* **184**, 539-546, (1979).

231 Wroblewska, B., Santi, M. R. & Neale, J. H. N-acetylaspartylglutamate activates cyclic AMP-coupled metabotropic glutamate receptors in cerebellar astrocytes. *Glia* **24**, 172-179, (1998).

232 Schoepp, D. D., Jane, D. E. & Monn, J. A. Pharmacological agents acting at subtypes of metabotropic glutamate receptors. *Neuropharmacology* **38**, 1431-1476, (1999).

233 Pacheco Otalora, L. F., Moffett, J. R. & Garrido-Sanabria, E. R. Selective vulnerability of hippocampal NAAGergic neurons in experimental temporal lobe epilepsy. *Brain Res* **1144**, 219-230, (2007).

234 Gonzalez-Burgos, G., Kroener, S., Seamans, J. K., Lewis, D. A. & Barrionuevo, G. Dopaminergic modulation of short-term synaptic plasticity in fast-spiking interneurons of primate dorsolateral prefrontal cortex. *J Neurophysiol* **94**, 4168-4177, (2005).

235 Baxter, M. G. & Murray, E. A. Opposite relationship of hippocampal and rhinal cortex damage to delayed nonmatching-to-sample deficits in monkeys. *Hippocampus* **11**, 61-71, (2001).

236 Aalto, S., Bruck, A., Laine, M., Nagren, K. & Rinne, J. O. Frontal and temporal dopamine release during working memory and attention tasks in healthy humans: a positron emission tomography study using the high-affinity dopamine D2 receptor ligand [11C]FLB 457. *J Neurosci* **25**, 2471-2477, (2005).

237 Wang, Y. & Goldman-Rakic, P. S. D2 receptor regulation of synaptic burst firing in prefrontal cortical pyramidal neurons. *Proc Natl Acad Sci U S A* **101**, 5093-5098, (2004).

238 Wan, F. J., Taaid, N. & Swerdlow, N. R. Do D1/D2 interactions regulate prepulse inhibition in rats? *Neuropsychopharmacology* **14**, 265-274, (1996).

239 Schwarzkopf, S. B., Bruno, J. P. & Mitra, T. Effects of haloperidol and SCH 23390 on acoustic startle and prepulse inhibition under basal and stimulated conditions. *Prog Neuropsychopharmacol Biol Psychiatry* **17**, 1023-1036, (1993).

240 Lavin, A., Moore, H. M. & Grace, A. A. Prenatal disruption of neocortical development alters prefrontal cortical neuron responses to dopamine in adult rats. *Neuropsychopharmacology* **30**, 1426-1435, (2005).